

Characterization of Doped Silicon and Endofullerenes by Raman Spectroscopy for Sensing and Transport Devices

Brian Burke

Condensed Matter Seminar, 4th Year Talk

4/9/2009 4:00 p.m.



Keith Williams' Nanophysics Group – University of Virginia

Outline

- Background
 - Raman Spectroscopy (FTIR)
 - Electron Transport Theory
 - Experimental Techniques (IETS, CV, STM)
- Current Projects
 - SurFET Device
 - Fano Interference in Doped Silicon
 - Raman Investigation of Endofullerenes
- Future Projects
 - Molecular Doping of Silicon
 - Field Dependence of SurFET Device (UV Raman and Transport)
 - IETS (Kondo effect) and Cyclic Voltammetry of Endofullerenes
 - Magneto-Raman of Endofullerenes
 - Development of Spin Logic Device

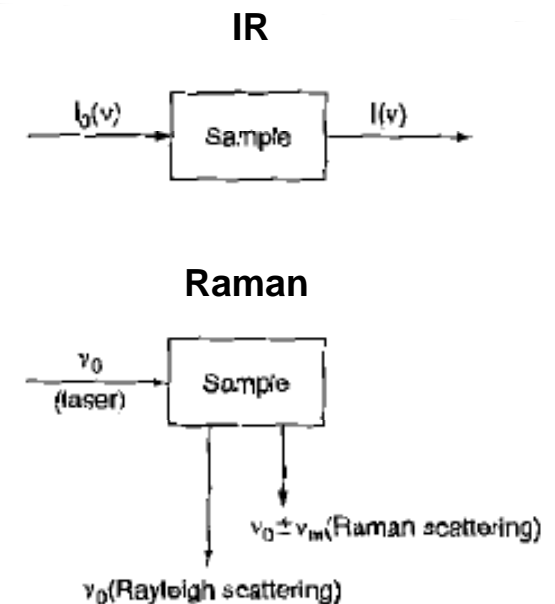


Raman and IR Spectroscopy

- Units in wavenumbers $\tilde{\nu} = \frac{\nu}{c} = \frac{1}{\lambda} \text{ (cm}^{-1}\text{)}$
- Transitions between vibrational levels (change in configuration)

Table 1-2 Spectral Regions and Their Origins

Spectroscopy	Range ($\tilde{\nu}$, cm^{-1})	Origin
γ -ray	$10^{10} - 10^8$	Rearrangement of elementary particles in the nucleus
X-ray (ESCA, PES)	$10^8 - 10^6$	Transitions between energy levels of inner electrons of atoms and molecules
UV-Visible	$10^6 - 10^4$	Transitions between energy levels of valence electrons of atoms and molecules
Raman and infrared	$10^4 - 10^2$	Transitions between vibrational levels (change of configuration)
Microwave	$10^2 - 1$	Transitions between rotational levels (change of orientation)
Electron spin resonance (ESR)	$1 - 10^{-2}$	Transitions between electron spin levels in magnetic field
Nuclear magnetic resonance (NMR)	$10^{-2} - 10^{-4}$	Transitions between nuclear spin levels in magnetic fields



J. Ferraro, *Introductory Raman Spectroscopy*, Elsevier (1994)



Raman Spectroscopy

- The electric field E from the laser beam fluctuates in time

$$E = E_0 \cos 2\pi\nu_0 t$$

- An electric dipole moment P is induced in the molecule or atoms under illumination

$$P = \alpha E$$

- For a small amplitude of vibration, α is a linear function of the nuclear displacement q

$$q = q_0 \cos 2\pi\nu_m t \quad \text{and} \quad \alpha = \alpha_0 + \left(\frac{\partial \alpha}{\partial q} \right)_0 q_0 + \dots$$

- Expanding P gives

$$P = \boxed{\alpha_0 E_0 \cos 2\pi\nu_0 t} + \left(\frac{\partial \alpha}{\partial q} \right)_0 q_0 E_0 \cos 2\pi\nu_0 t \cos 2\pi\nu_m t$$

Rayleigh \swarrow Stokes \swarrow

$$\Rightarrow \frac{1}{2} \left(\frac{\partial \alpha}{\partial q} \right)_0 q_0 E_0 \left[\boxed{\cos \{2\pi(\nu_0 + \nu_m)t\}} + \boxed{\cos \{2\pi(\nu_0 - \nu_m)t\}} \right]$$

Anti-Stokes \swarrow

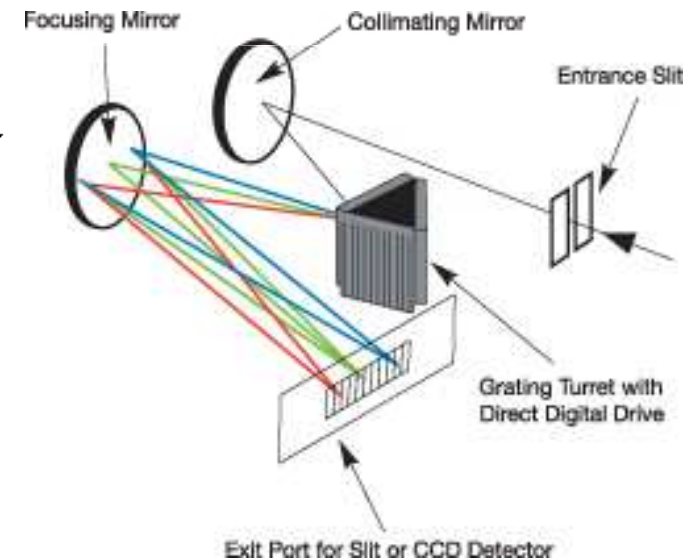
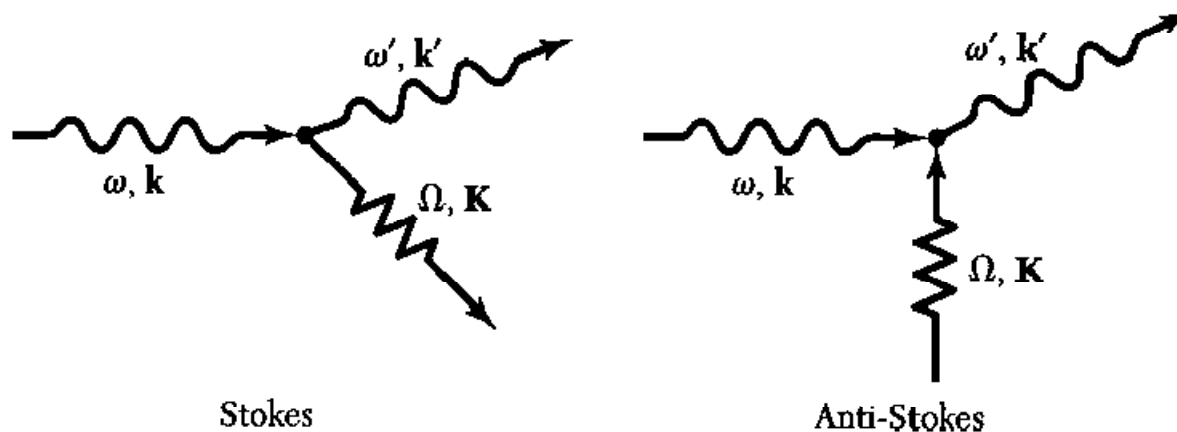
J. Ferraro, *Introductory Raman Spectroscopy*, Elsevier (1994)



Raman Spectroscopy

- Scattering event between incoming and outgoing photons and quantized vibrations (vibrons and phonons)
- Interaction is through an intermediate electronic transition
- Electron de-excites, emitting a Raman-scattered photon, the frequency of which is shifted by an amount equal to the frequency of the phonon
- The selection rules for first-order Raman scattering are

$$\omega = \omega' \pm \Omega \quad \text{and} \quad \mathbf{k} = \mathbf{k}' \pm \mathbf{K}$$



C. Kittel, *Introduction to Solid State Physics*, Wiley (2004)

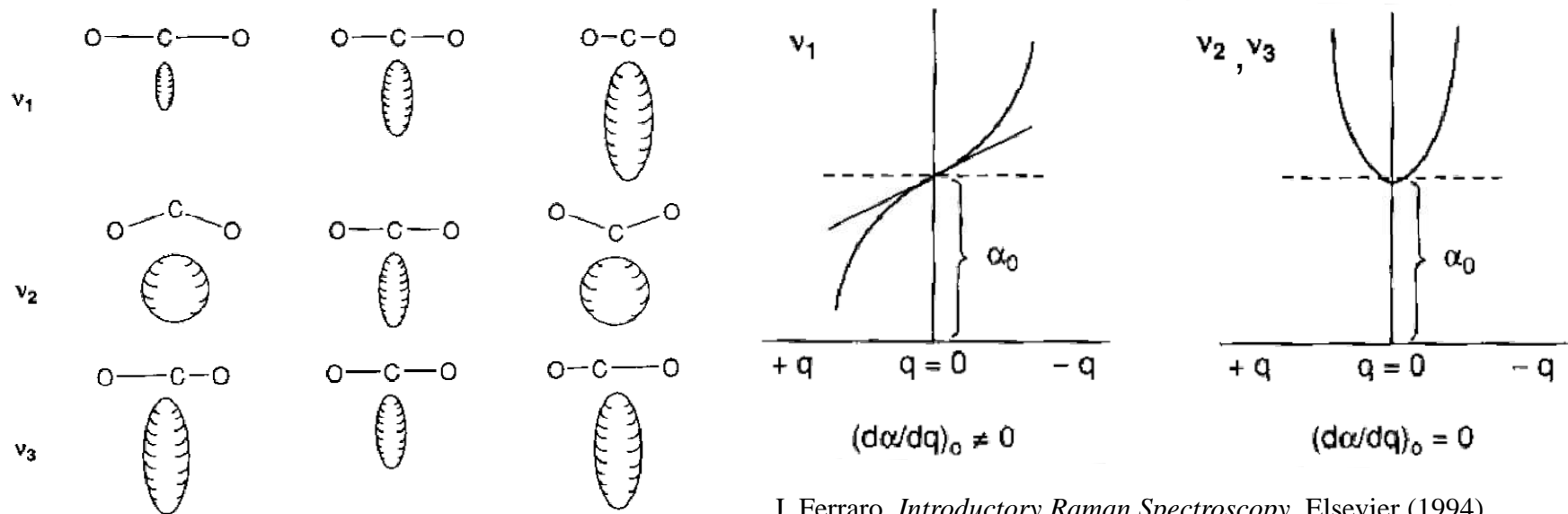


Selection Rules for Raman Spectra

- A vibration is IR-active if the dipole moment is changed during the vibration and is Raman-active if the polarizability is changed

$$\begin{bmatrix} P_x \\ P_y \\ P_z \end{bmatrix} = \begin{bmatrix} \alpha_{xx} & \alpha_{xy} & \alpha_{xz} \\ \alpha_{yx} & \alpha_{yy} & \alpha_{yz} \\ \alpha_{zx} & \alpha_{zy} & \alpha_{zz} \end{bmatrix} \begin{bmatrix} E_x \\ E_y \\ E_z \end{bmatrix}$$

- If we plot $1/\sqrt{\alpha_i}$ (polarizability ellipsoid), the vibration is Raman-active if the size, shape or orientation changes

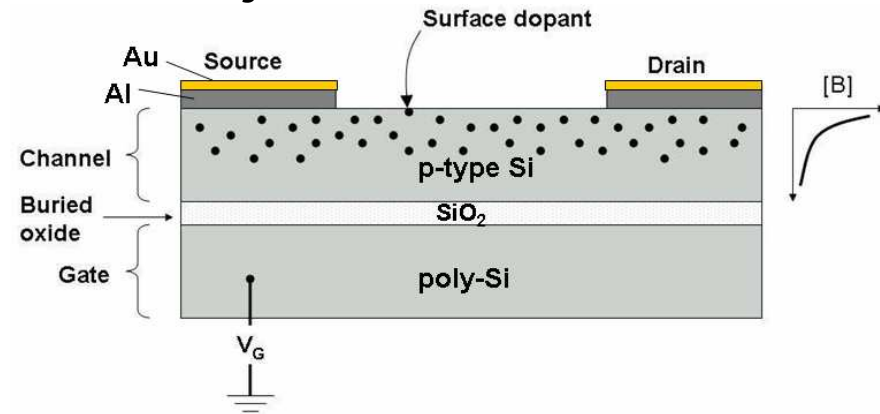


J. Ferraro, *Introductory Raman Spectroscopy*, Elsevier (1994)

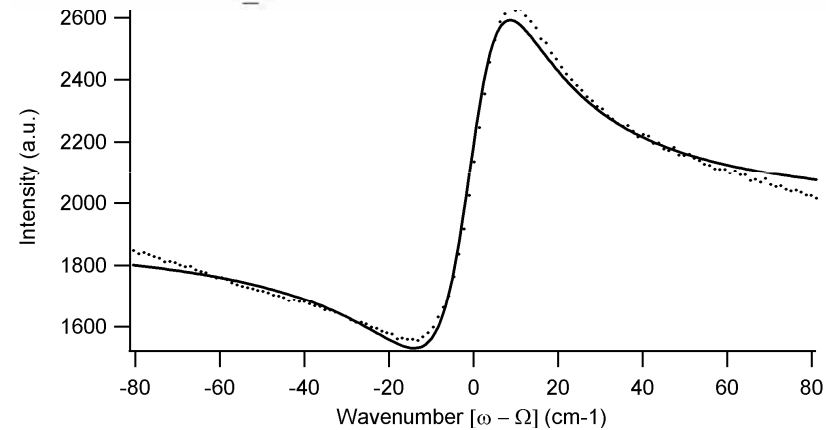


Current Projects

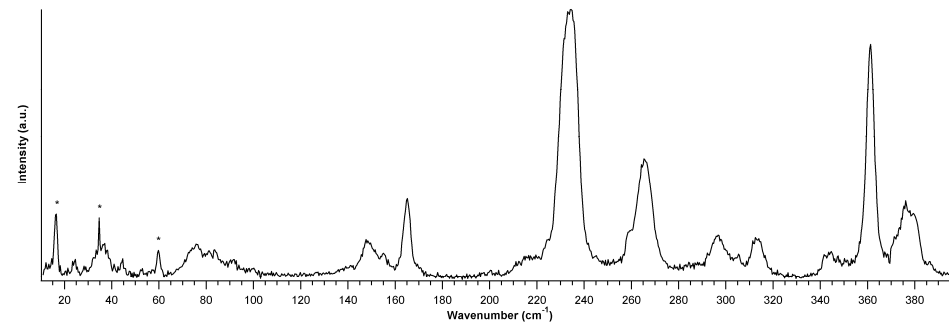
- SurFET Device



- Fano Interference in Doped Silicon

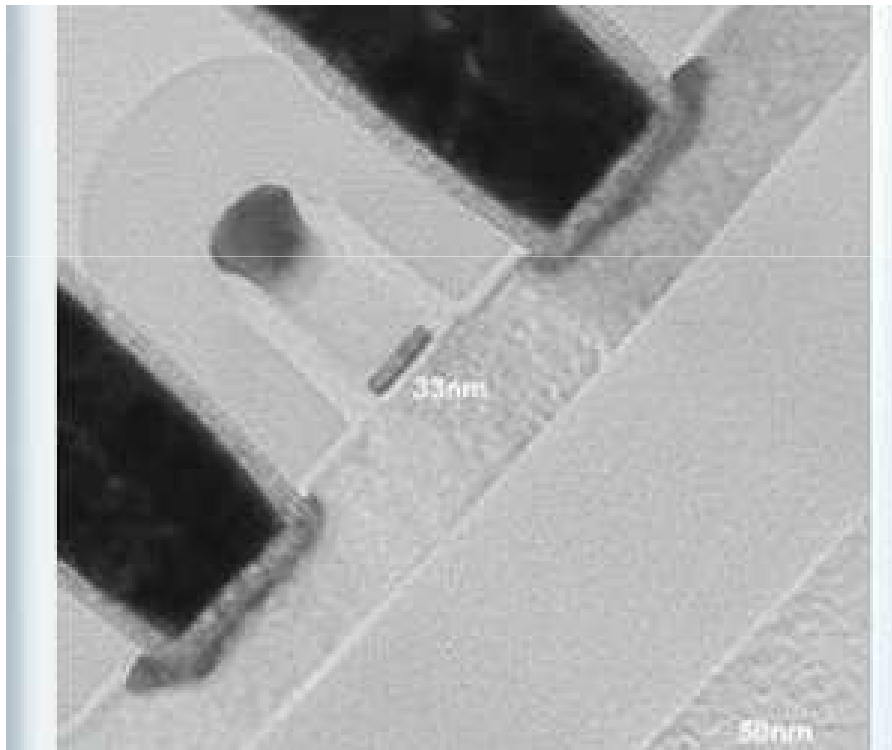


- Raman Investigation of Endofullerenes

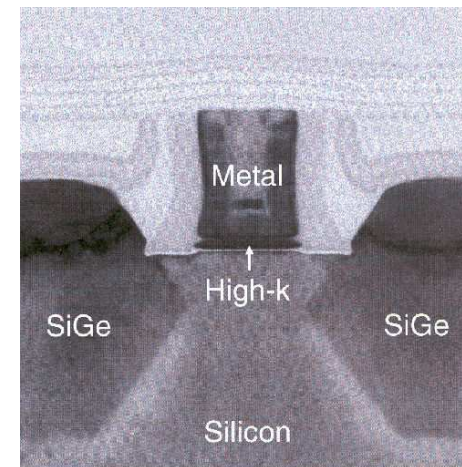
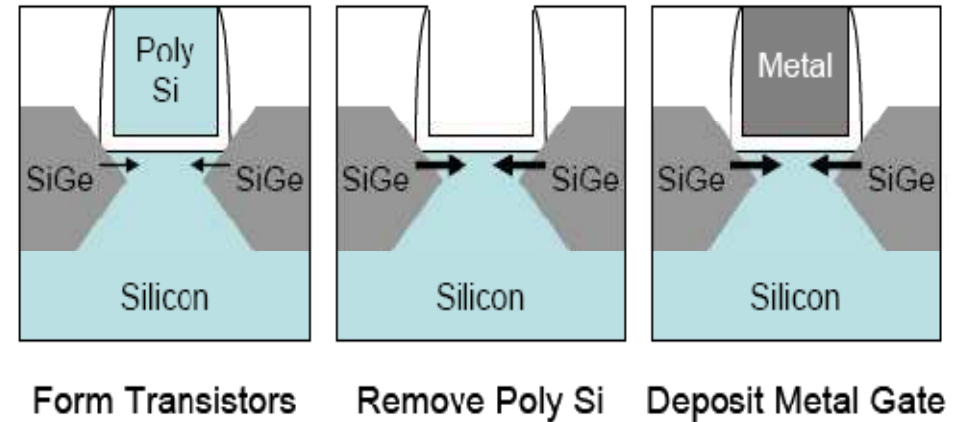


Research Motivation

- Scaling down of silicon transistors leads to new surface physics
- Need to bridge the gap between top-down silicon technology and molecular electronics



AMD-IBM 33 nm high-k metal gate transistor

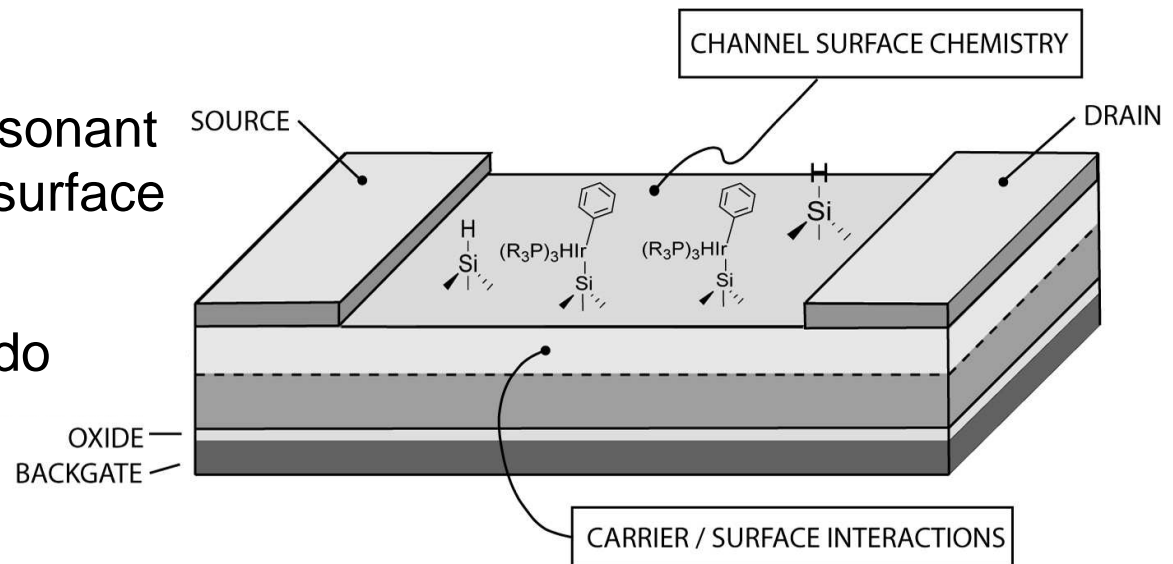


Intel 45 nm high-k metal gate transistor



New Transistor Design: SurFET

- Field effect transistor (FET) is fabricated atop a silicon-on-insulator (SOI) wafer
- The exposed channel surface is decorated with molecules that define scattering centers
- Scattering introduces resonant levels into the channel
- Transport is not through the molecule, but parallel to the channel surface
- Device is a FET with resonant on/off levels mediated by surface scattering
- Fano interference, Kondo scattering, RTS can be observed



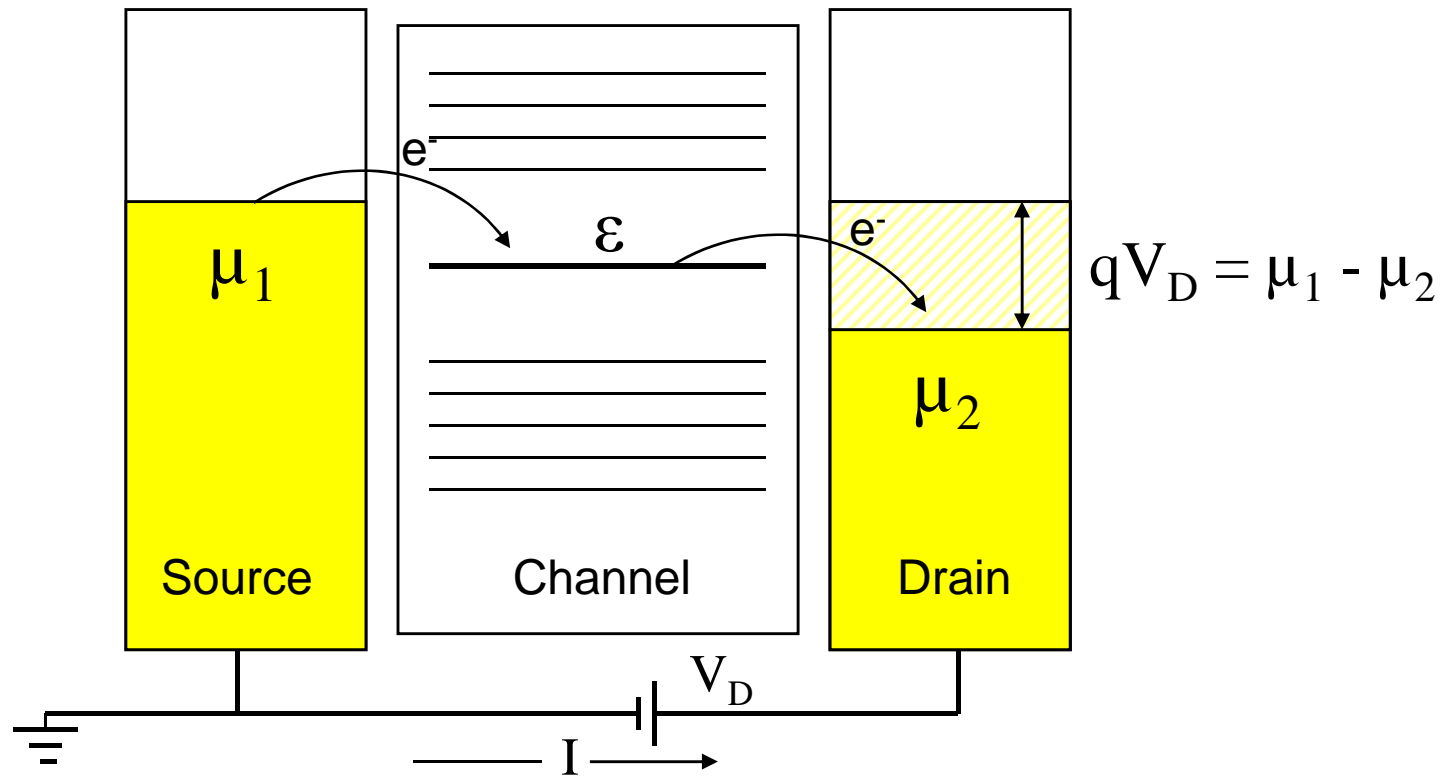
Surface scattering field effect transistor (SurFET)



Electron Transport Theory

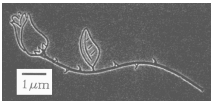
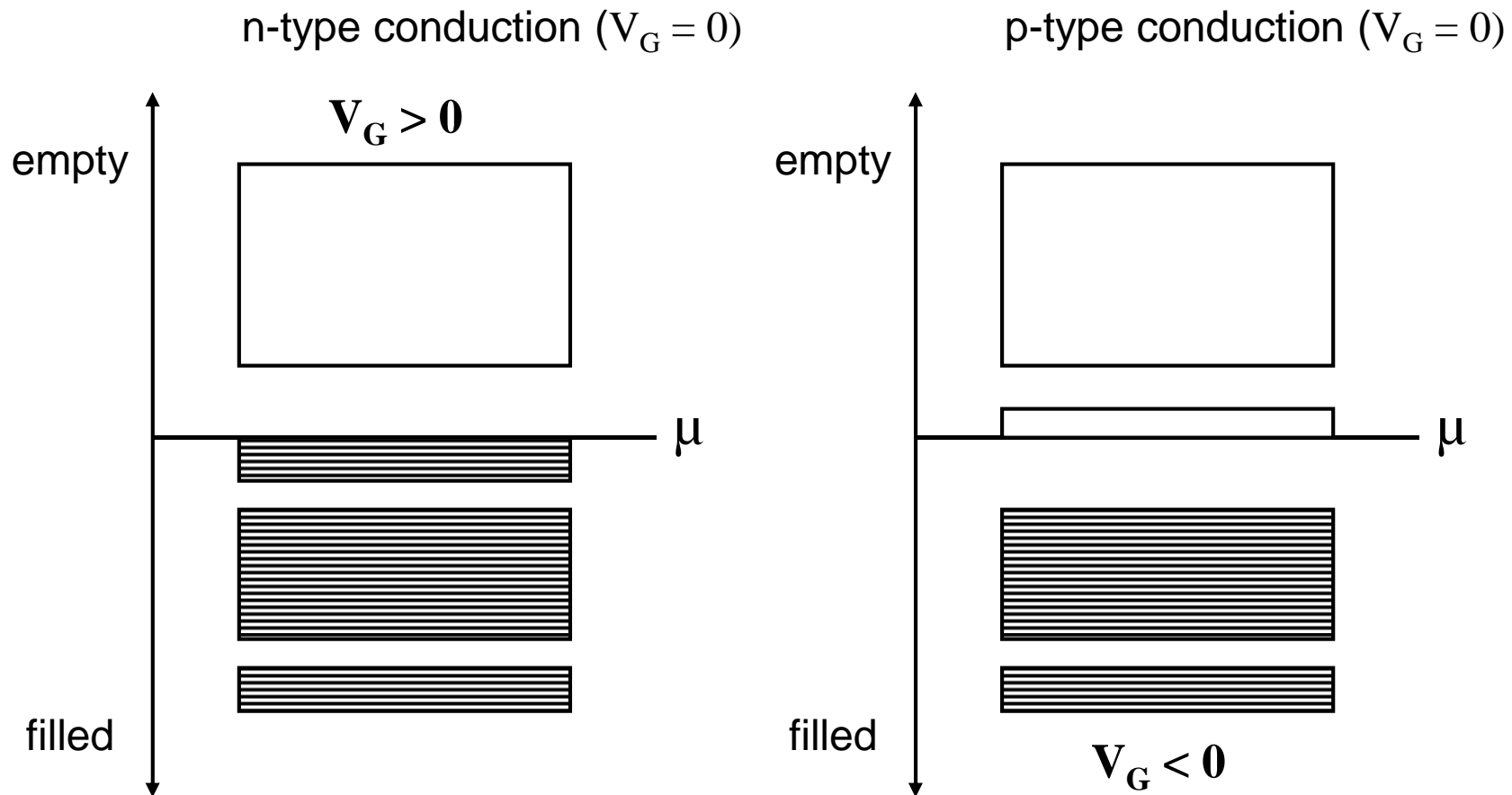
- What makes electrons flow?

Conduction depends on the availability of states around $E = \mu$, not the number of electrons. Additionally, it does not matter if the states are empty or filled.



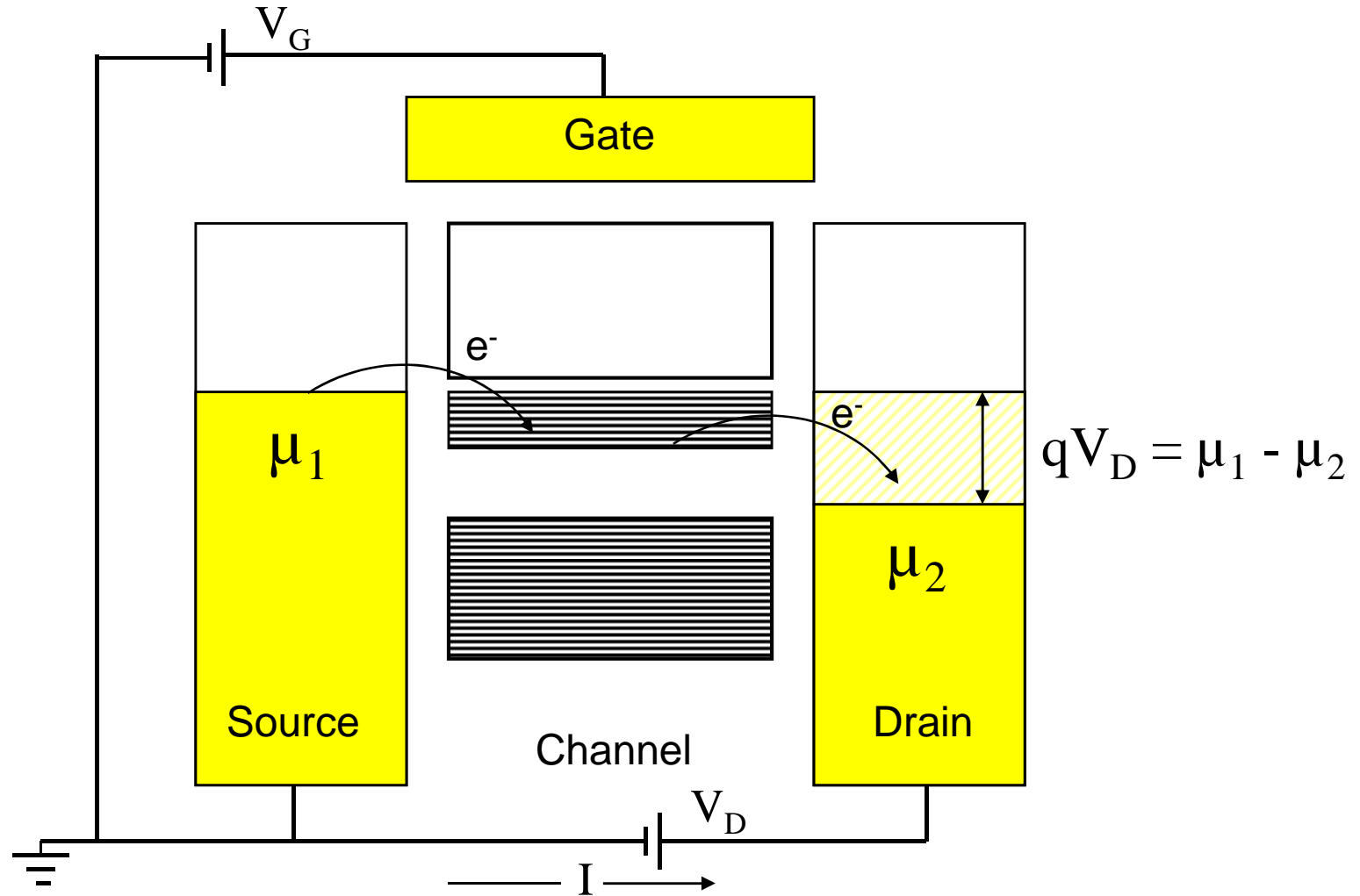
Electron Transport Theory

- How does a Gate Voltage affect conduction?

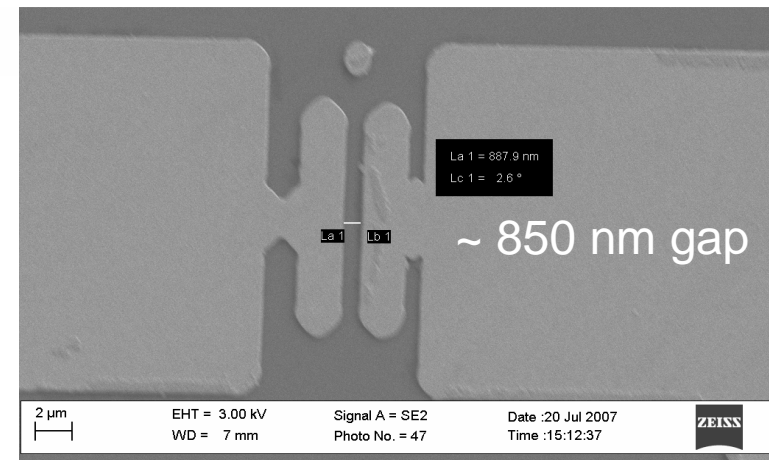
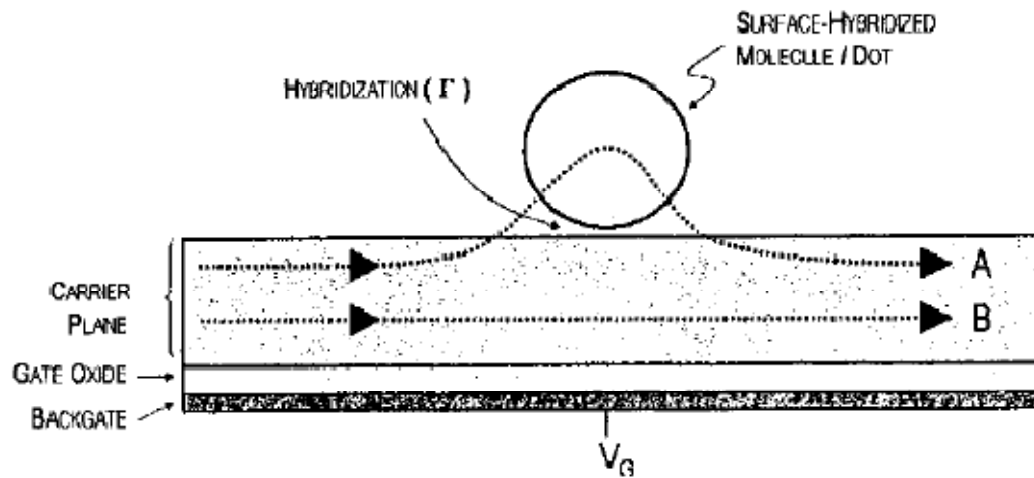
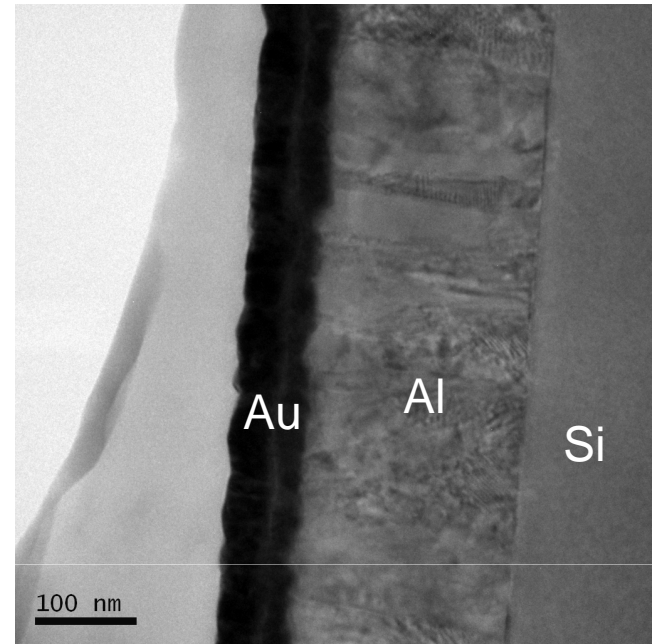
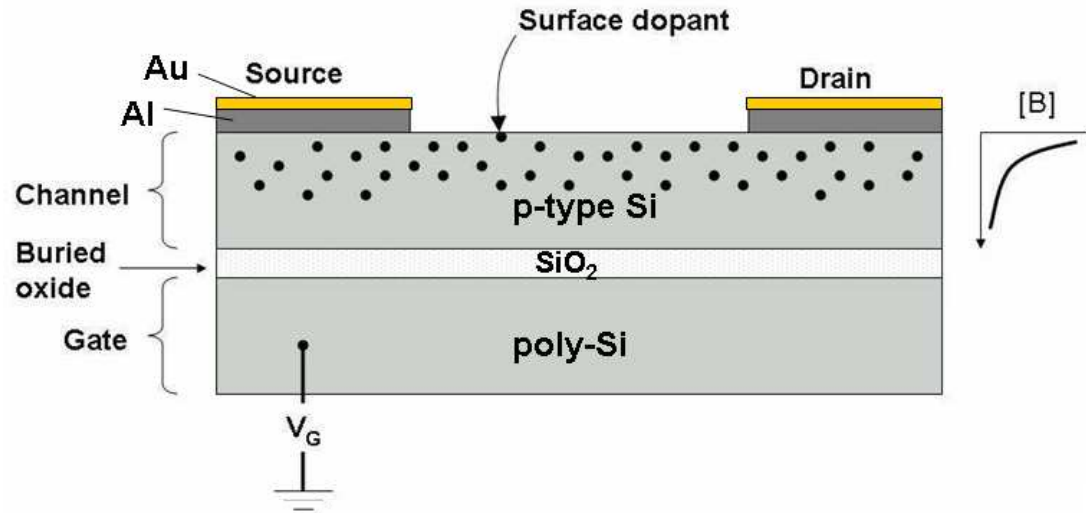


Electron Transport Theory

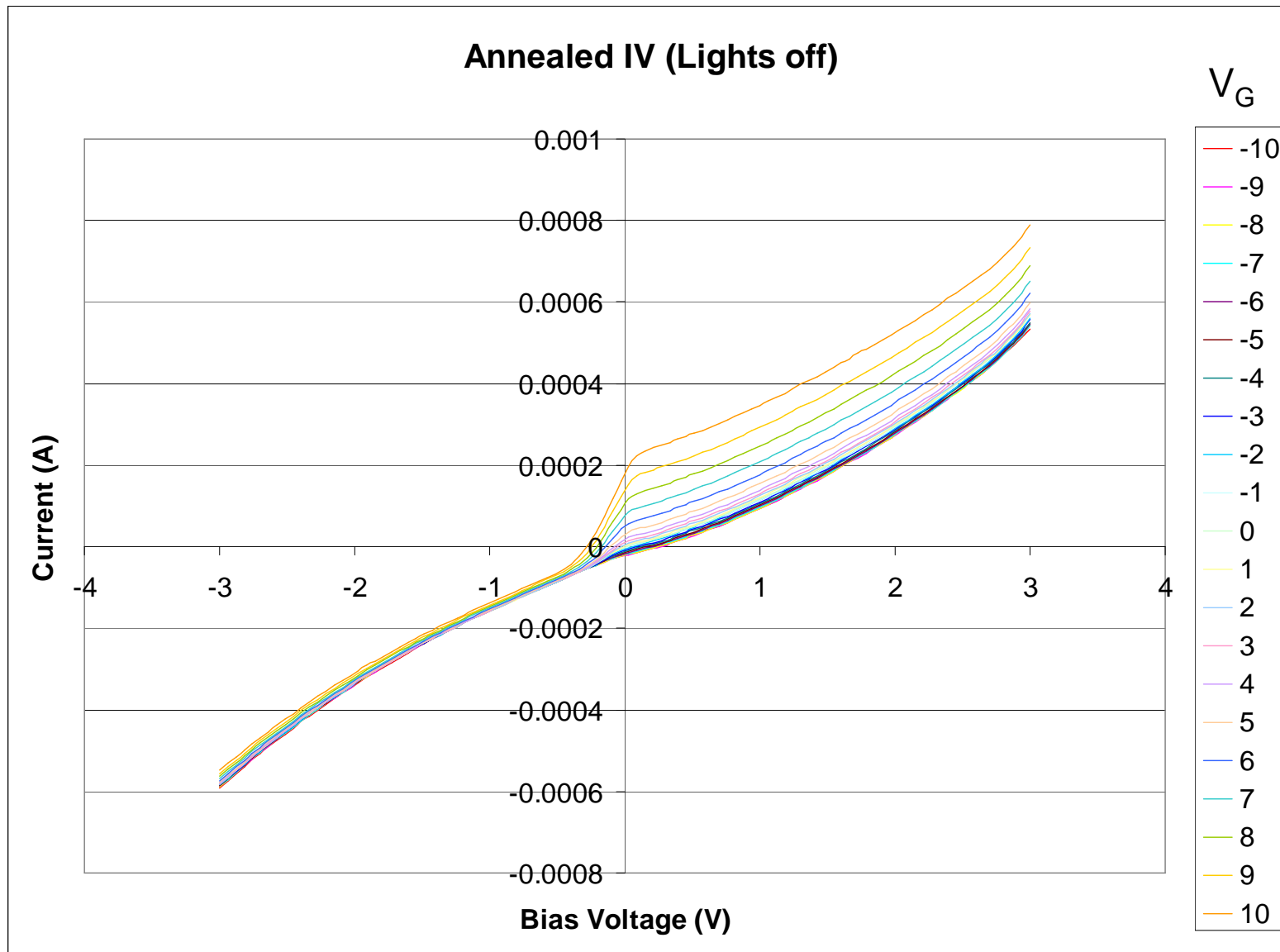
- How does a Gate control conduction in our SurFET?



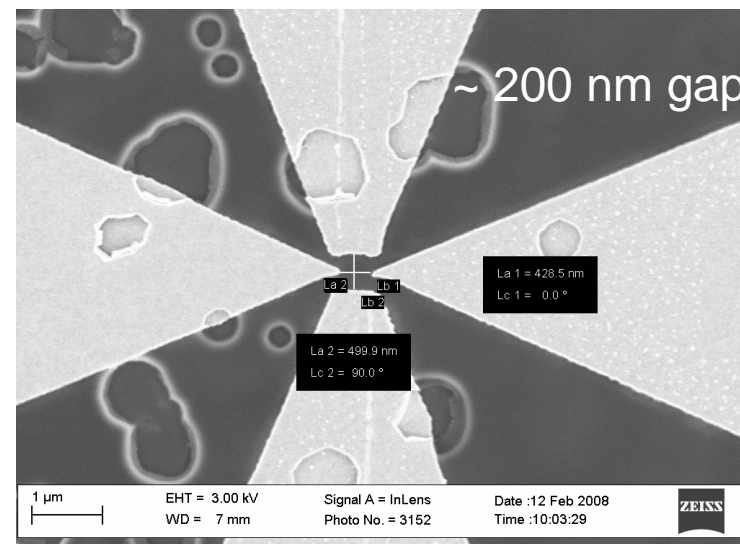
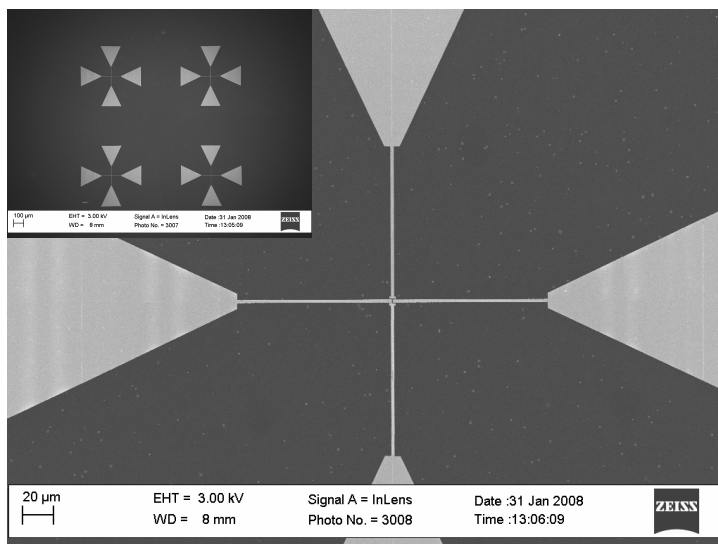
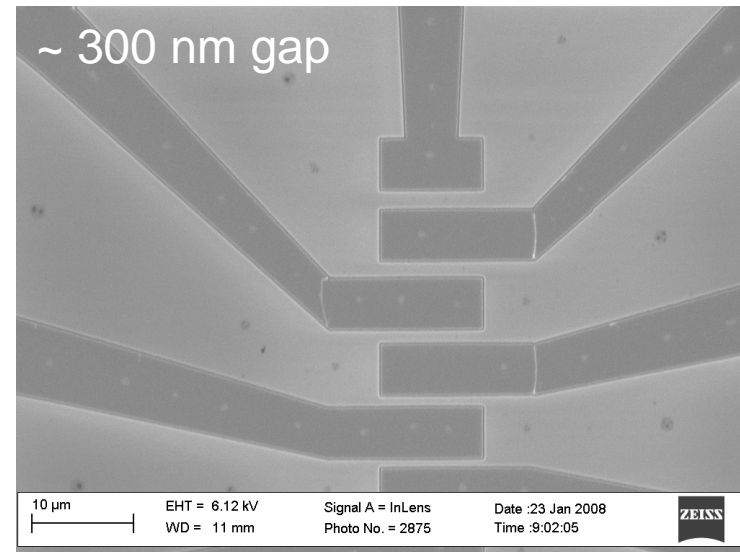
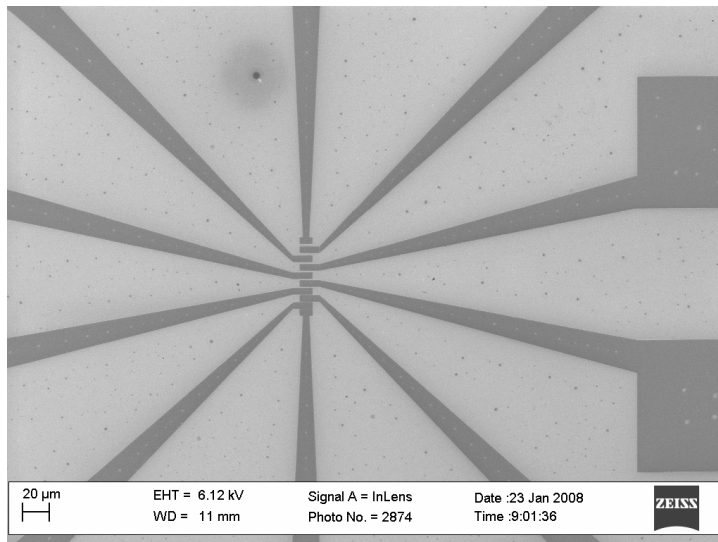
SurFET Design



SurFET Characteristics (RT)

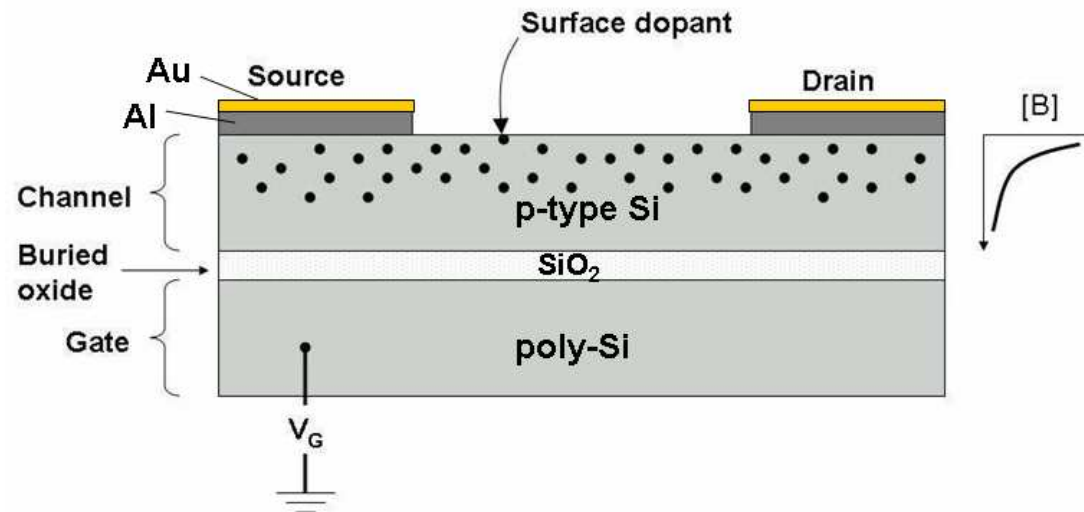


SurFET Designs (EBL)



SurFET Design for Fano Interference

- Surface doping (Boron complexes) and thermal annealing techniques produce a highly doped p-type silicon region
- The backgate pushes the carriers into a 2DEG-like state at the surface
- By controlling the carrier concentration via the backgate, one can tune the overlap between the 2DEG-like channel continuum and the dot-like adsorbate scatterers (discrete states)



Fano interference device using SurFET design



Fano Interference

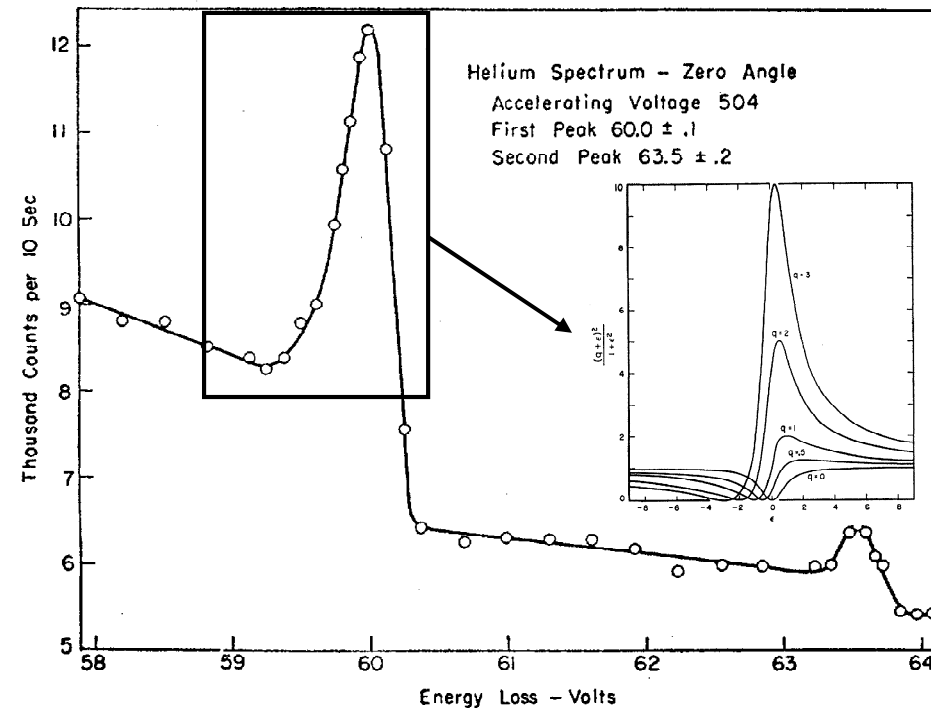
- Discovered by U. Fano in 1961 (EELS of He)
- The theory is extended to the interaction of one discrete level with two or more continua and of a set of discrete levels with one continuum

φ – discrete state

$\psi_{E'}$ – continuum of states

$$\Psi_E = a\varphi + \int dE' b_{E'}\psi_{E'}$$

$$\frac{|(\Psi_E | T | i)|^2}{|(\psi_E | T | i)|^2} = \frac{(q + \epsilon)^2}{1 + \epsilon^2}$$

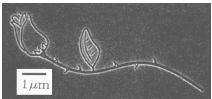
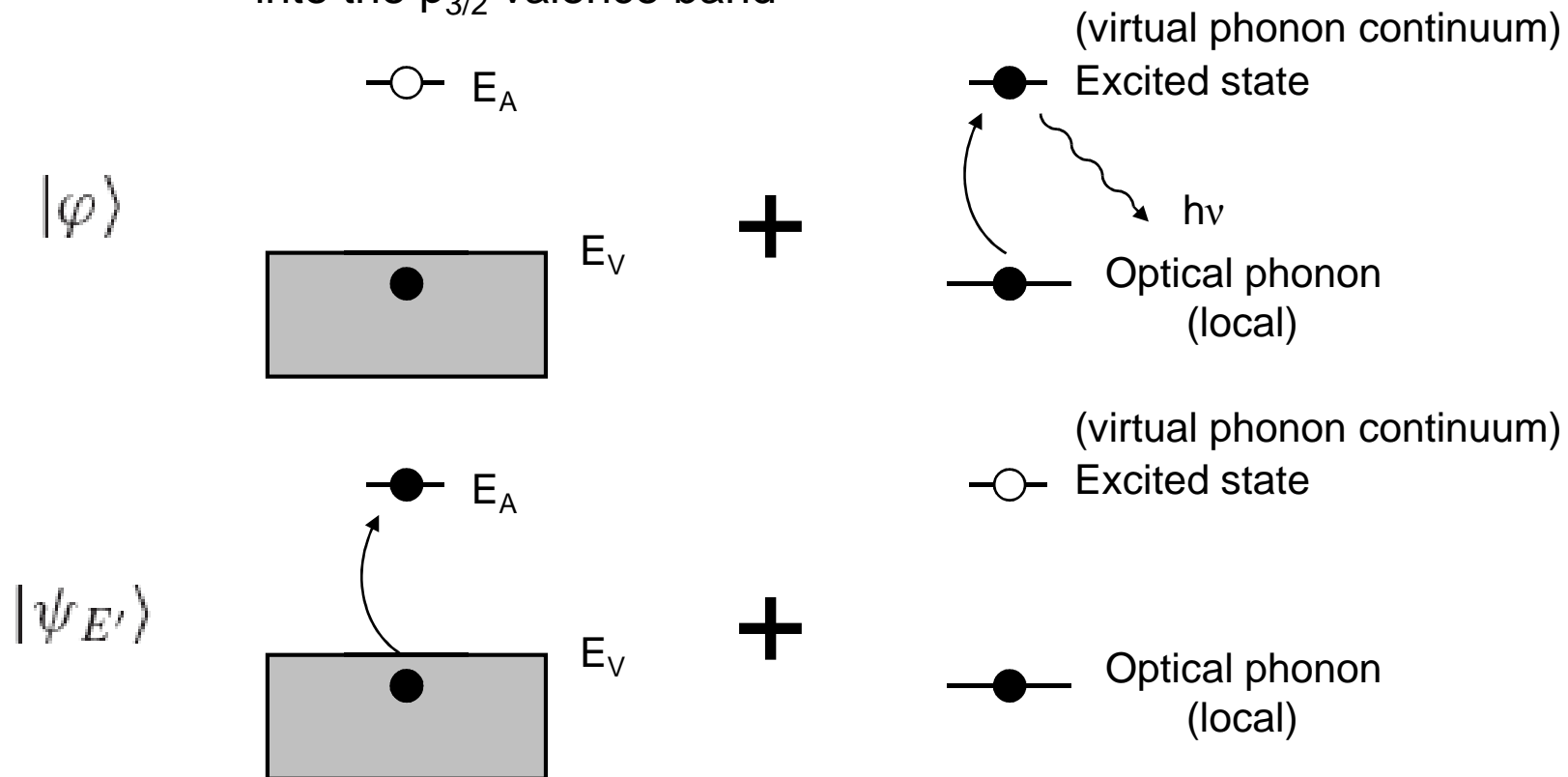


U. Fano, Phys. Rev. **124**, 1866 (1961)



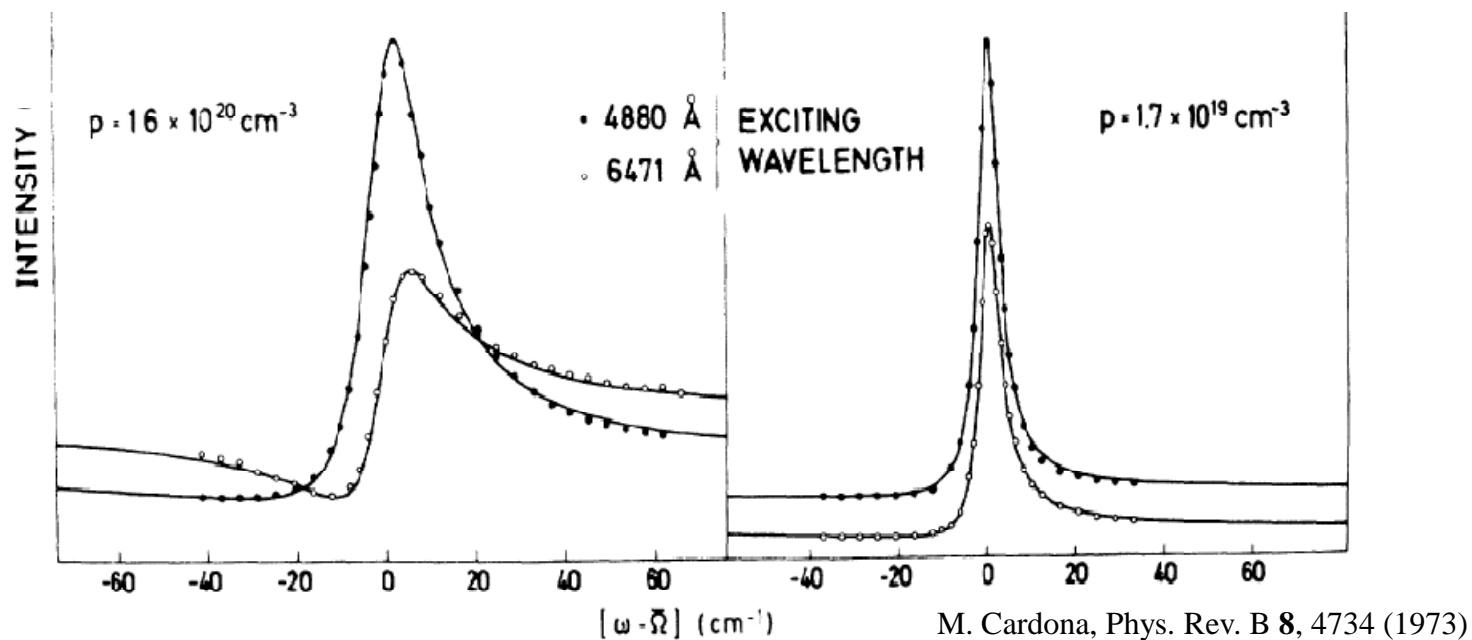
Fano Interference in Silicon

- The Fano effect in p-type silicon is associated with the resonant interaction of two states:
 - Discrete state, $|\varphi\rangle$, which represents the hole in its acceptor ground state (G) and one locally excited optical phonon
 - The state, $|\psi_{E'}\rangle$ with no phonons created and the hole excited into the $p_{3/2}$ valence band



Fano Interference in Silicon

- In p-type silicon, Fano resonances have been observed in photoconductivity and Raman spectroscopy experiments
- The asymmetry due to the zone center ($\mathbf{k} = 0$) optical phonon ($515\text{-}521\text{ cm}^{-1}$) changes as a function of temperature, exciting wavelength and doping concentration
- Interaction with only the hole continuum is due to the fact that shallow acceptor levels in Si are separated by energies comparable to phonons



Fano Fitting Parameters

$$I(\epsilon, q) = (q + \epsilon)^2 / (1 + \epsilon^2)$$

$$\epsilon = (\omega - \Omega - \delta\Omega) / \Gamma$$

- Γ is the squared matrix element of the coupling between the continuum and the discrete state (phonon self-energy), which depends on carrier concentration and not the excitation wavelength.

$$\hbar\Gamma = \frac{\pi}{4} \left(\frac{95}{78} \right) \frac{\hbar a}{M\Omega} d_0^2 \rho(\hbar\omega) (1 + n_B)$$

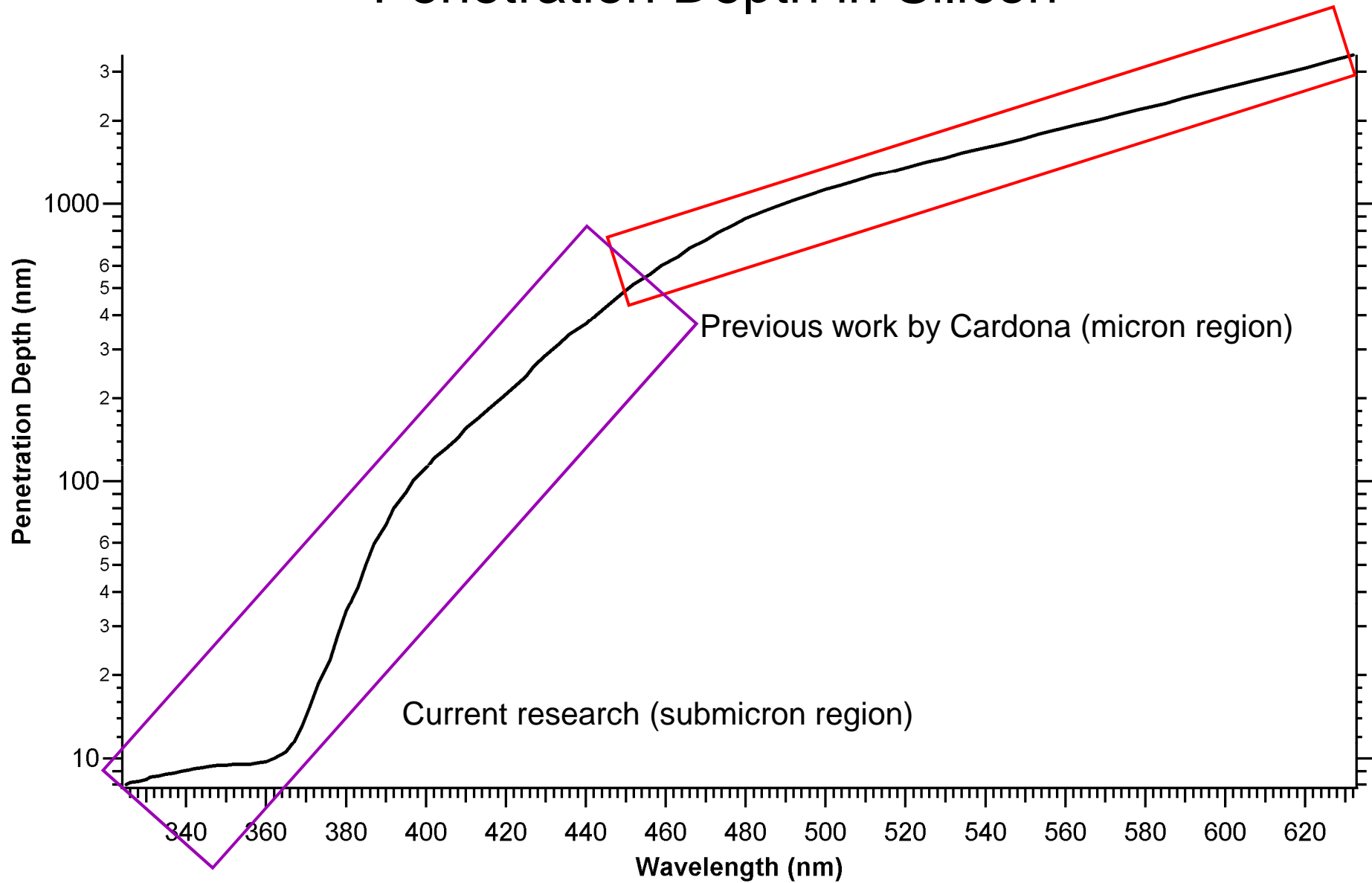
- q squared represents the ratio of the scattering probability of the discrete state to that of the continuum, which depends on both carrier concentration and the excitation wavelength (the two processes may have different frequency dependences).

$$\Gamma q^2 = \frac{1}{\pi} \frac{|\langle \Phi | T | i \rangle|^2}{|\langle \psi_E | T | i \rangle|^2} \propto |R_p / R_e|^2$$

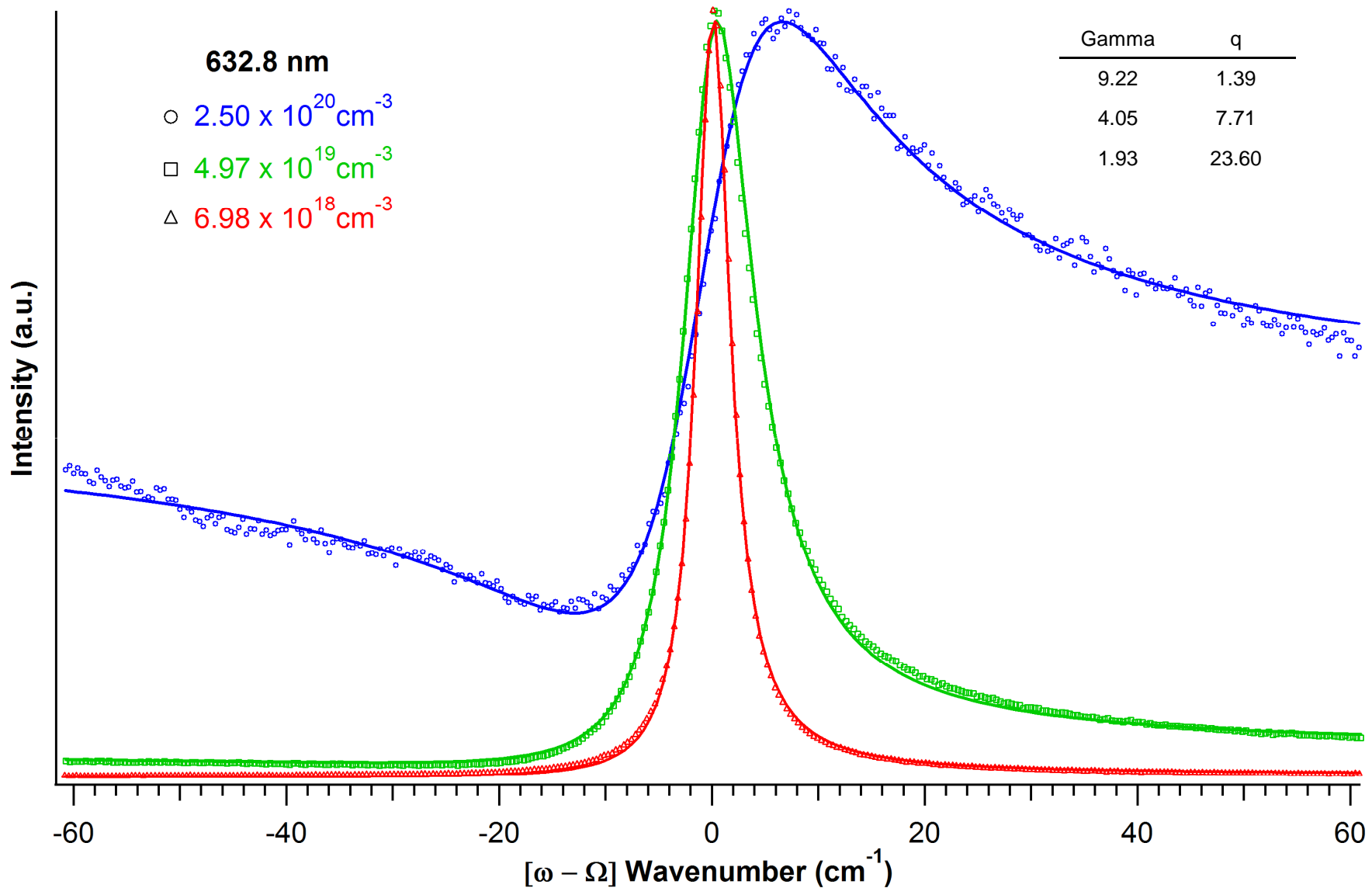
M. Cardona, Phys. Rev. B **8**, 4734 (1973)



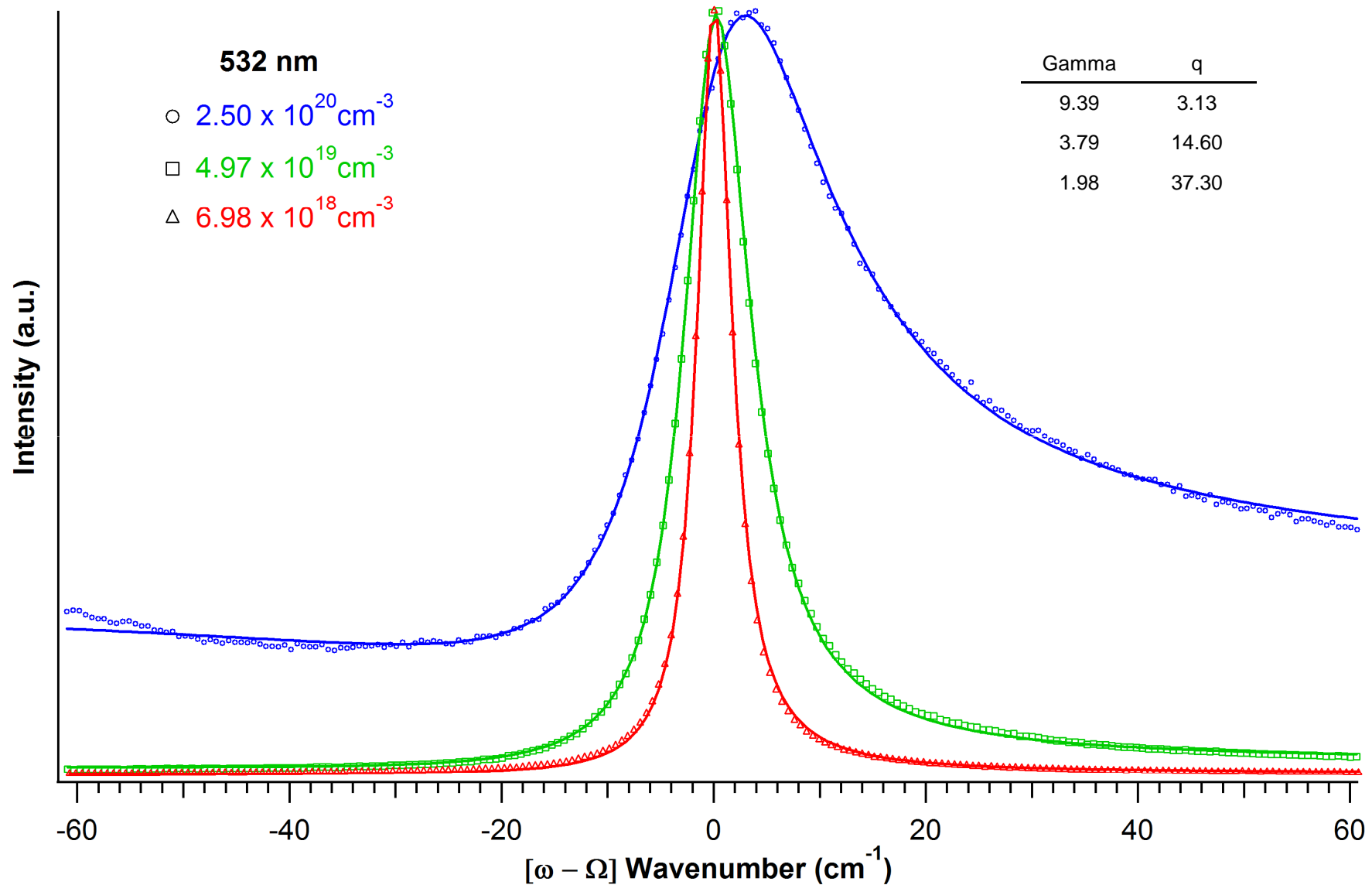
Penetration Depth in Silicon



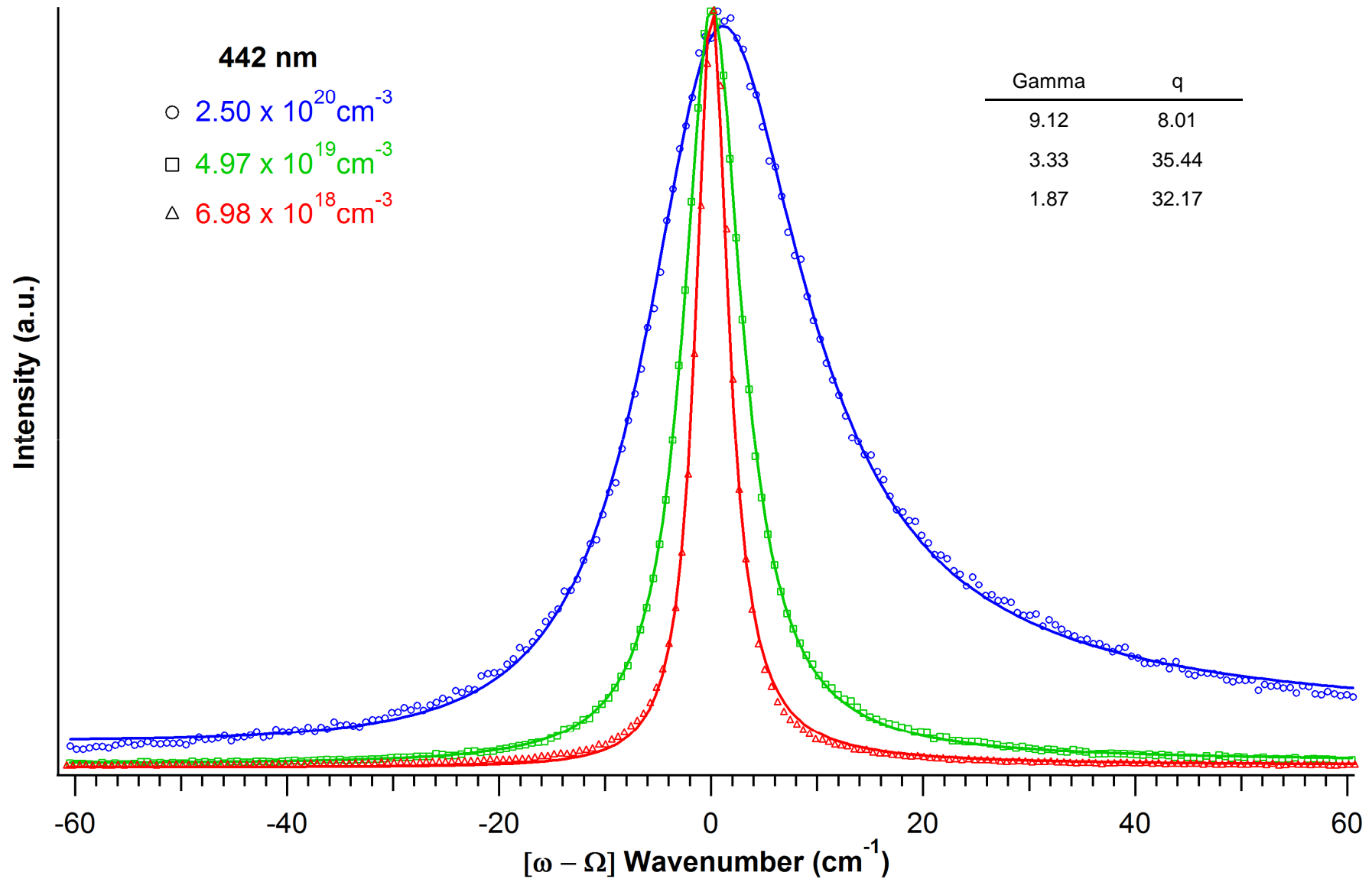
Comparison with Cardona's Work



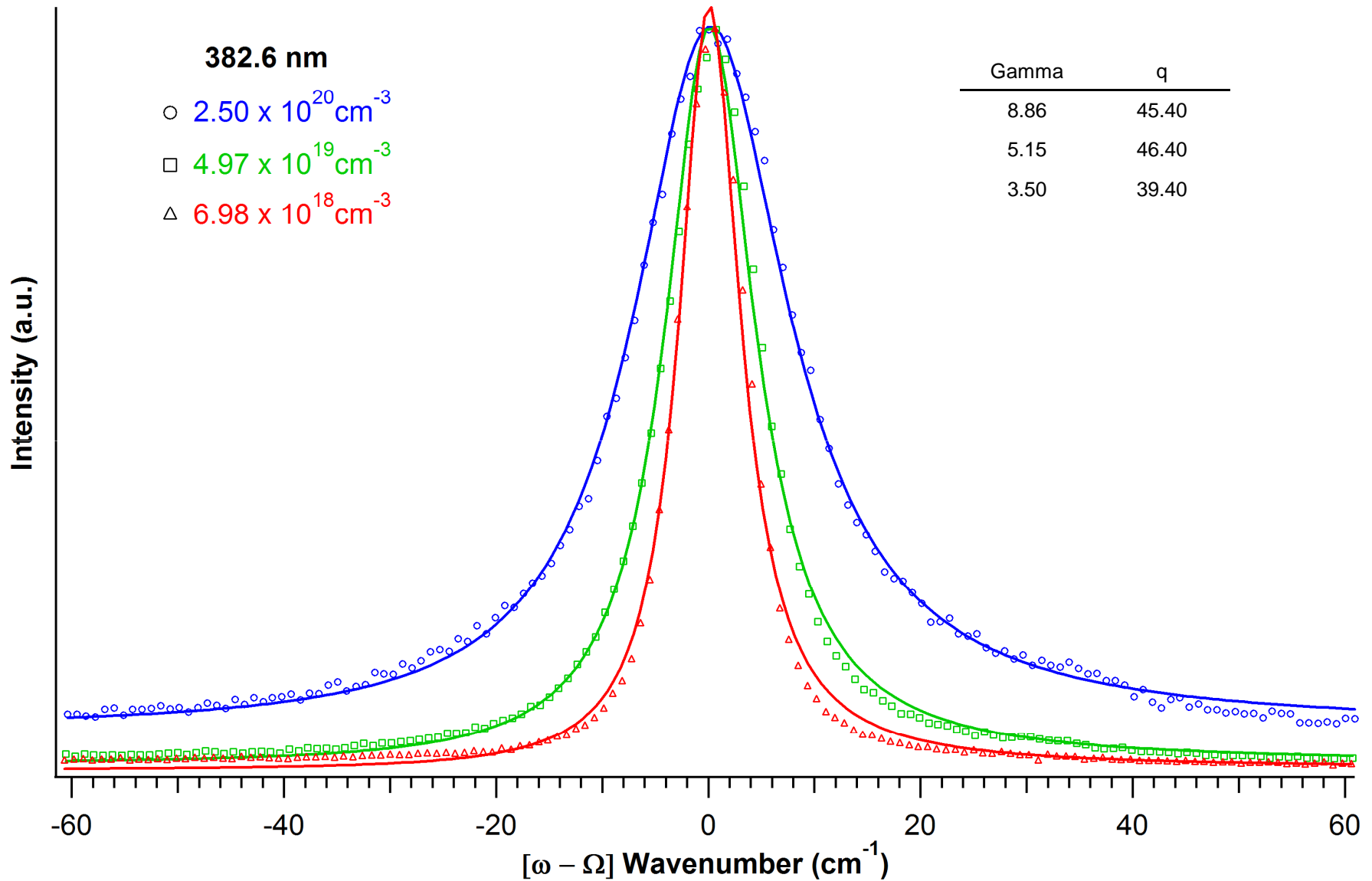
Comparison with Cardona's Work



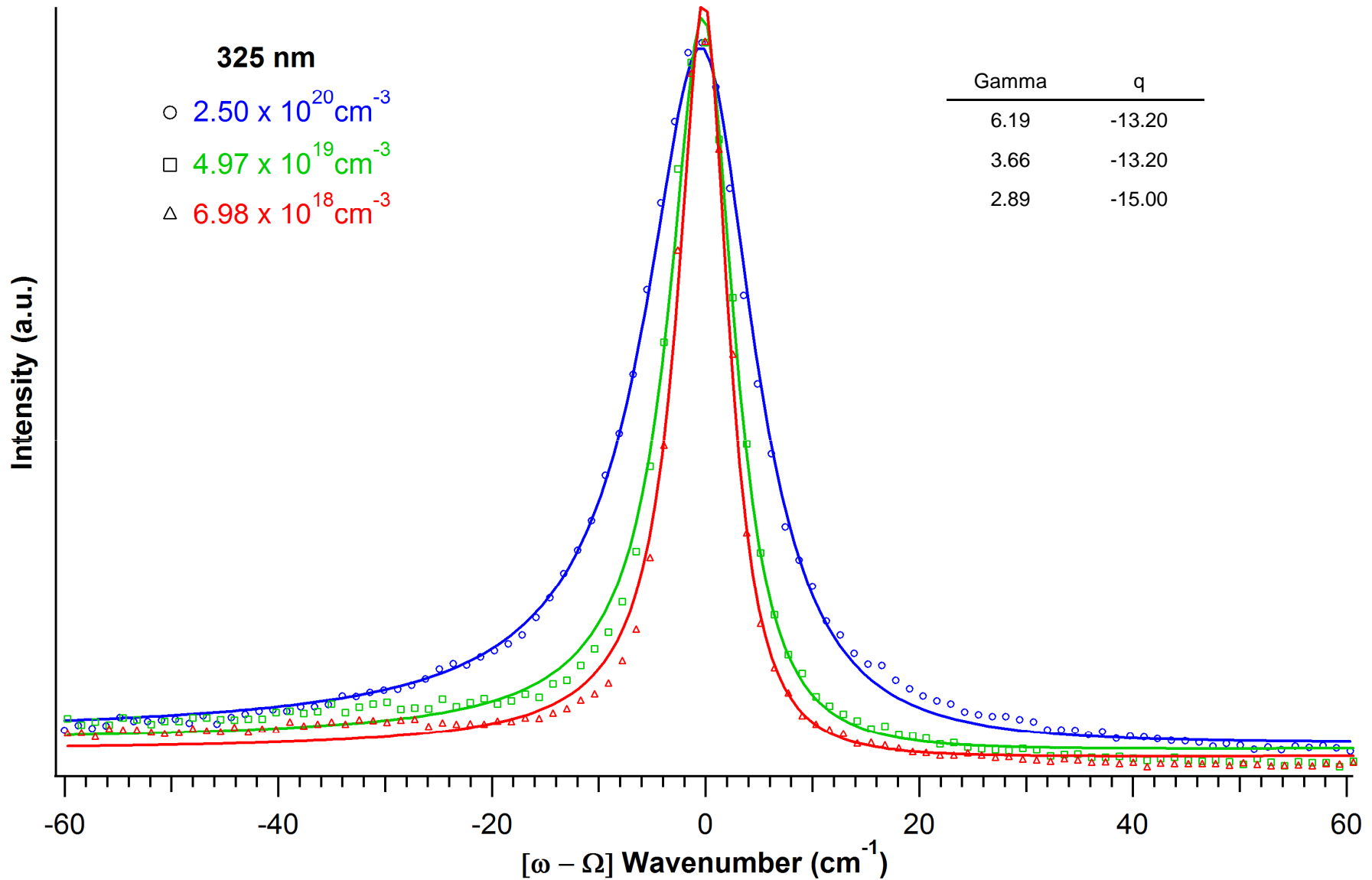
Extension of Cardona's Work



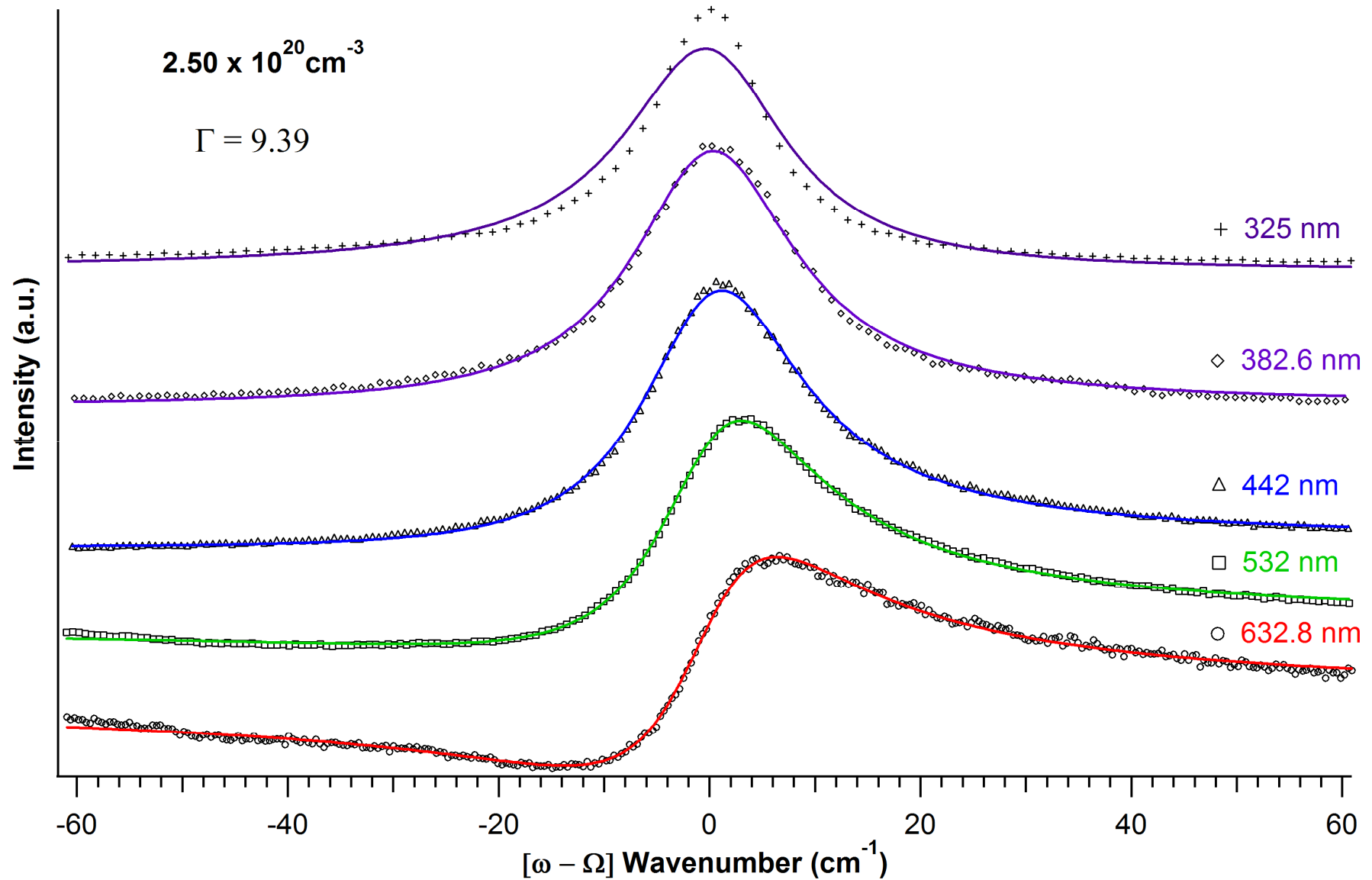
Extension of Cardona's Work



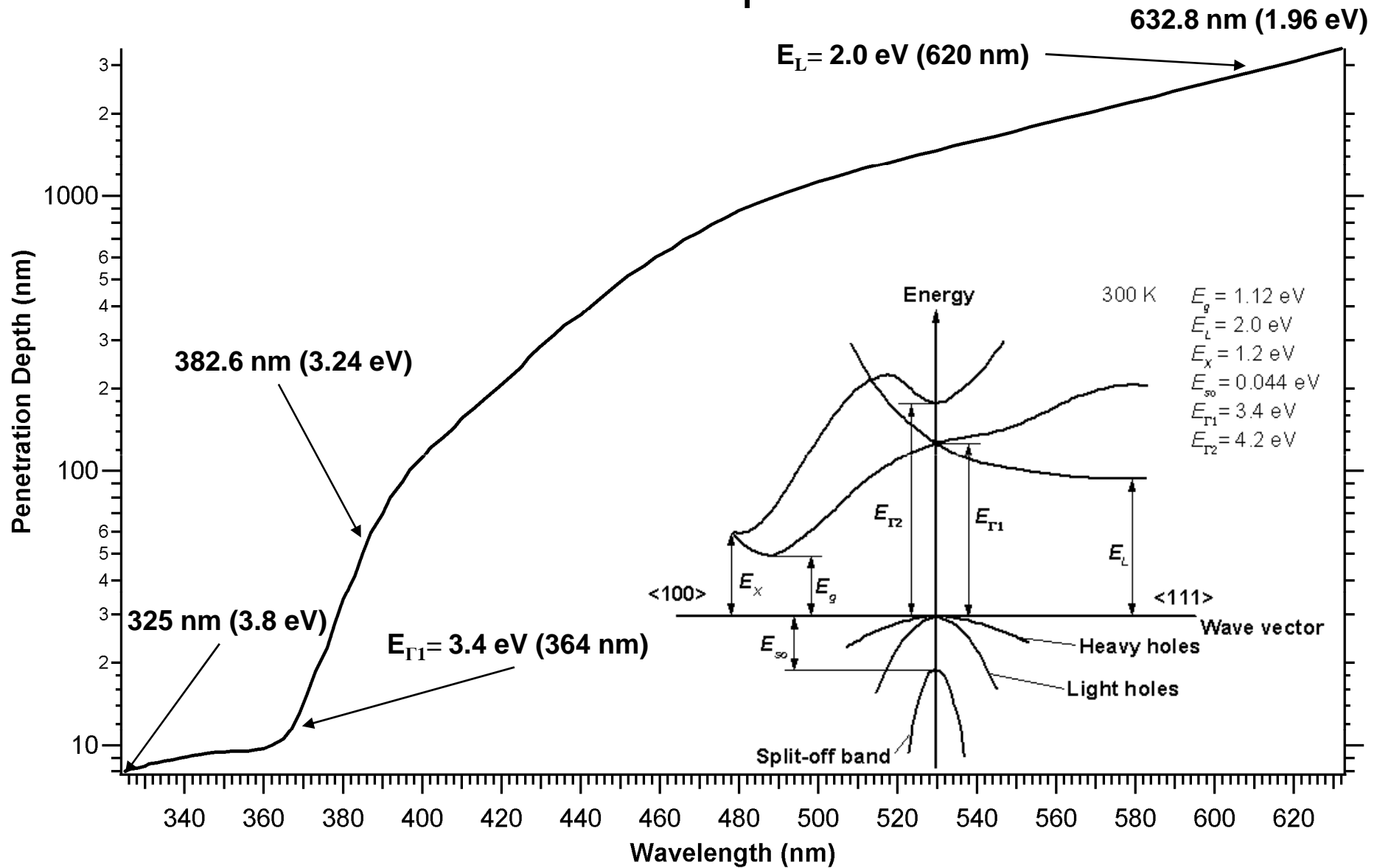
Extension of Cardona's Work



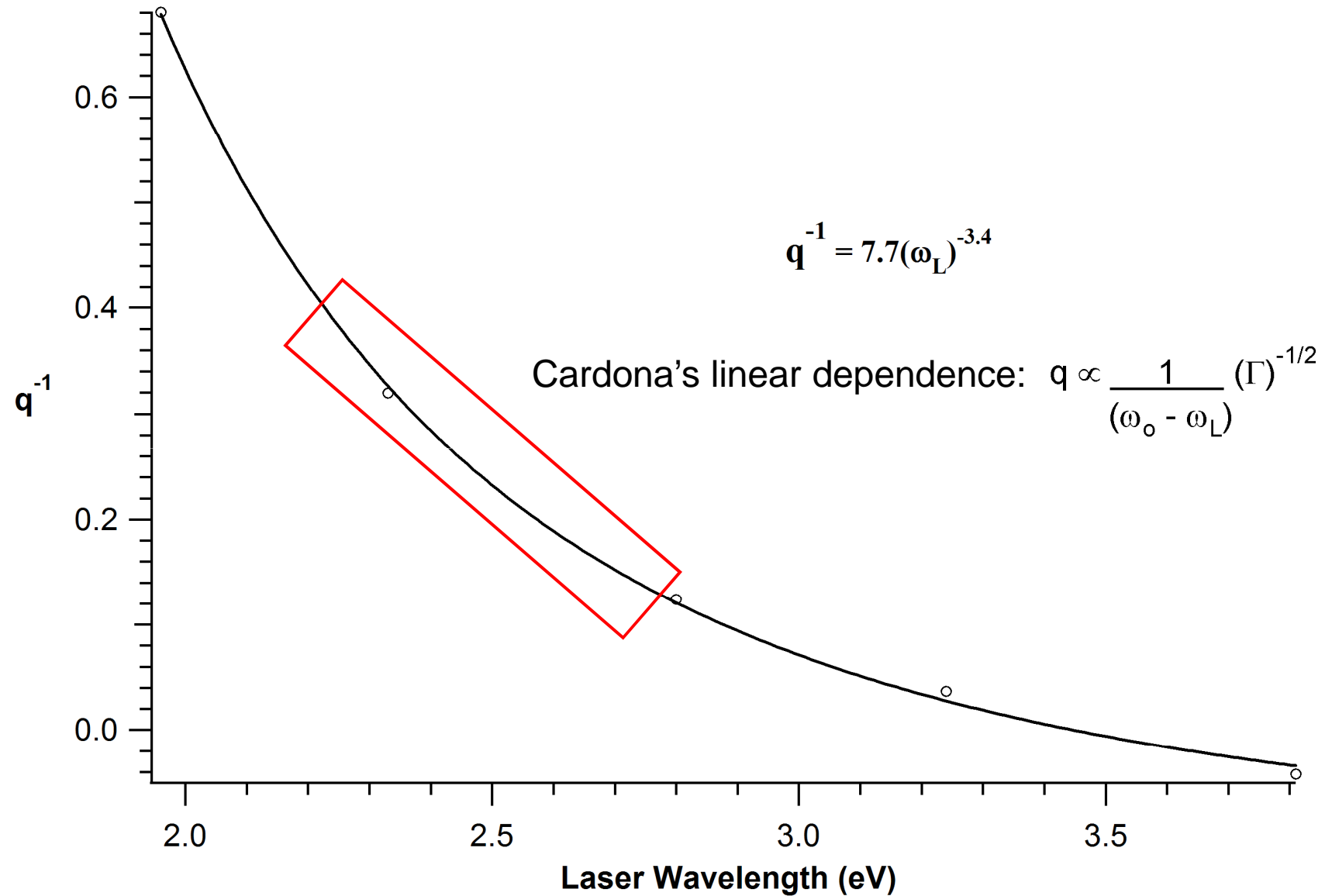
Fano Interference (Γ held constant)



Electronic Excitation Spectrum in Silicon

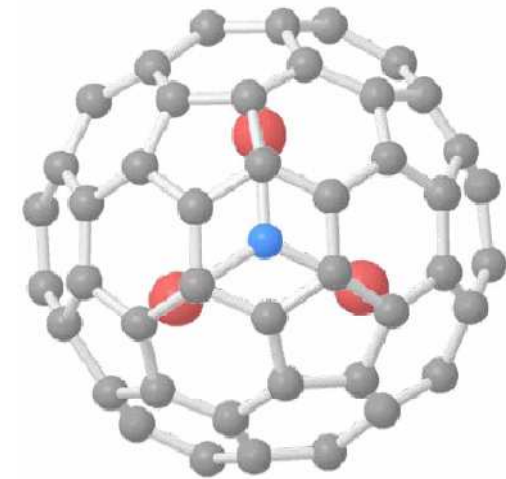
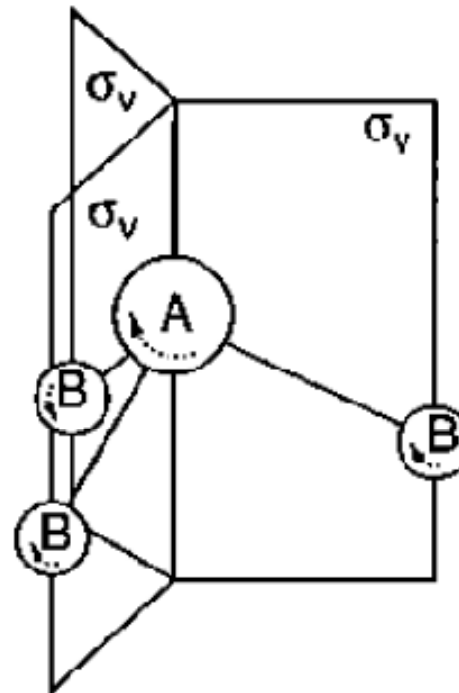
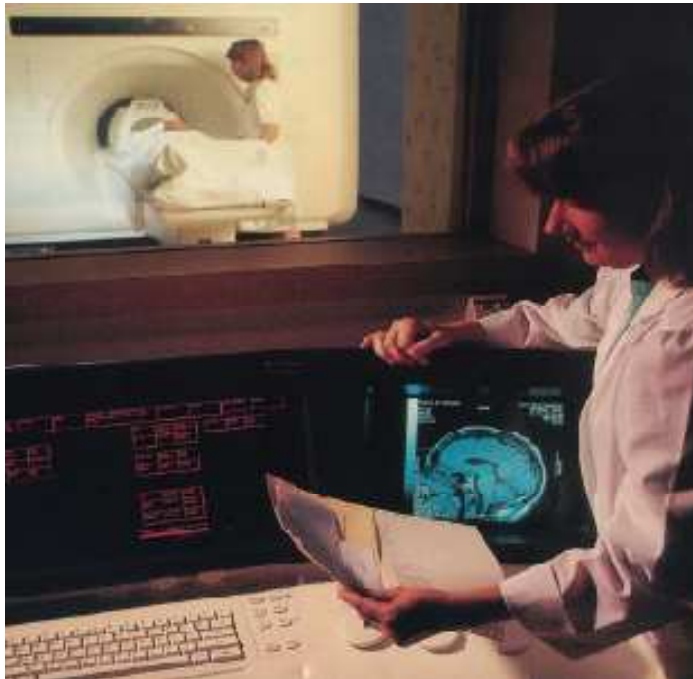


Parameter q Dependence on Wavelength



Research Motivation

- Encapsulated Metal Species
- Symmetries and Orientation of Endocomplex
- Medical Nanotechnology Applications (MRI Contrast Agent and Radiopharmaceuticals)
- Spin Logic Device

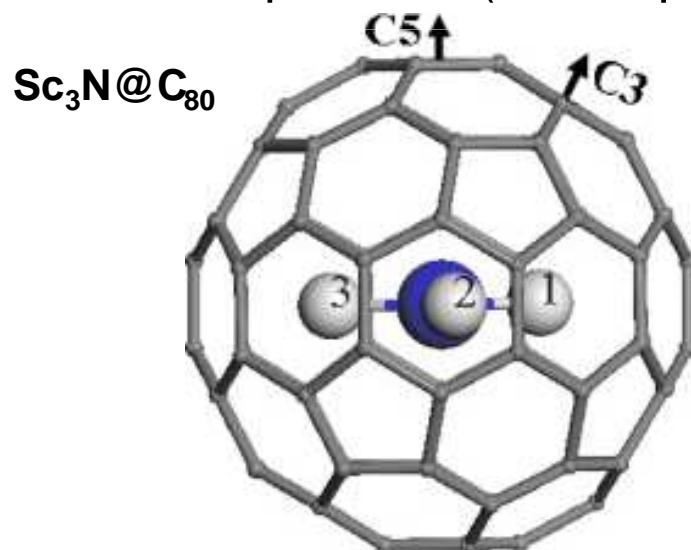


$\text{Gd}_3\text{N}@C_{80}$

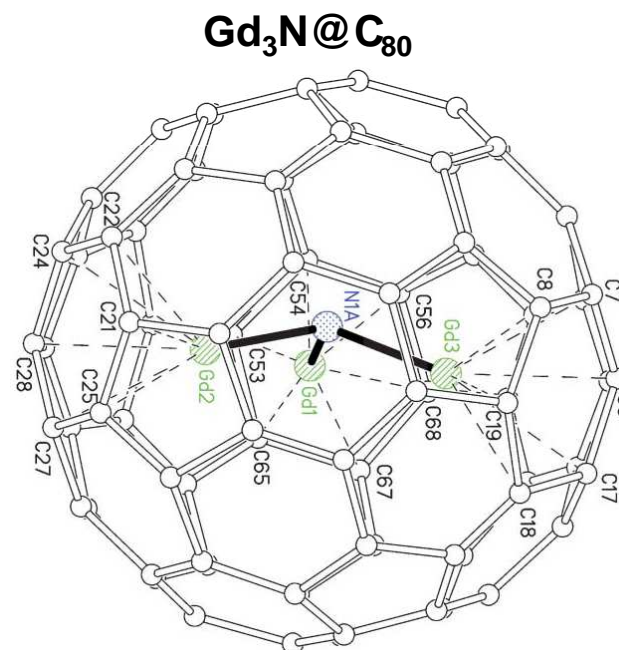


Optimizing $M_3N@C_{80}$ Geometry

- $M = Sc, Y$ and Lanthanides (Gd, Lu, La ...)
- No experimental data available for vibrational assignment of M_3N cluster modes or $I_h - C_{80}$ cage modes (only stable when combined)
- Some endocomplexes are planar ($Sc_3N@C_{80}$) and others are pyramidal ($Gd_3N@C_{80}$) determined by X-ray diffraction
- $Sc_3N@C_{80}$ is found to freely rotate at room temperature (NMR spectrum)



Y. Zhu *et al*, *Chem. Phys. Lett.* **461**, 285 (2008)

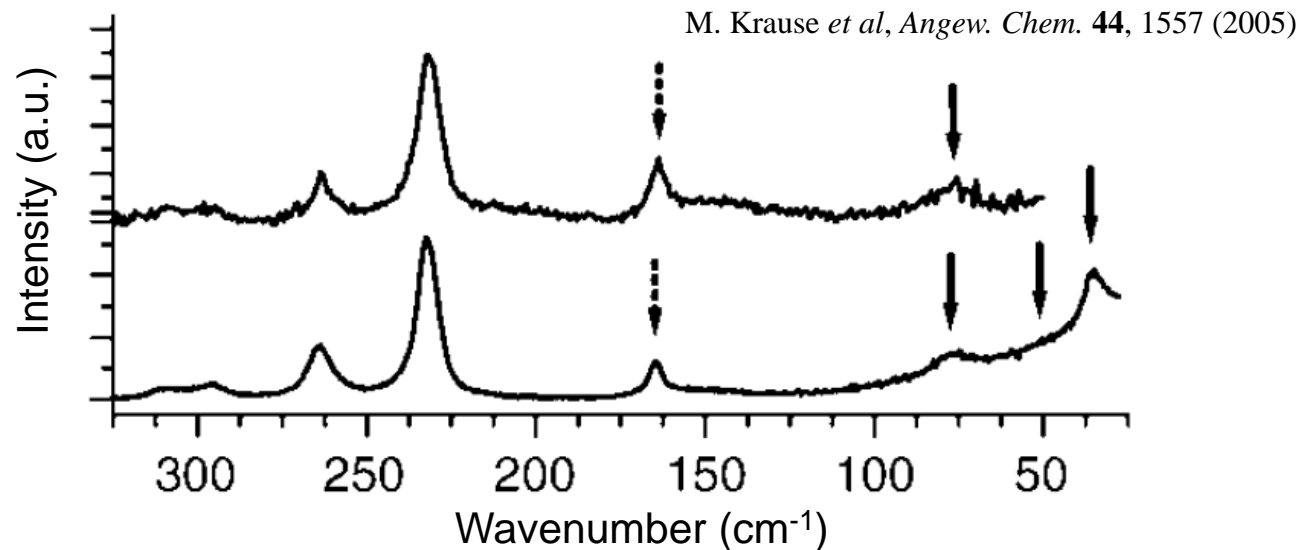
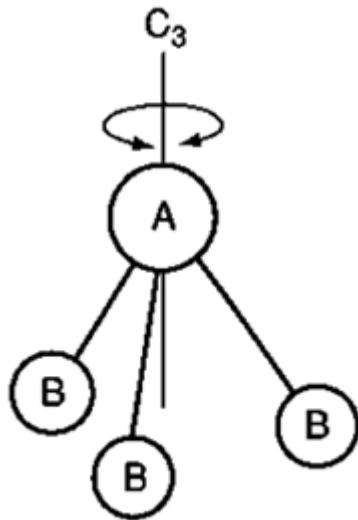


S. Stevenson *et al*, *Chem. Commun.* **2004**, 2814

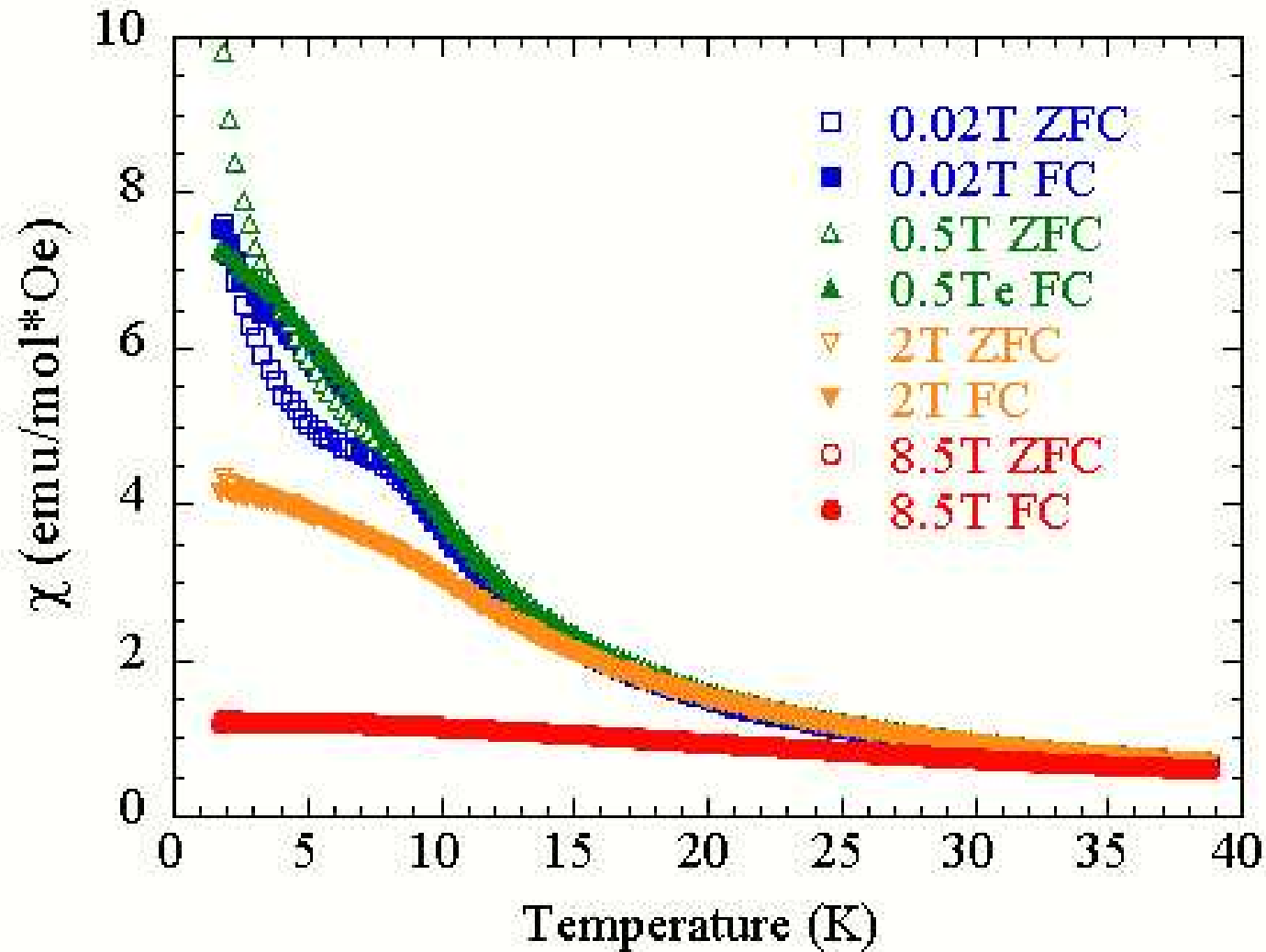


Investigation of $\text{Gd}_3\text{N}@C_{80}$

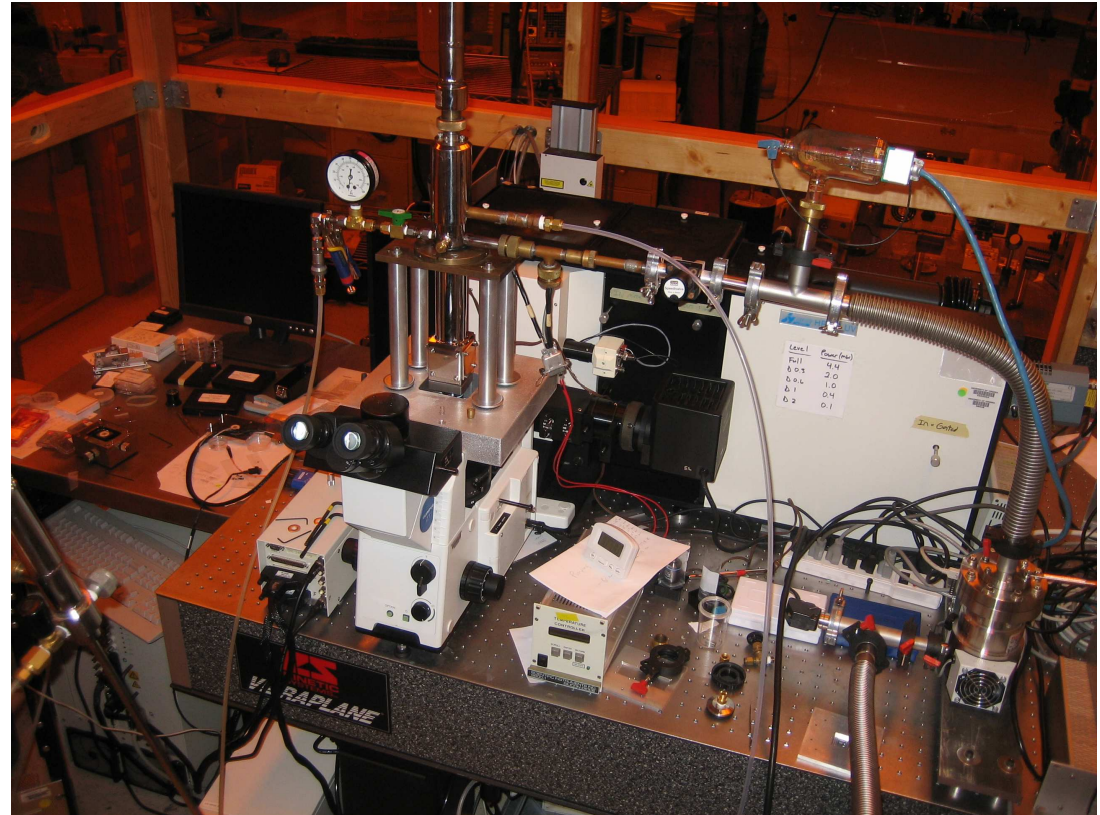
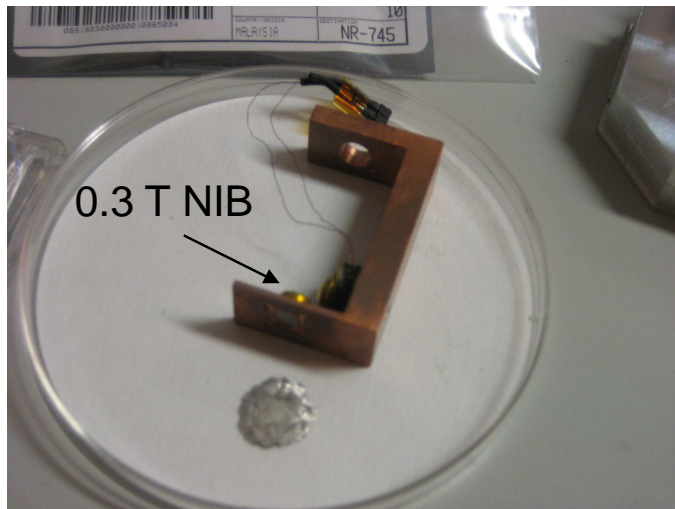
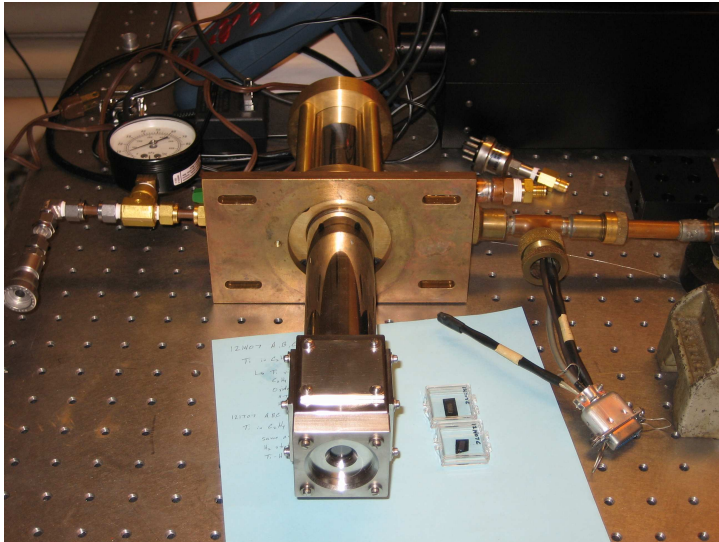
- Is the Gd_3N cluster rotating freely inside C_{80} ?
 - Raman spectra of $\text{Gd}_3\text{N}@C_{80}$ show peaks below 100 cm^{-1} , which are absent in smaller/lighter clusters ($\text{Sc}_3\text{N}@C_{80}$ and $\text{Y}_3\text{N}@C_{80}$)
 - Temperature dependent measurements (4 – 400 K)
- Does the cluster form a chemical bond and is there a particular bonding site?
 - Raman data suggests a hindered rotation inside the cage
 - Recent DFT studies determined the lowest energy to be with C_3 symmetry and Gd atoms centered over hexagons



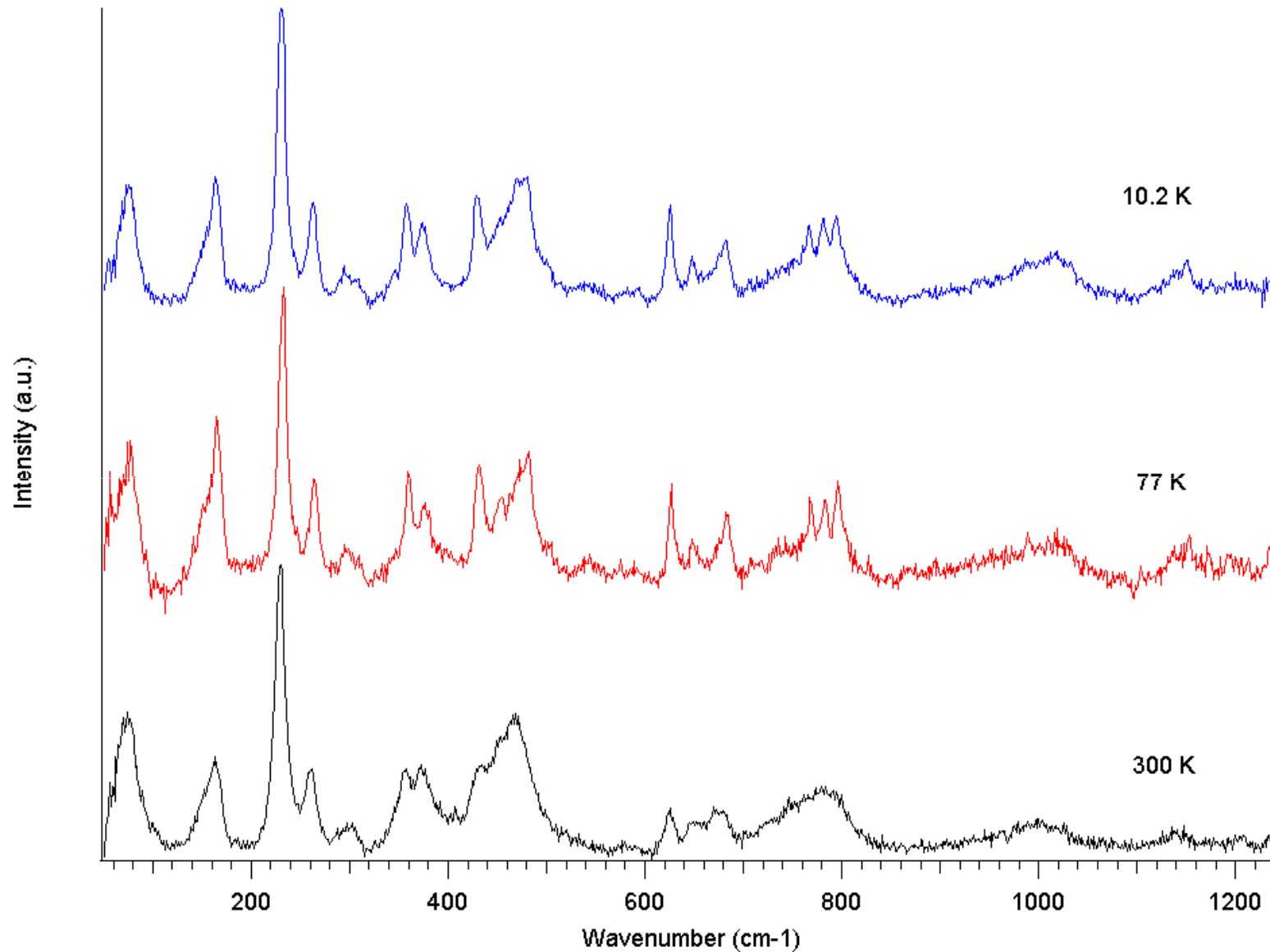
Convincing Data of Inflection Point (Gd₃N@C₈₀)



Modified Optical Cryostat (10.2 – 300 K)



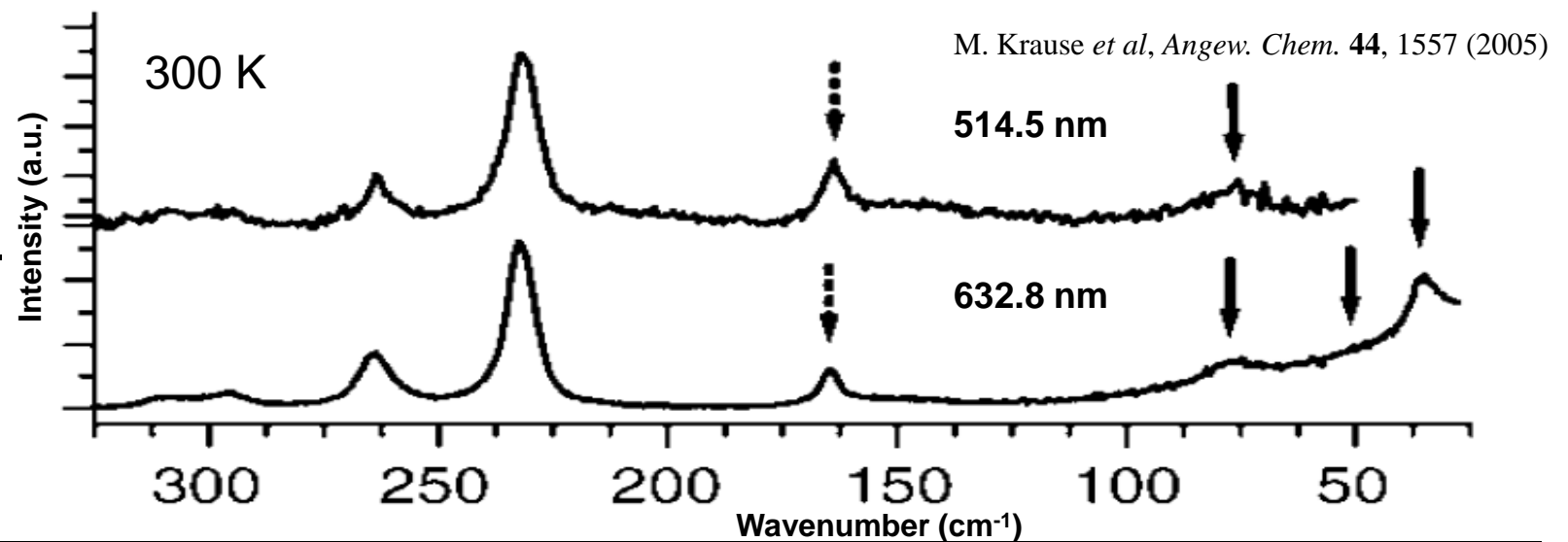
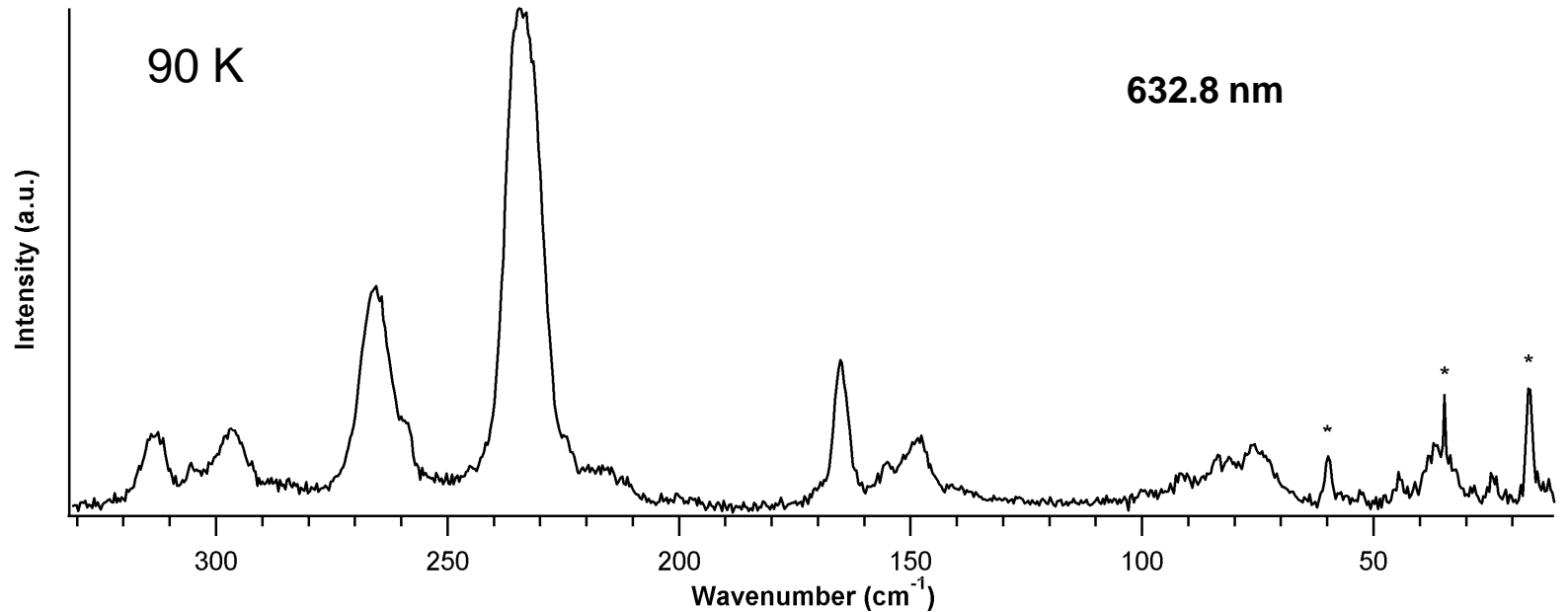
Initial Raman Data of $\text{Gd}_3\text{N}@C_{80}$



Gd₃N@C₈₀ (cm⁻¹)

Raman Spectra of Gd₃N@C₈₀ (CNMS)

- 165.2
- 155
- 148.4
- 141.4
- 100
- 91.5
- 83.6
- 81.2
- 76
- 57
- 52.6
- 44.6
- 36.4
- 35
- 28.2
- 24.6



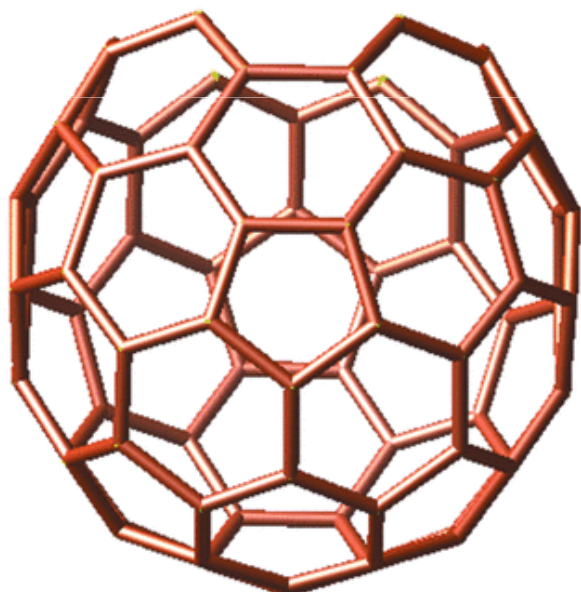
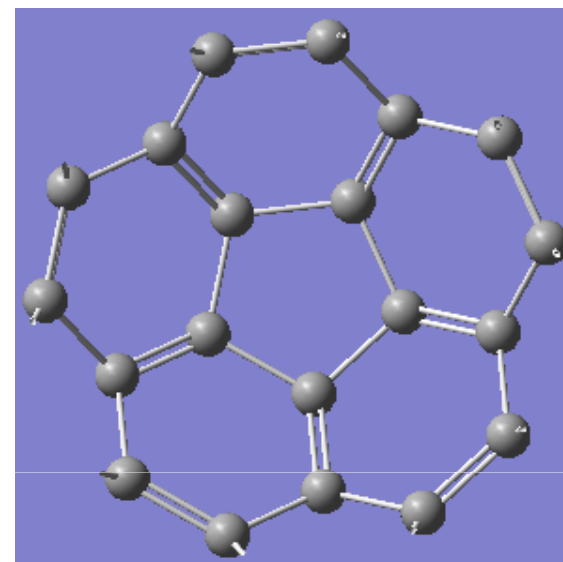
Gd₃N@C₈₀ (cm⁻¹)

- 165
- 77
- 54
- 34



C₈₀ Geometry (I_h symmetry)

- C₈₀ cage consists of 12 pentagons and 30 hexagons (Euler's polyhedron formula)
- Two types of C–C bonds exist
- 6:6 ring bonds (between hexagons) are double bonds and are shorter than the 6:5 ring bonds (between pentagon and hexagon)



I_h – C₈₀

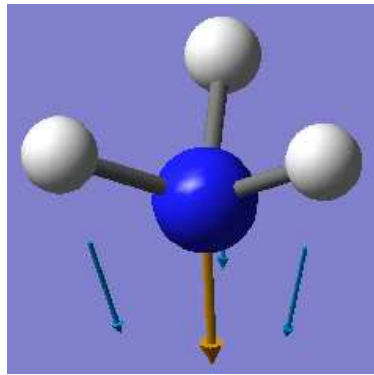
$$\Gamma_{\text{vib}, I_h - C_{80}} = 3A_g(\text{Ra}) + 1A_u + 4F_{1g} + 6F_{1u}(\text{IR}) + 5F_{2g} + 7F_{2u} + 8G_g + 8G_u + 11H_g(\text{Ra}) + 9H_u$$

- 62 normal modes
- 6 are IR active and 14 are Raman active

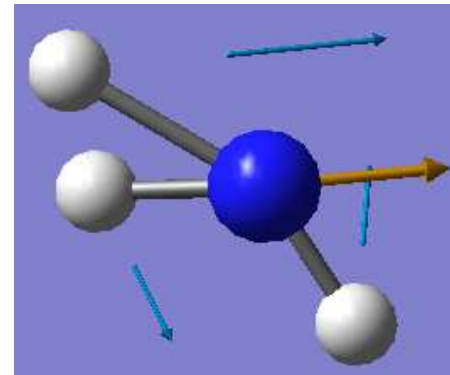
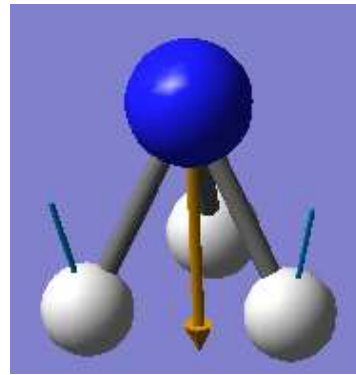
K. Krause *et al.*, *J. Chem. Phys.* **115**, 6596 (2001)



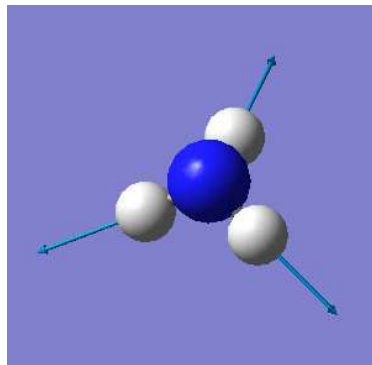
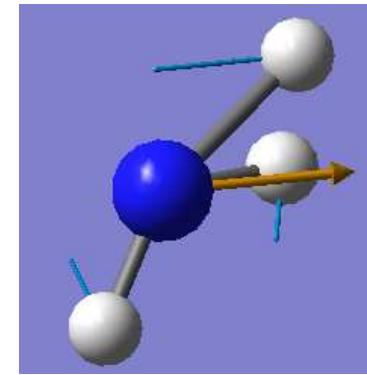
Ammonia (NH₃) Calculation



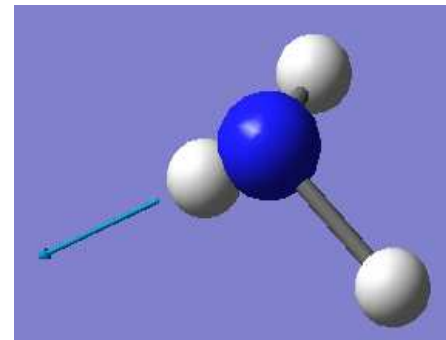
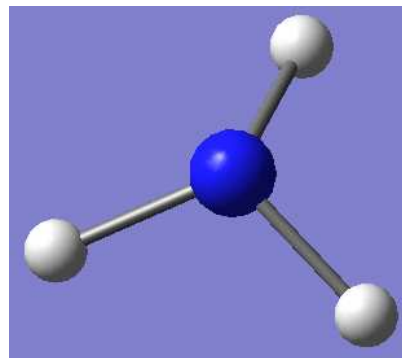
N-H Wagging mode 780 cm⁻¹
(1139 cm⁻¹)



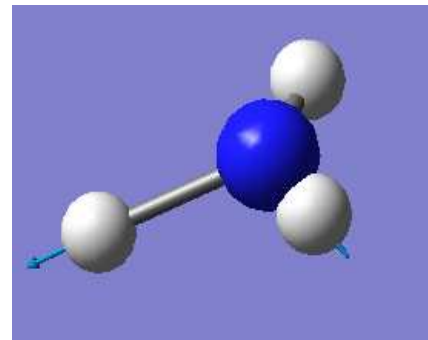
H-N-H Scissoring mode 1747 cm⁻¹
degenerate (1765 cm⁻¹)



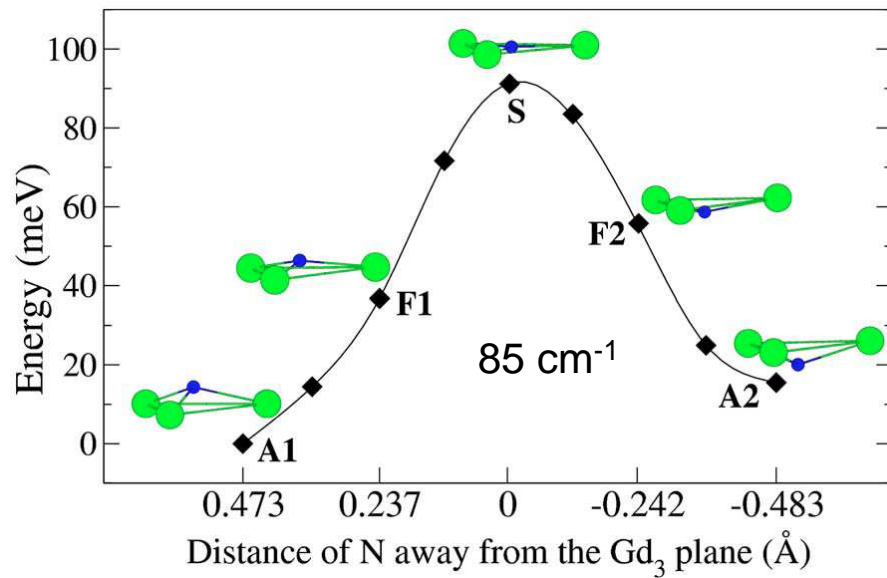
N-H Symmetric stretch 3384.5 cm⁻¹
(3464 cm⁻¹)



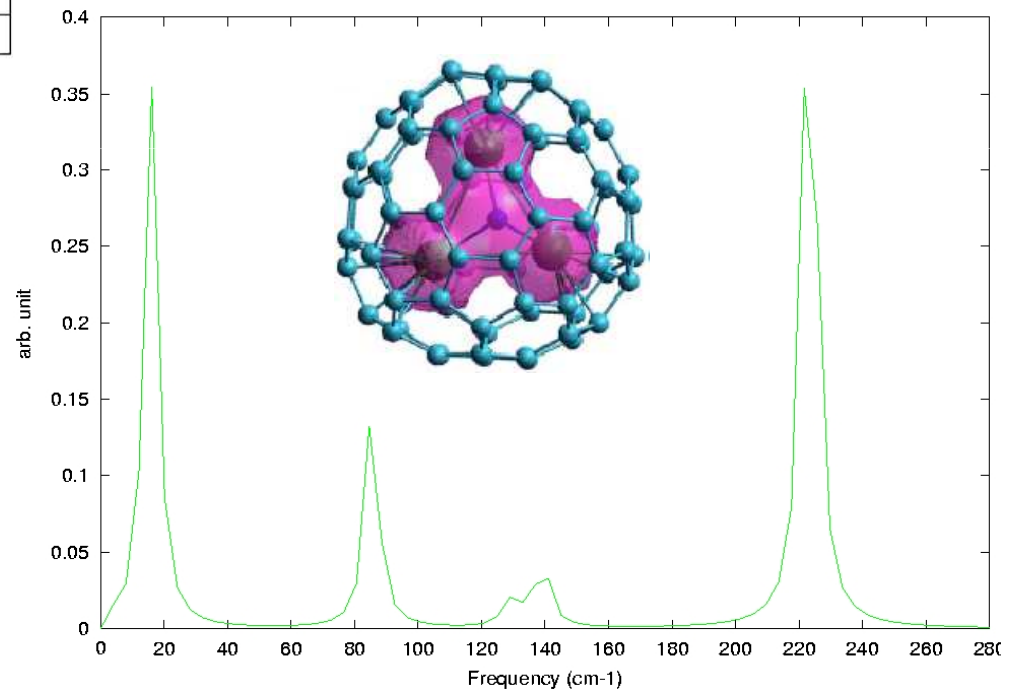
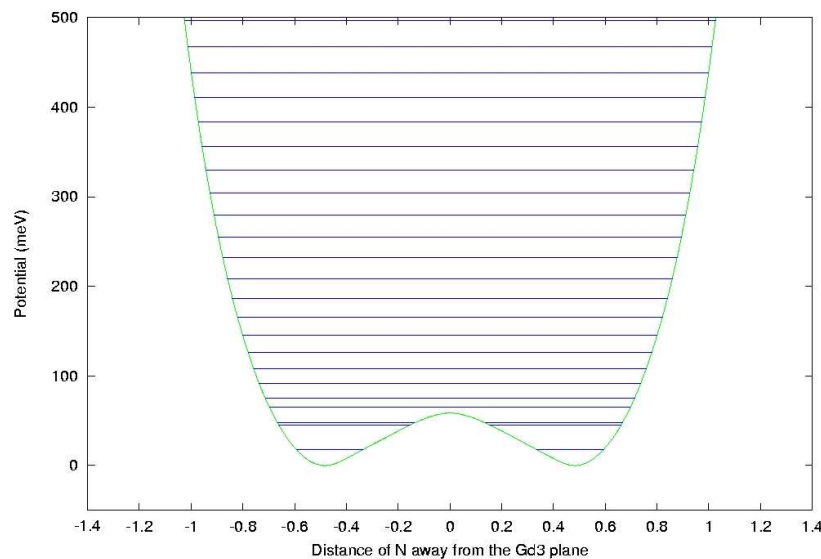
N-H Asymmetric stretch 3536 cm⁻¹
degenerate (3534 cm⁻¹)



Gd₃N@C₈₀ Calculation (VCU)



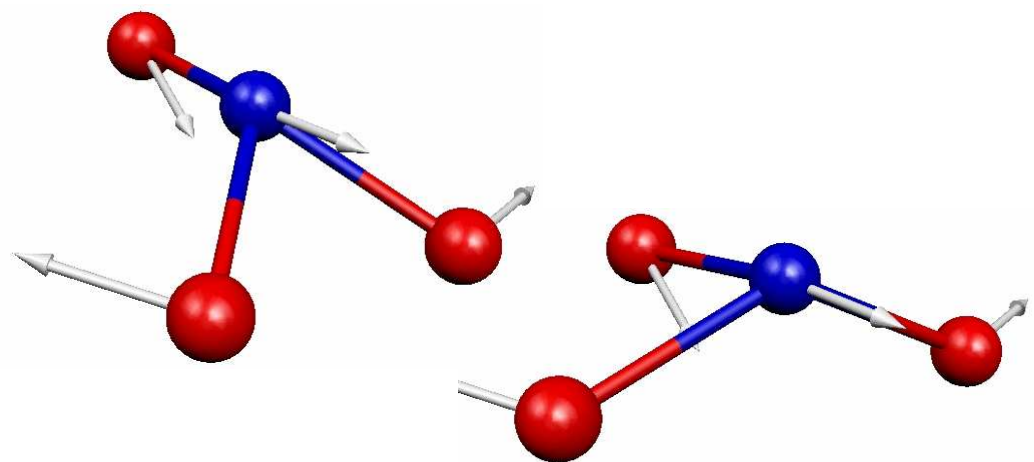
- Double-potential well used to model N wagging mode (VASP, DFT)
- To properly treat Gd f states, a LDA + U method was adopted
- Able to plot Raman intensities and frequencies



M. Qian *et al.*, *Phys. Rev. B* **75**, 104424 (2007)

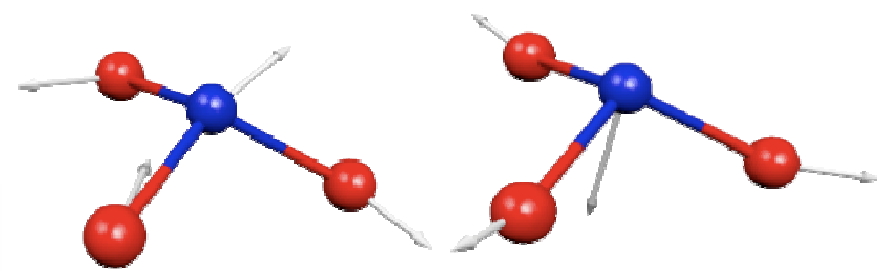
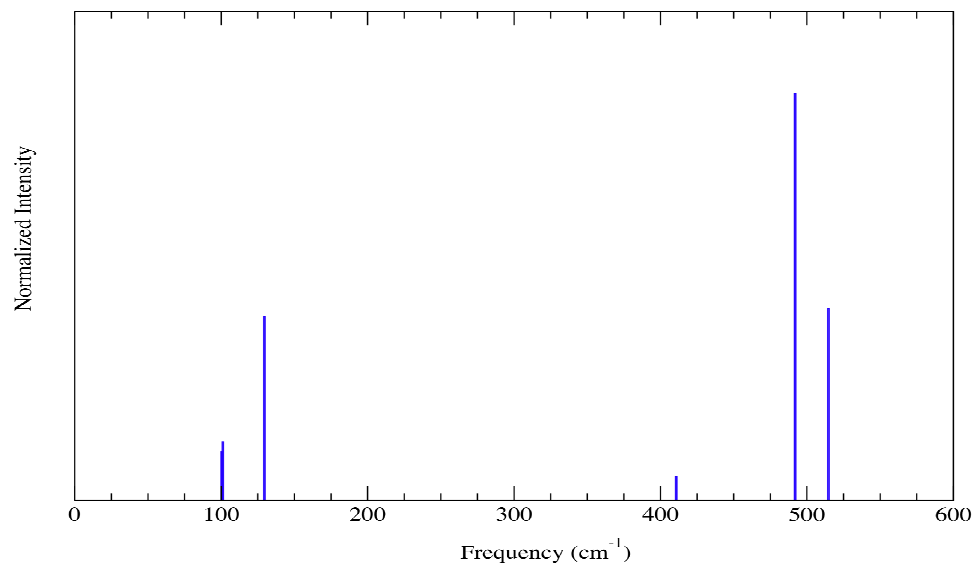


Gd₃N Calculation (VCU)



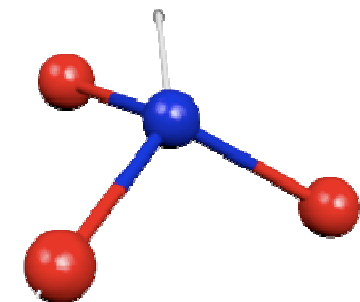
100.4 cm⁻¹

Gd₃N Raman Modes

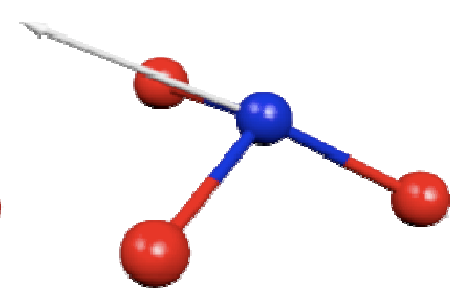


101.1 cm⁻¹

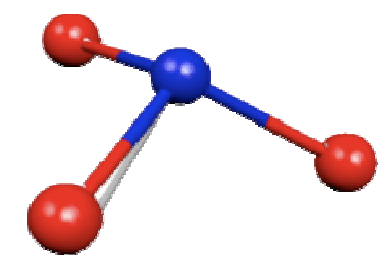
129.6 cm⁻¹



491.9 cm⁻¹



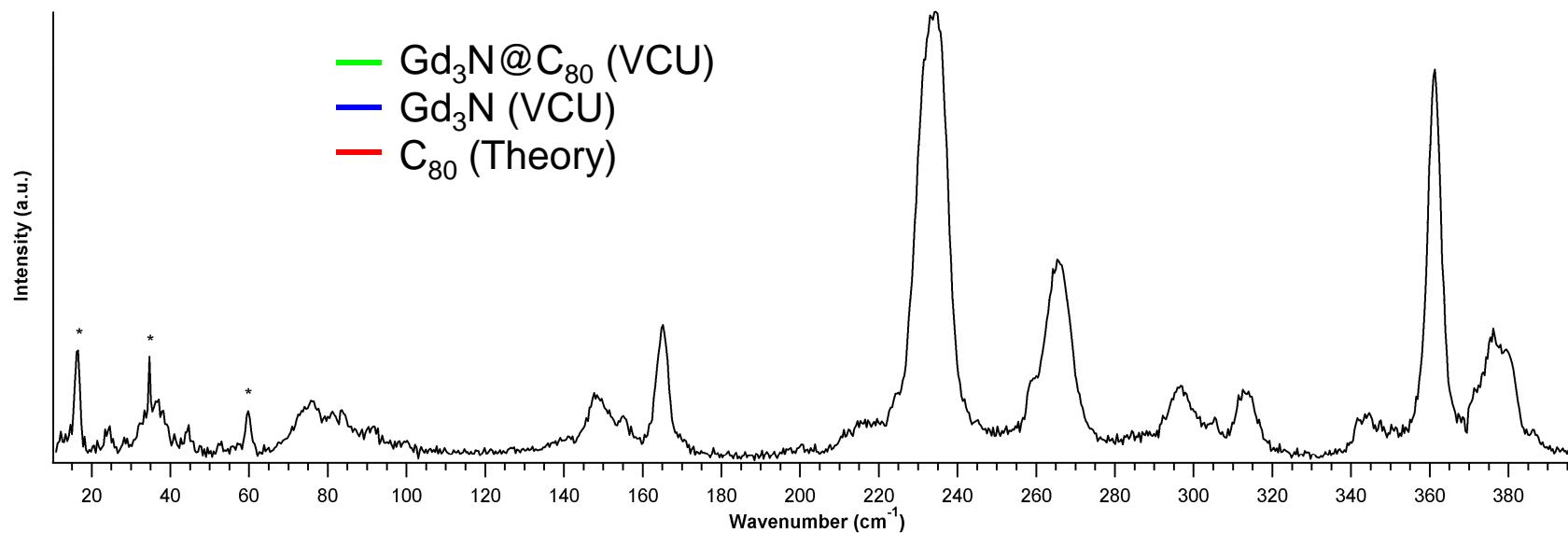
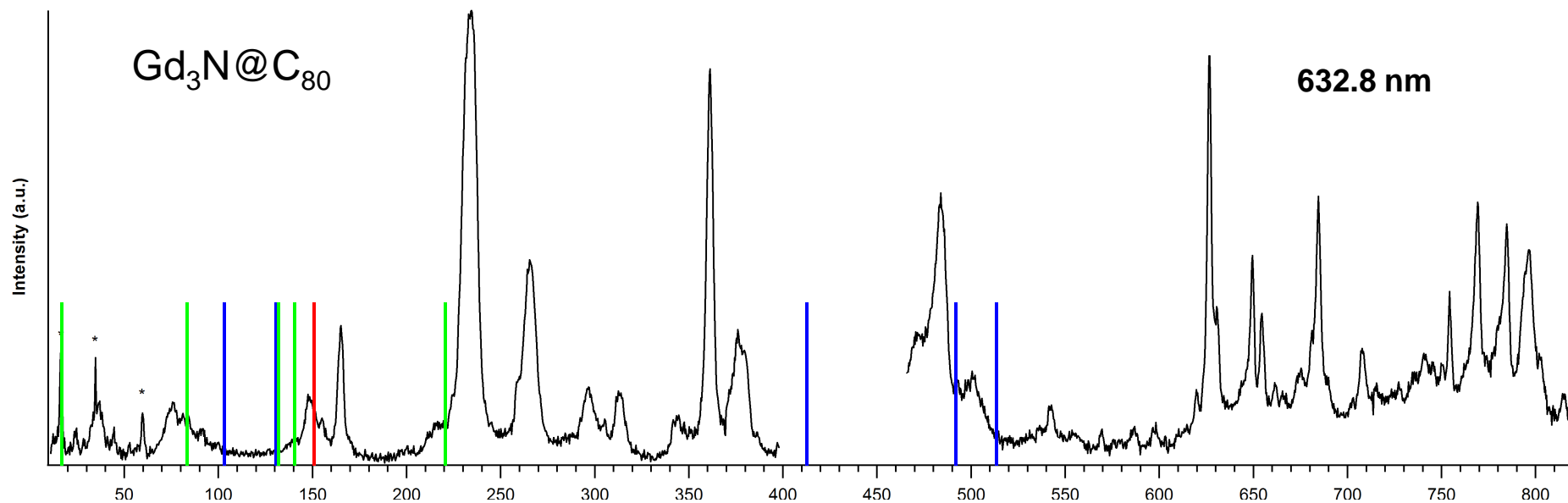
514.7 cm⁻¹



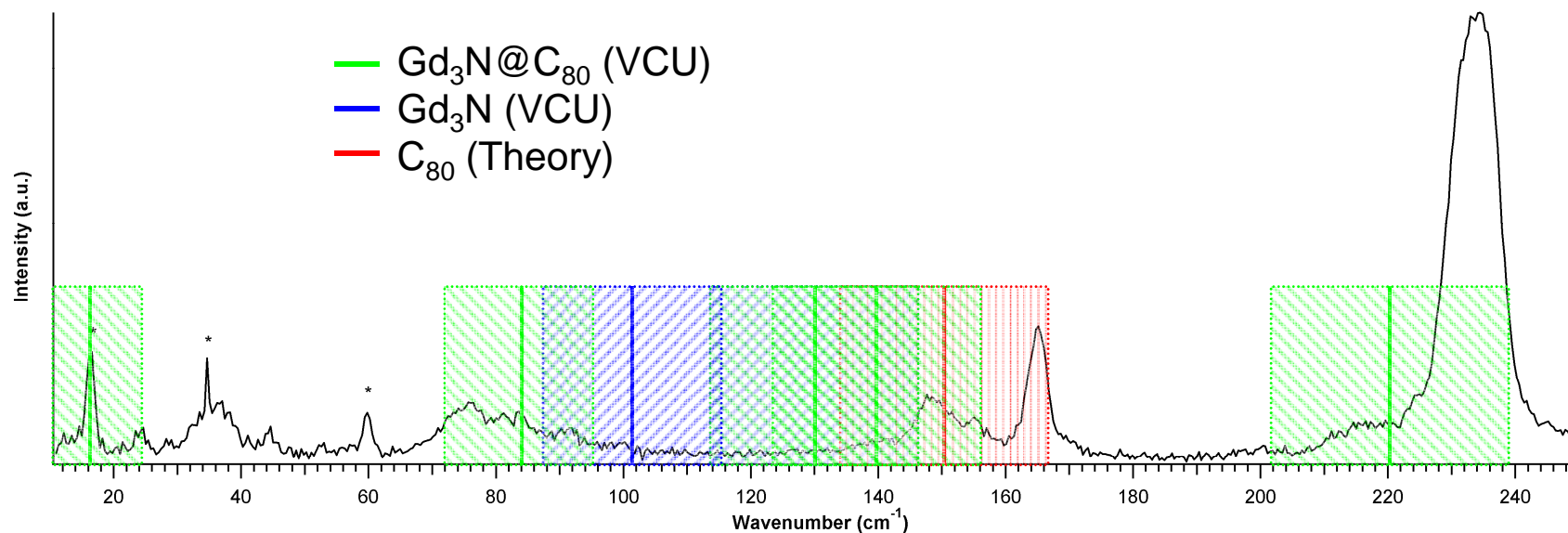
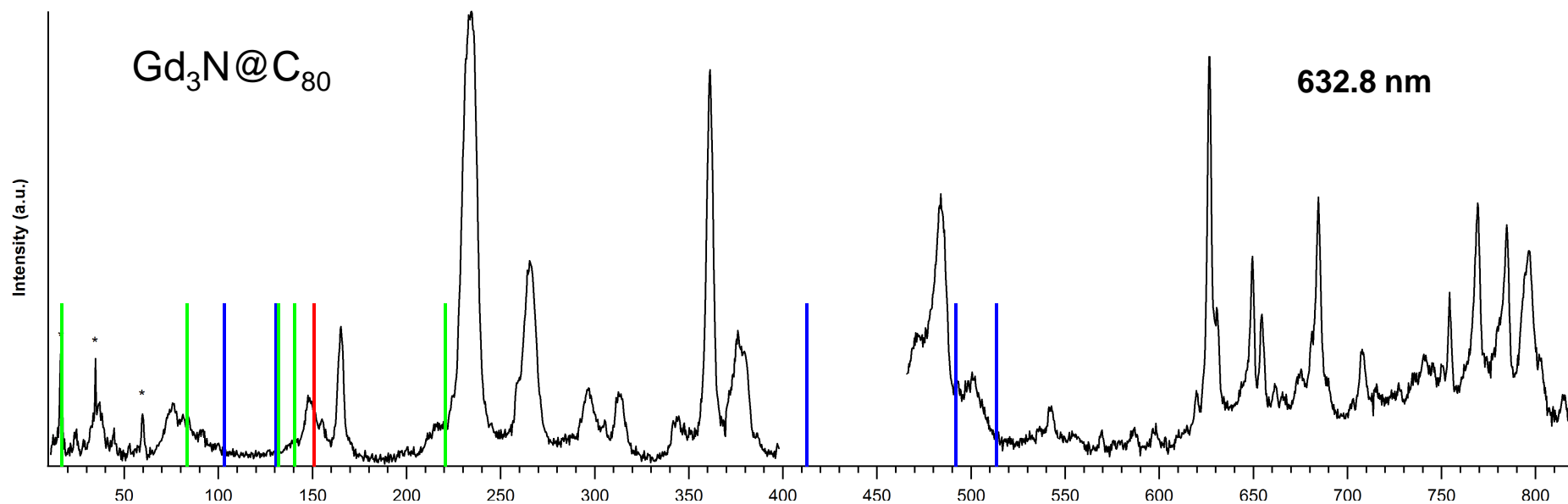
410.7 cm⁻¹



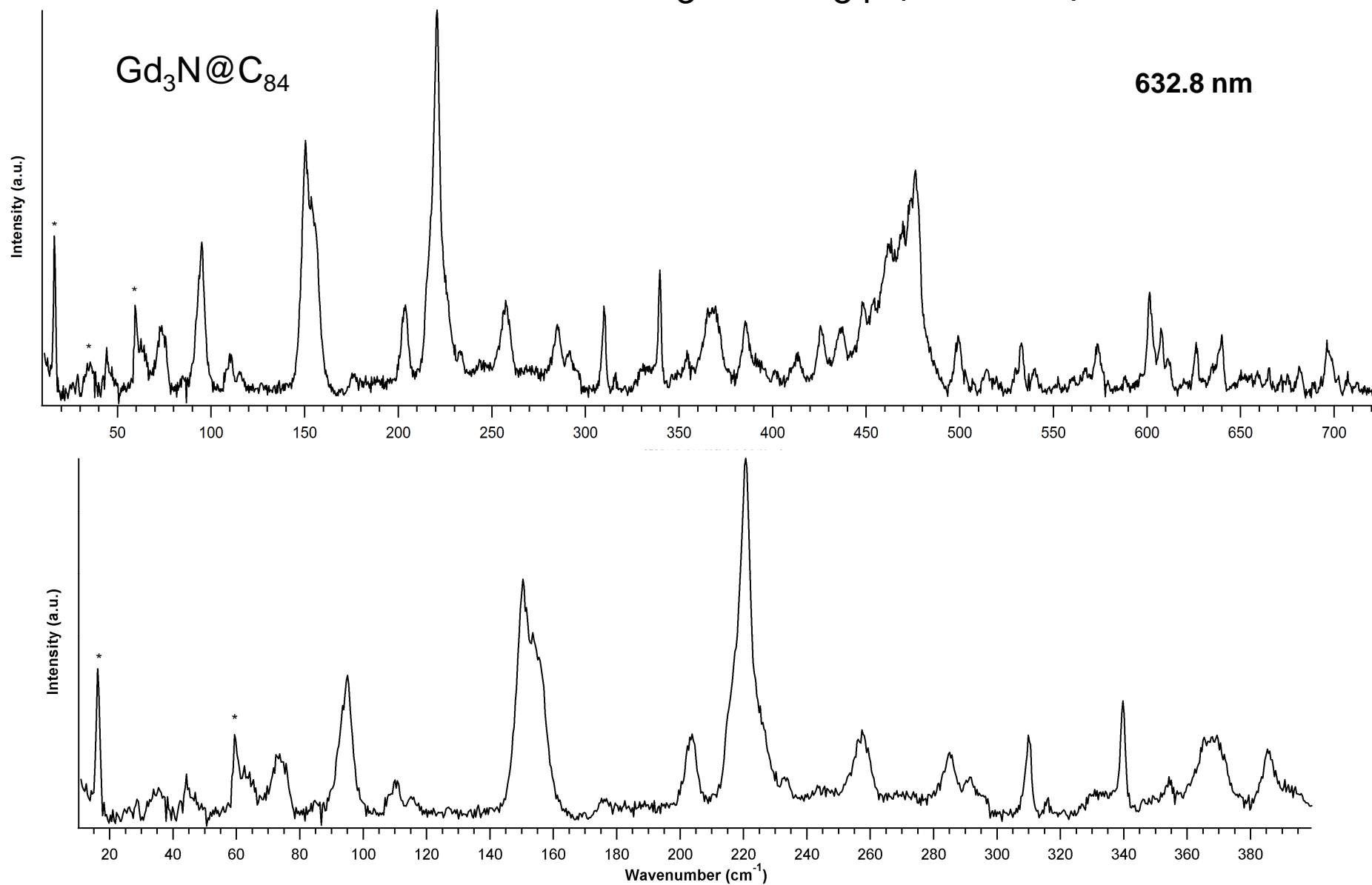
Raman of $\text{Gd}_3\text{N}@C_{80}$ (CNMS)



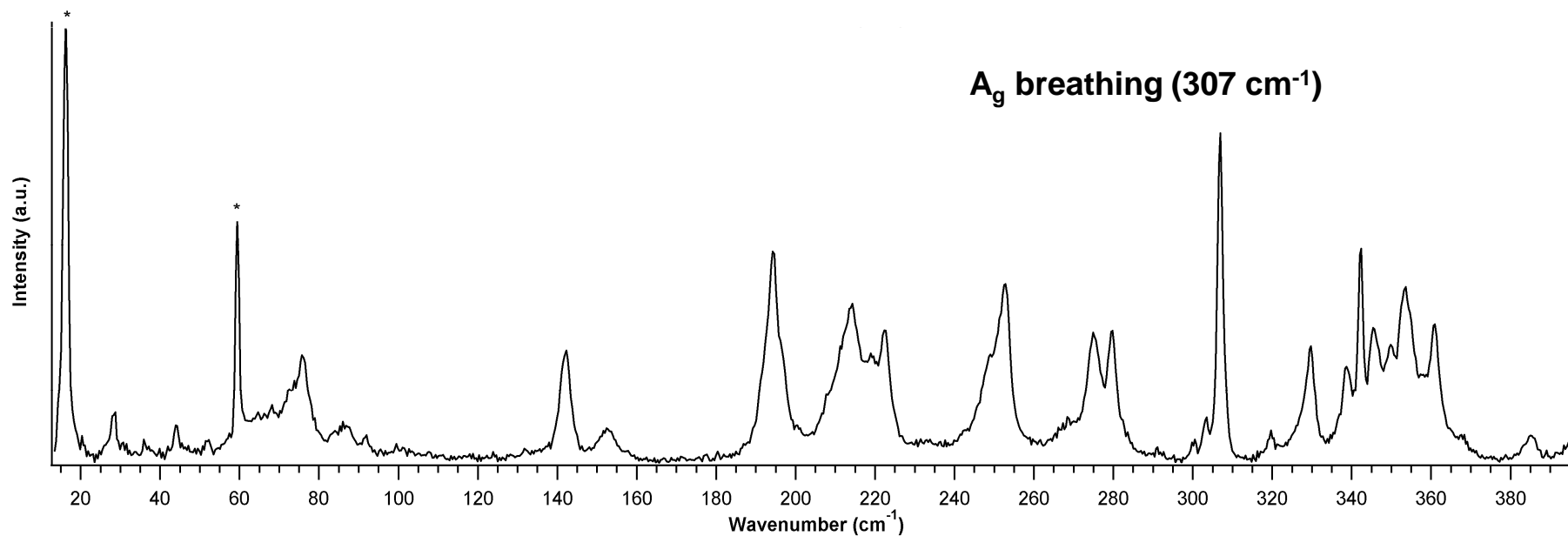
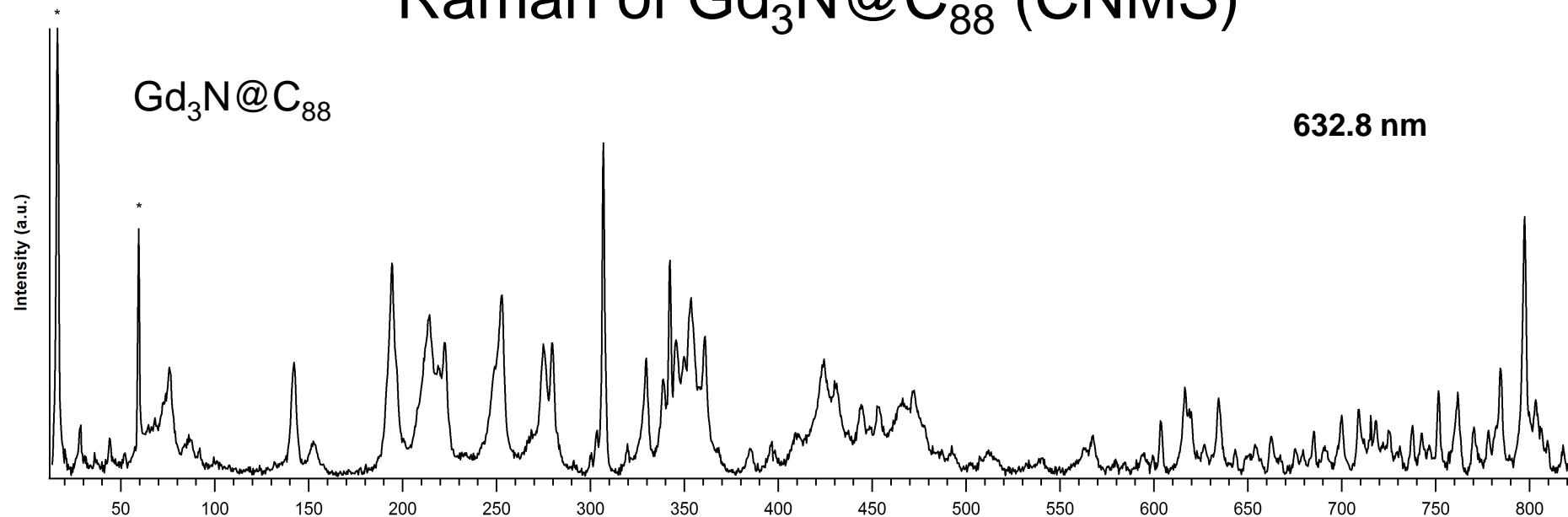
Raman of $\text{Gd}_3\text{N}@C_{80}$ (CNMS)



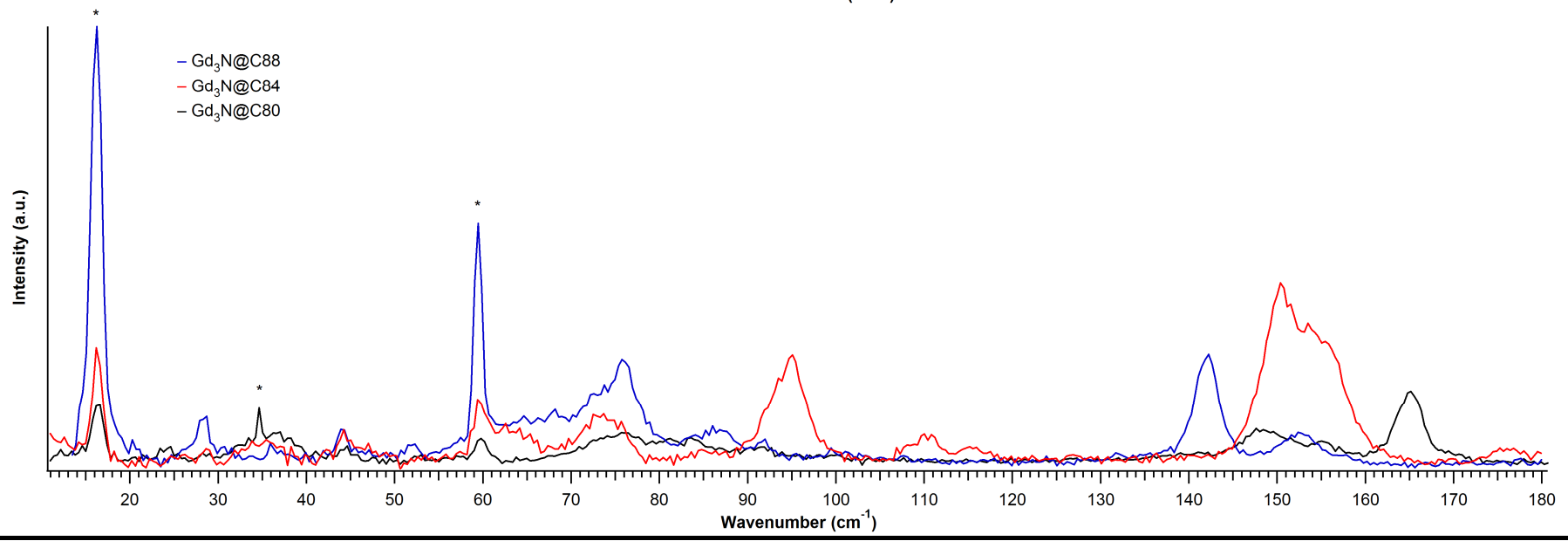
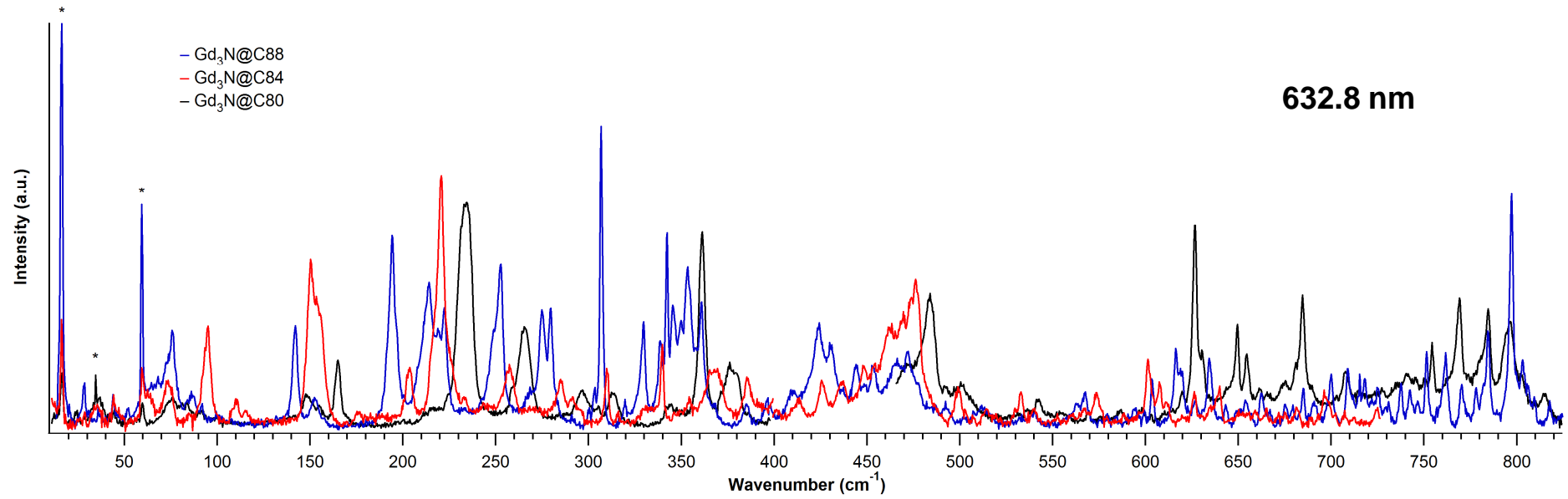
Raman of $\text{Gd}_3\text{N}@C_{84}$ (CNMS)



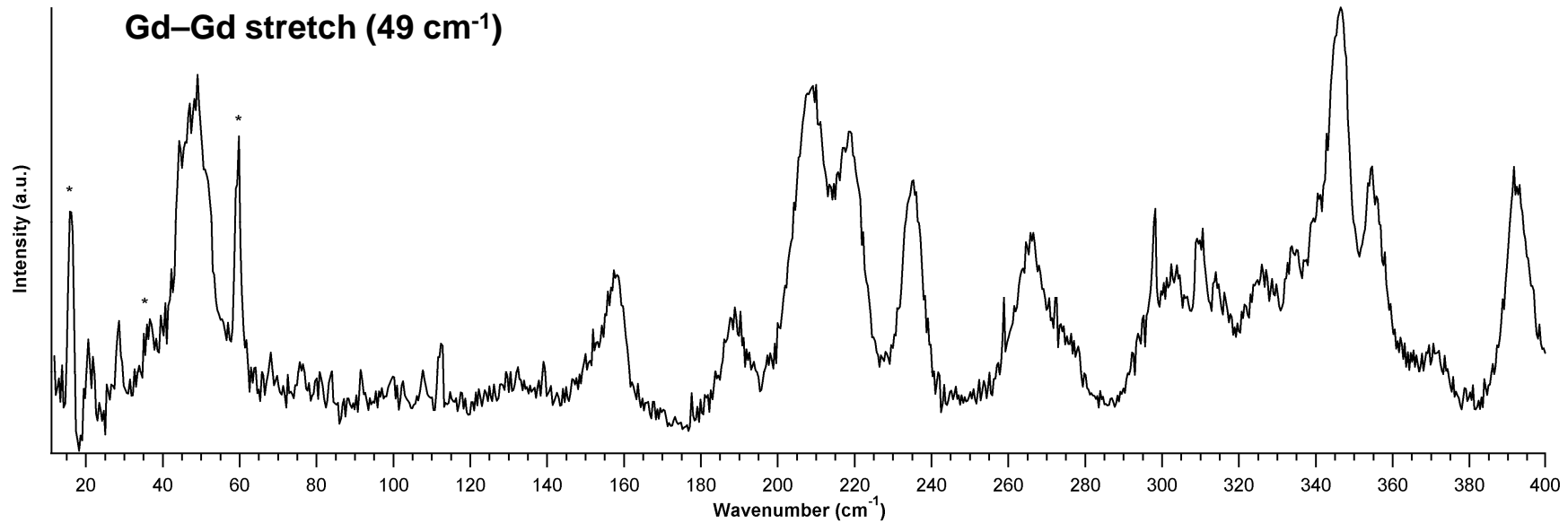
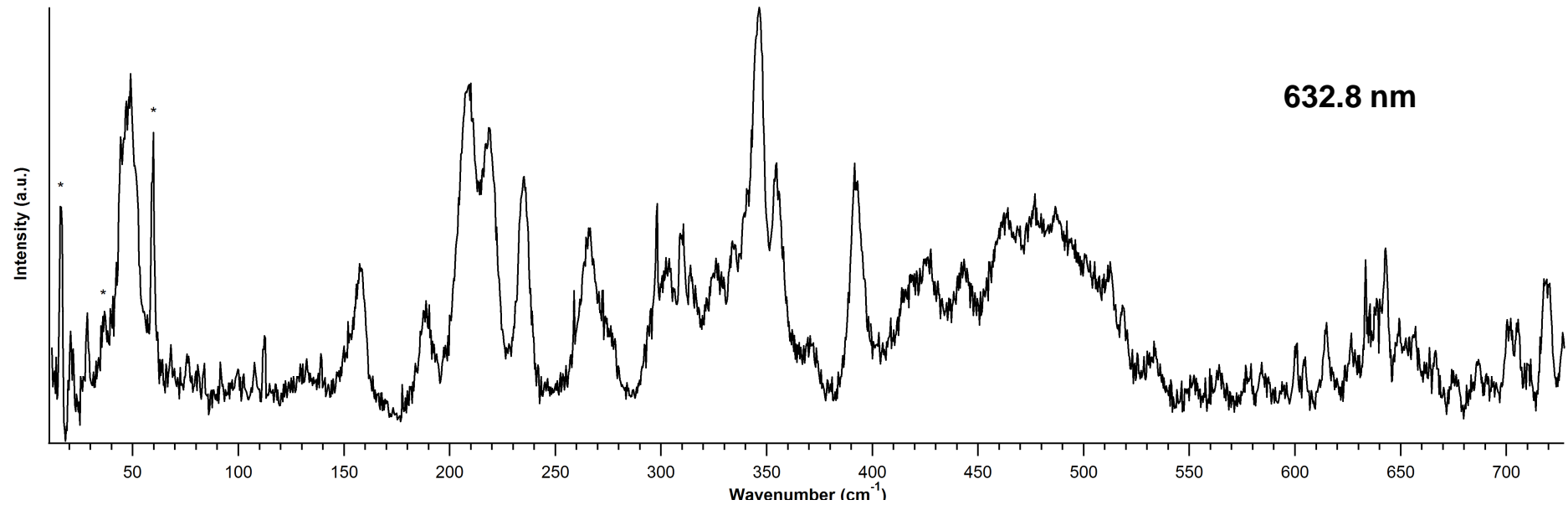
Raman of $\text{Gd}_3\text{N}@C_{88}$ (CNMS)



Gd₃N@C_{8x} (90 K) Comparison

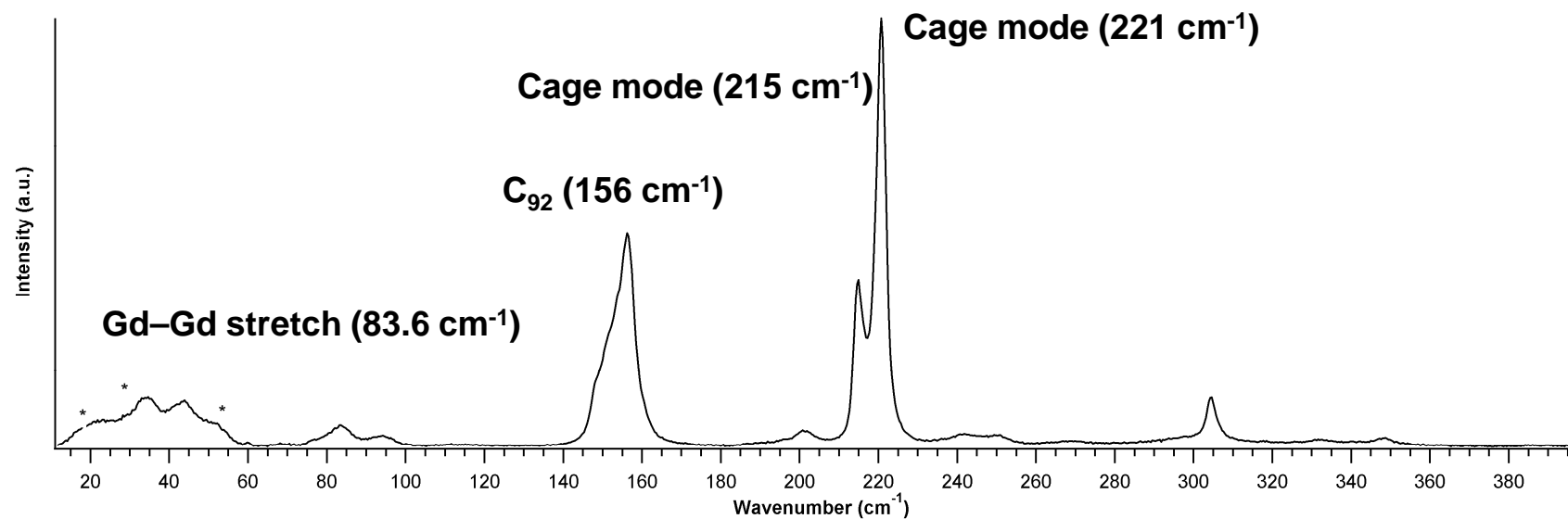
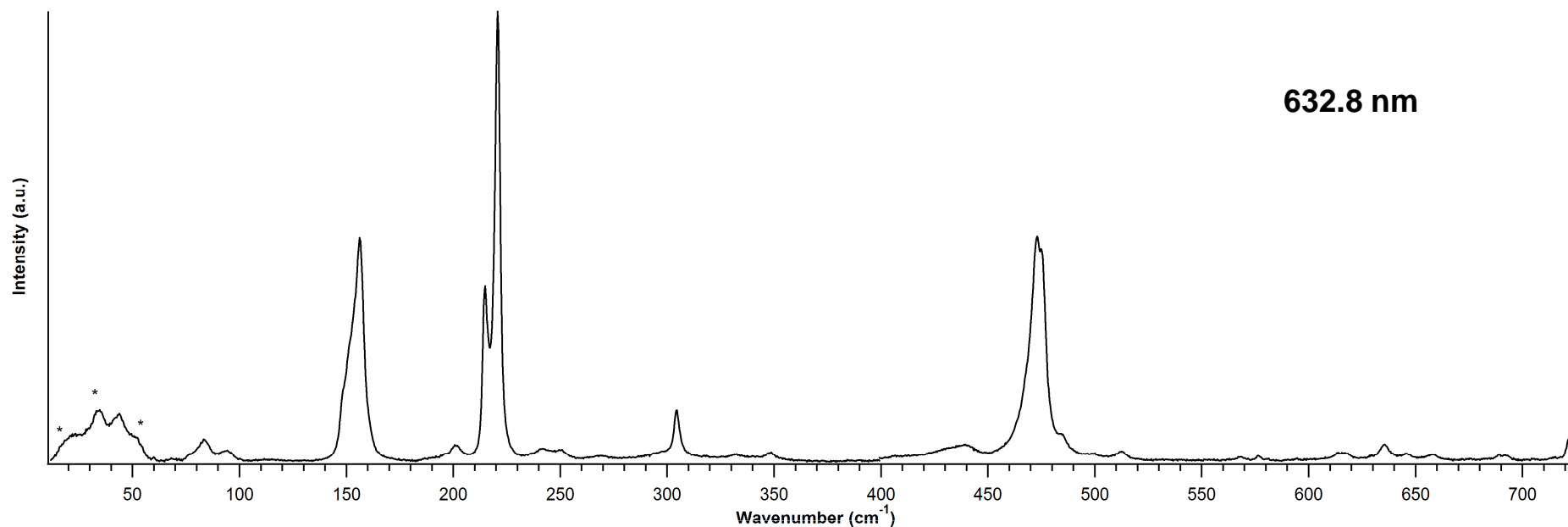


Gd₂@C₉₀ (90 K)



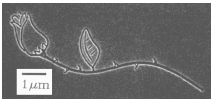
Gd₂C₂@C₉₂ (90 K)

632.8 nm



Future Projects

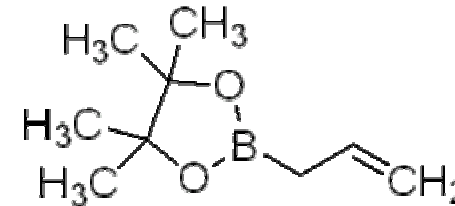
- Molecular Doping of Silicon
- Field Dependence of SurFET
- IETS (Kondo effect) and Cyclic Voltammetry
- Magneto-Raman of Endofullerenes
- Development of Spin Logic Device



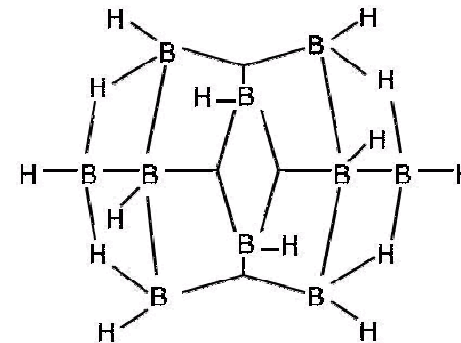
Molecular Doping of Silicon

- We have formed molecular monolayers on hydrogen terminated silicon (SOI) wafers, from thicknesses of 20 nm – 200 nm.

- Allylboronic Acid Pinacol Ester is used to form a Si-C bond, which is 20 times stronger than a hydrogen bond and prevents any oxide from forming. However, only one boron atom acts as a dopant per molecule. Estimated coverage is $\sim 4.9 \times 10^{14} \text{ cm}^{-2}$.



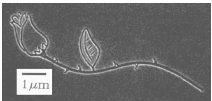
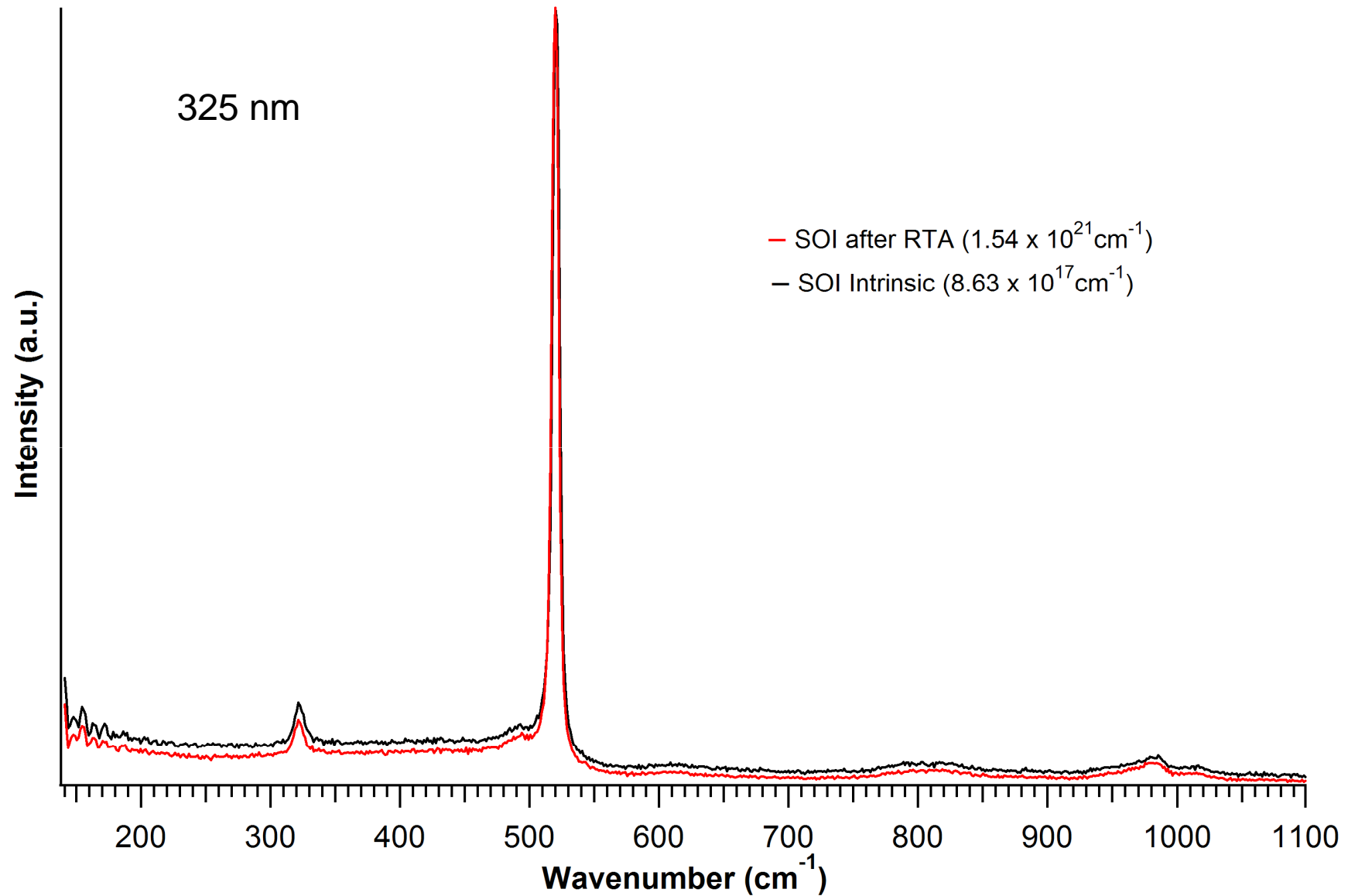
- Decaborane is used to form a Si-H bond, contributing 10 boron atoms per molecule. Estimated coverage is $\sim 7.8 \times 10^{14} \text{ cm}^{-2}$.



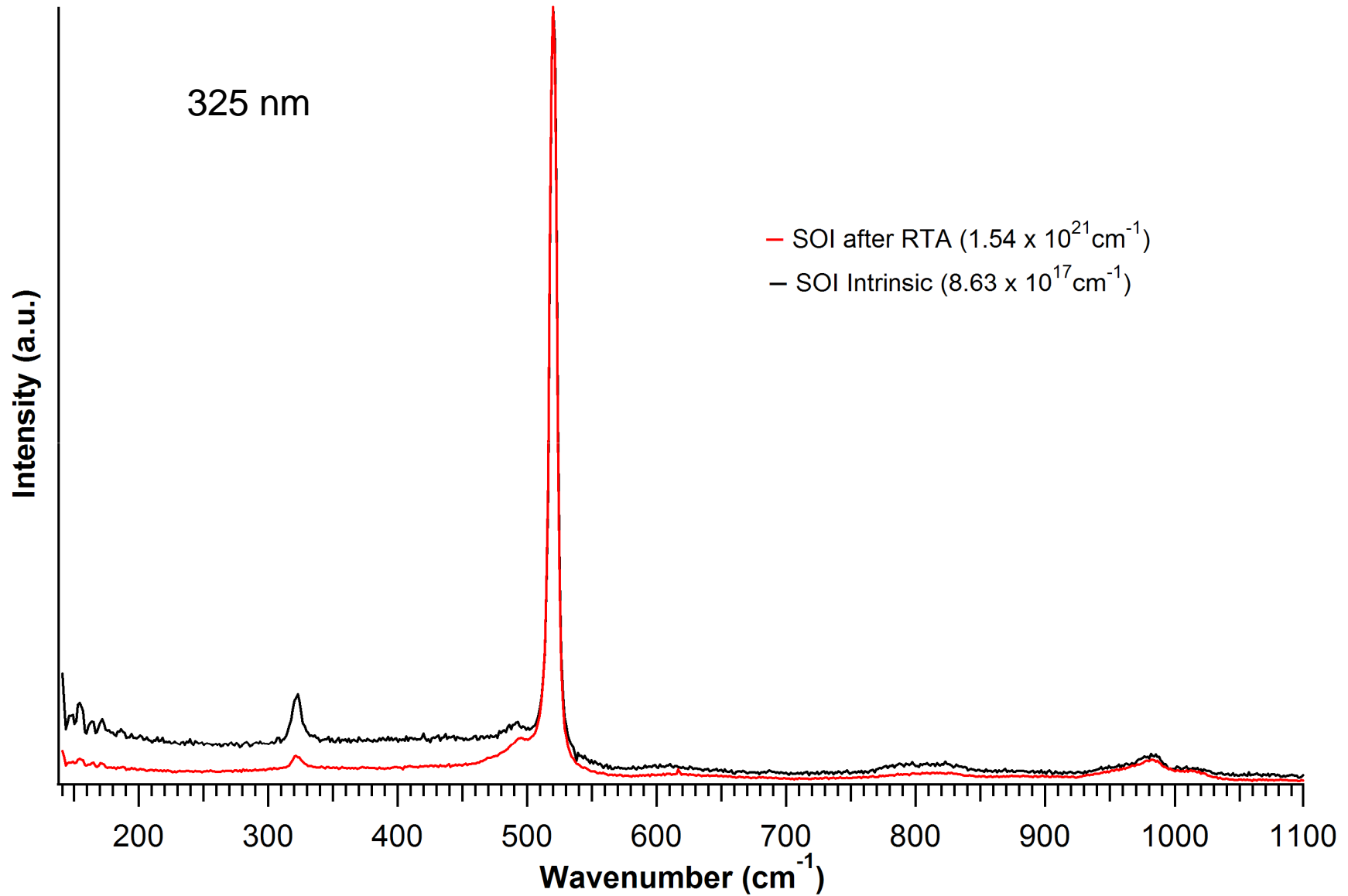
- The samples undergo RTA and analysis by sheet resistance and Hall effect measurements and then Raman spectroscopy. We have observed an average increase in doping from $2.5 \times 10^{15} \text{ cm}^{-3}$ to $4.21 \times 10^{19} \text{ cm}^{-3}$ (200 nm SOI) and from $8.63 \times 10^{17} \text{ cm}^{-3}$ to $5.3 \times 10^{20} \text{ cm}^{-3}$ (75 nm SOI).



Molecularly Doped SOI (75 nm)

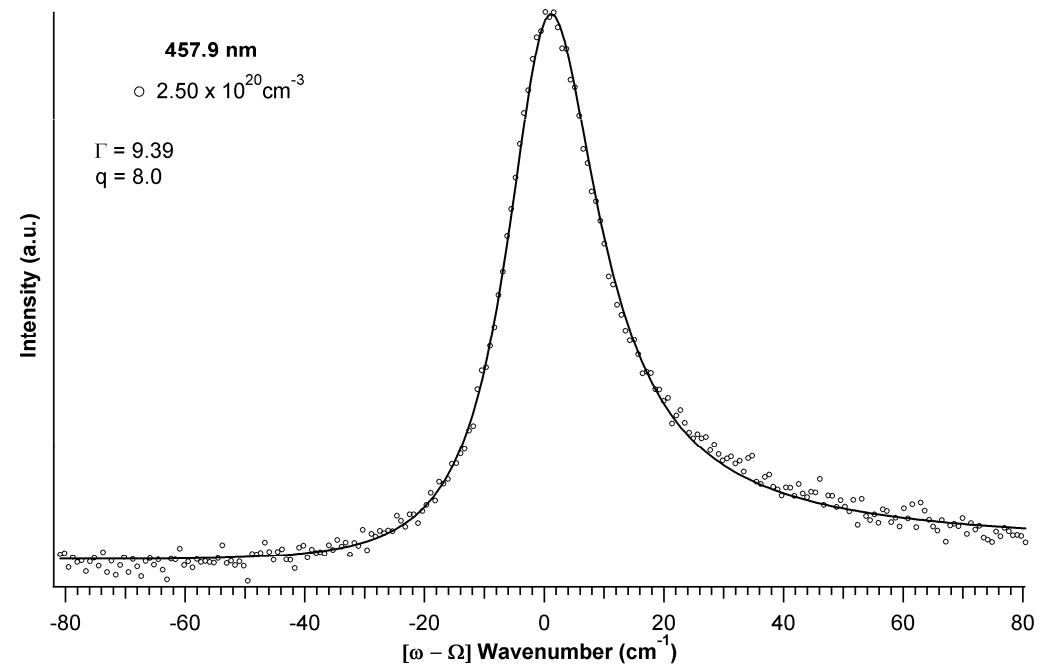
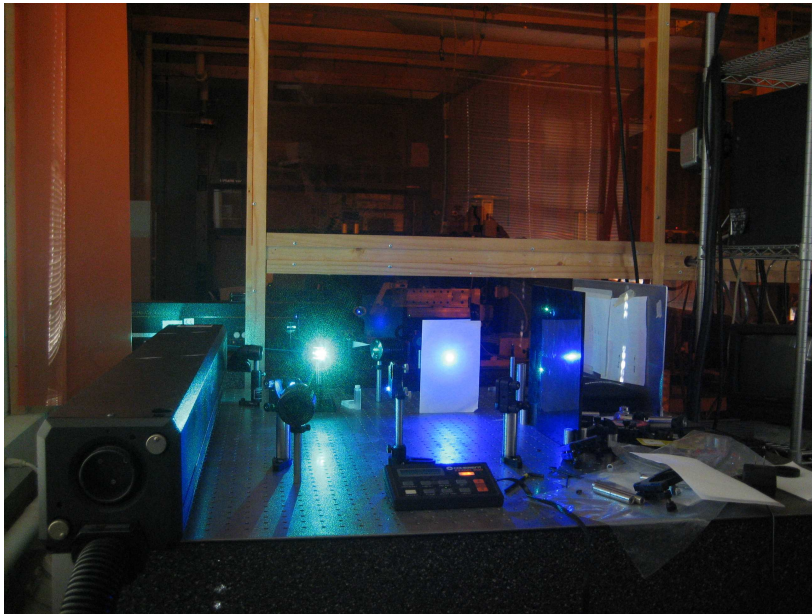


Molecularly Doped SOI (23 nm)

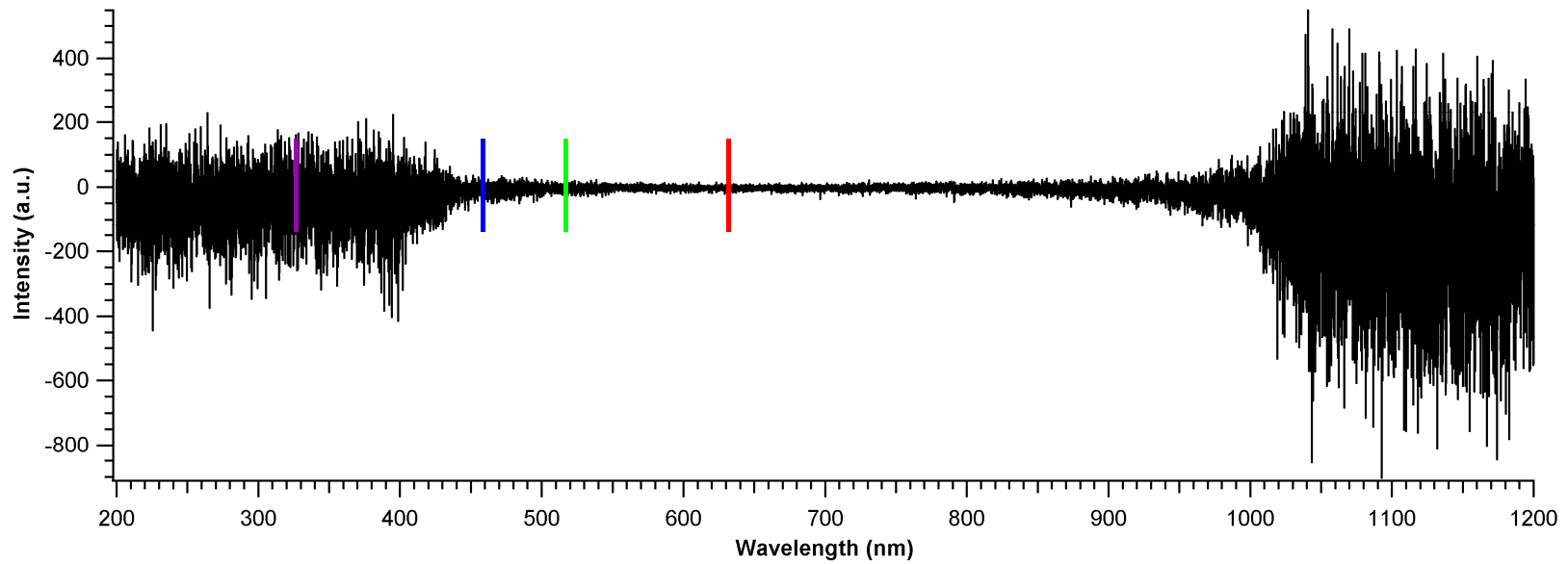
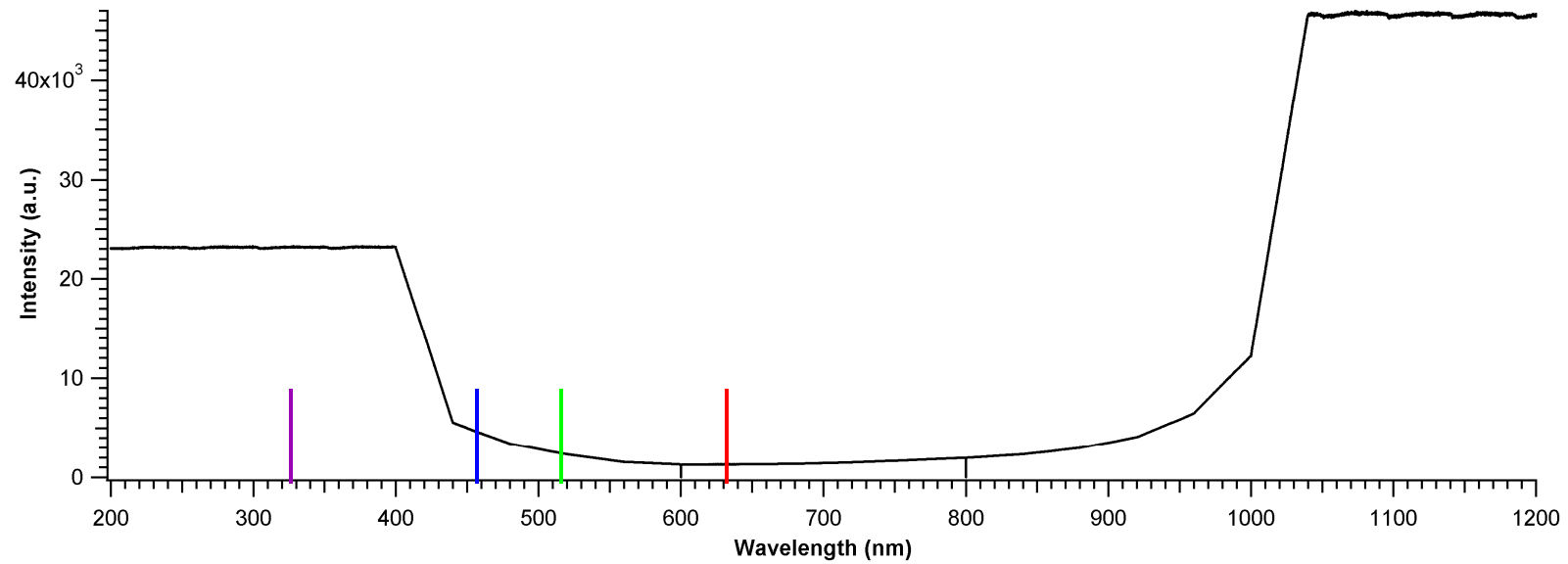


Additional Ar Ion and HeCd Laser Lines

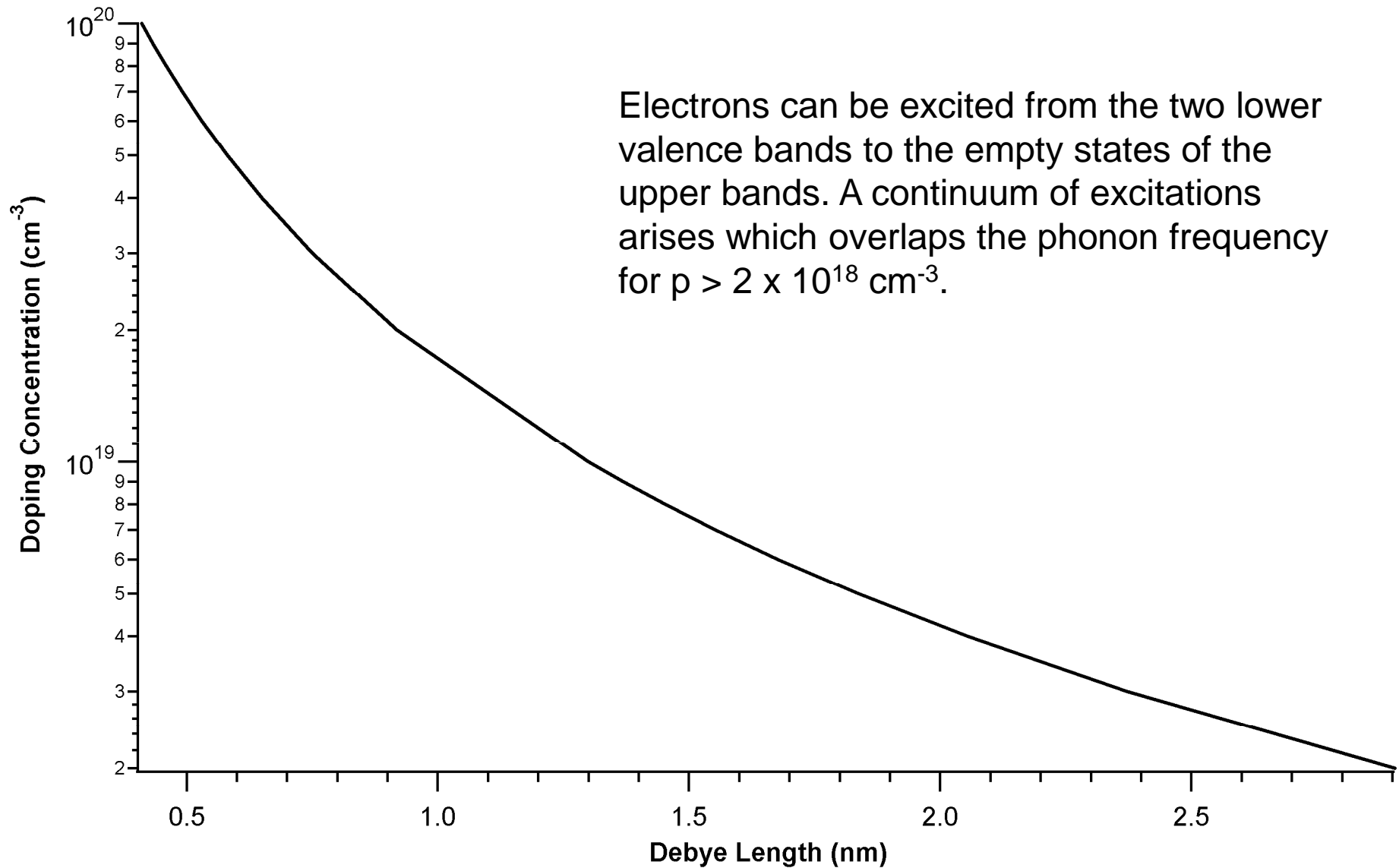
- Ar⁺ laser (514.5 nm and 457.9 nm) and HeCd (325 nm) have been added to Raman setup
- Field dependence (confocal Raman) and mapping studies of doped silicon with 457.9 nm line (~500 nm penetration depth)
- Analysis of deuterium and hydrogen for nuclear studies (Norum Group)



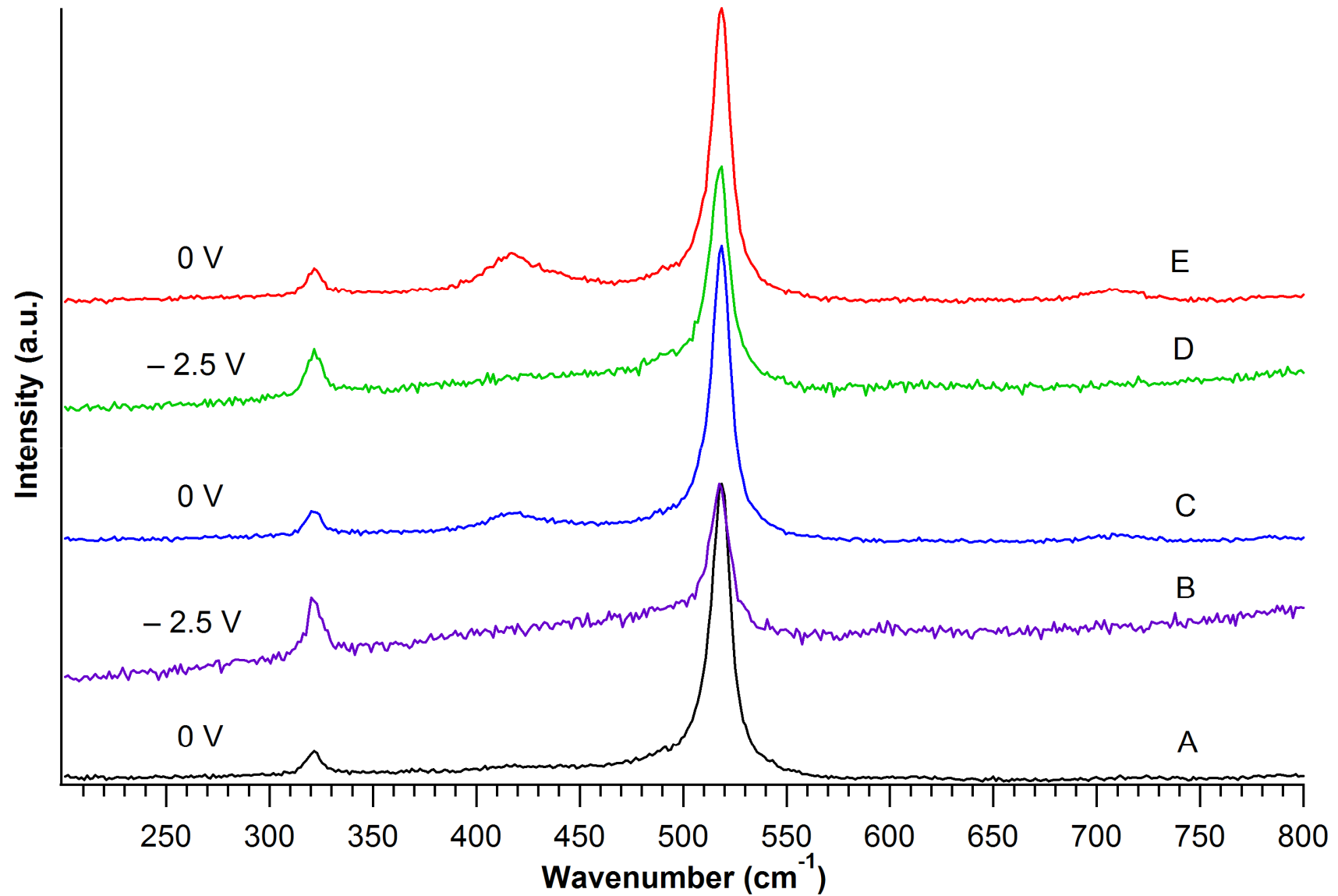
Detector Limitations



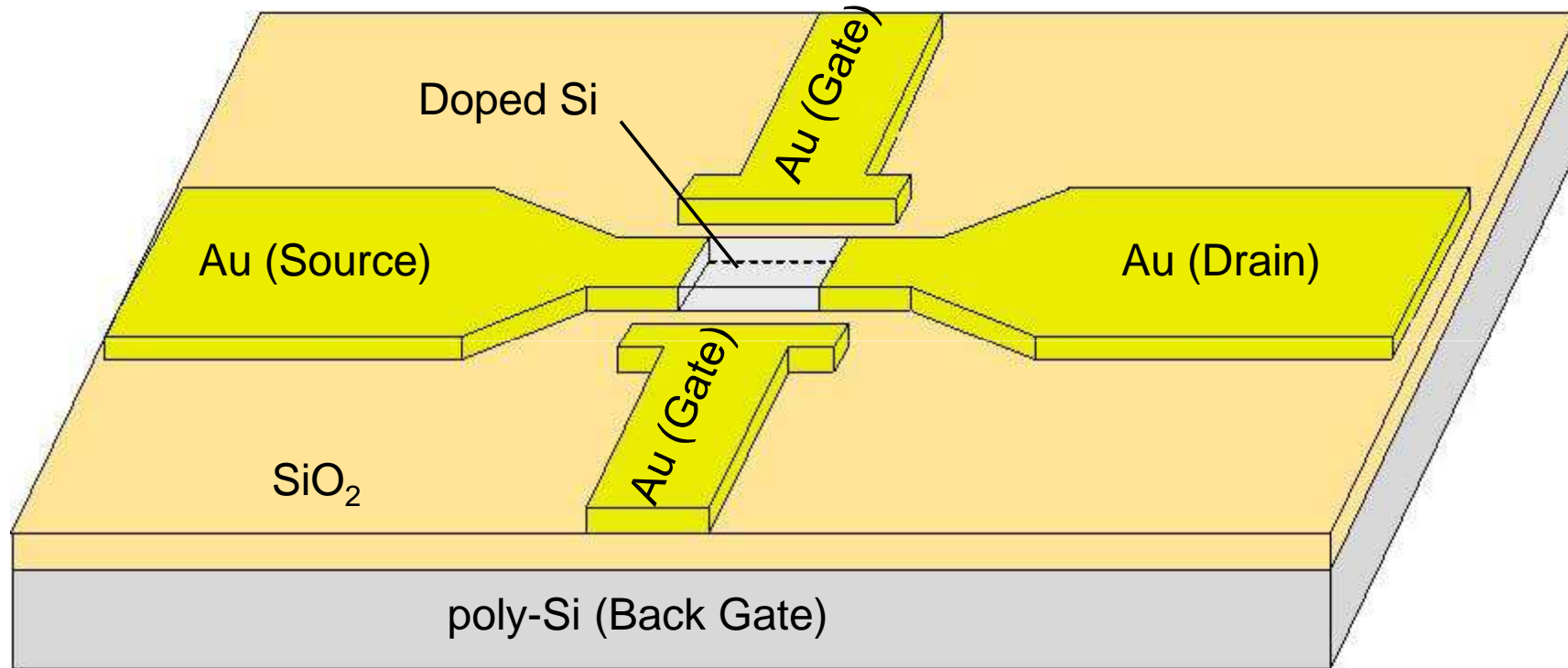
Debye Length in Doped Silicon



Possible Field Dependence

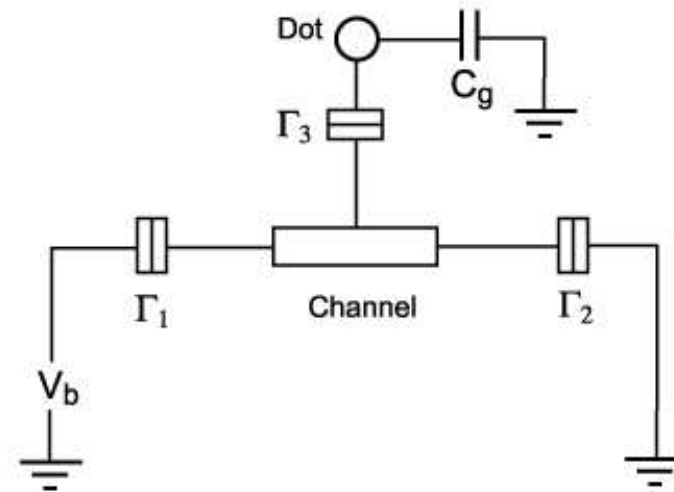
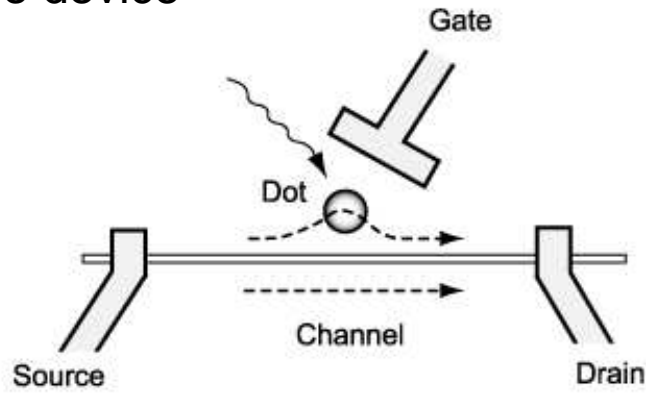


Future SurFET Design

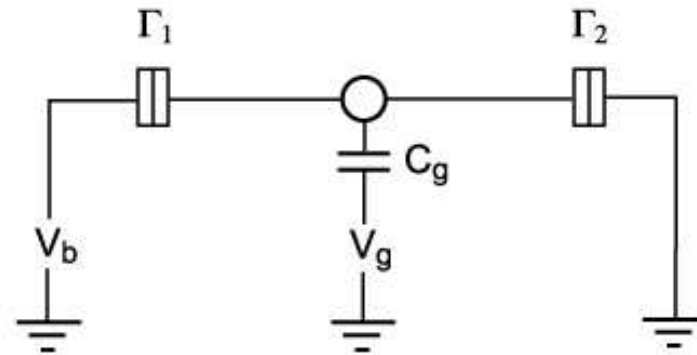
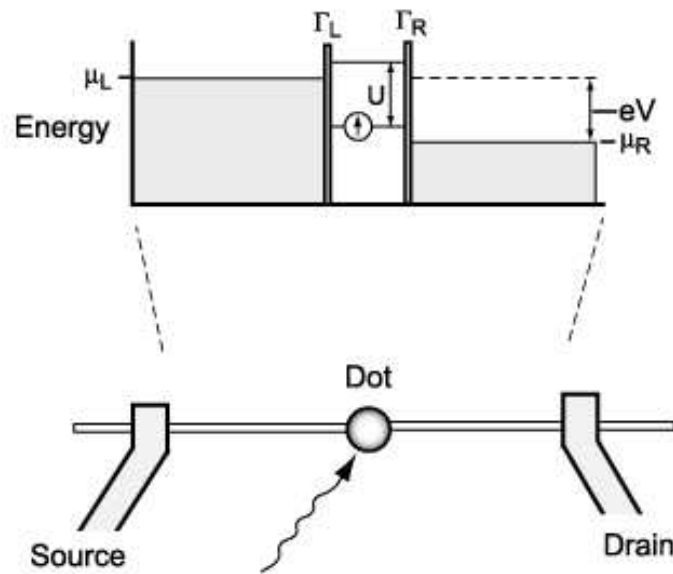


Fano and Kondo Effect

Fano device

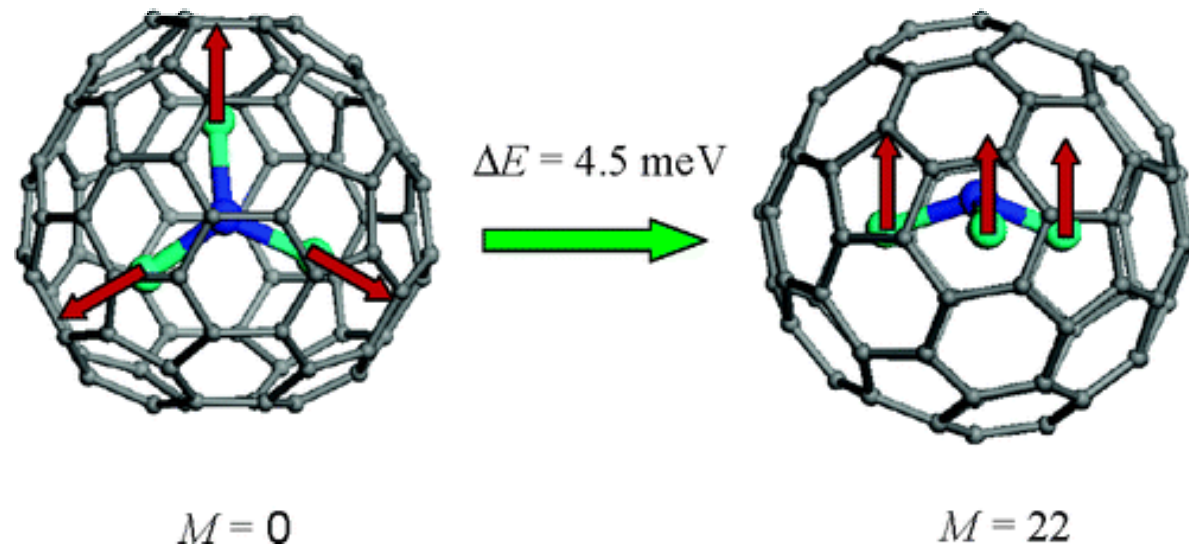


Kondo device



Investigation of $\text{Gd}_3\text{N}@C_{80}$

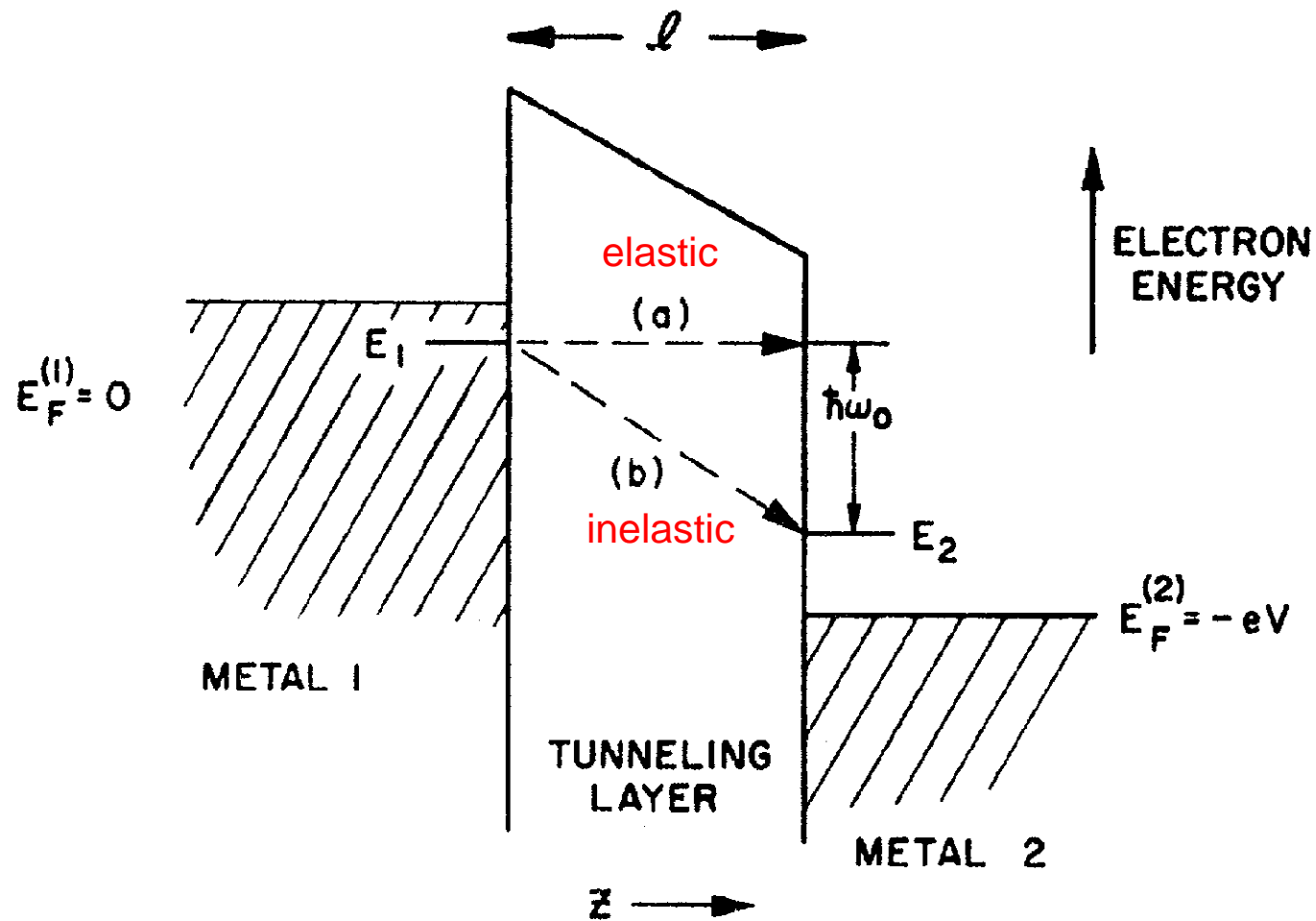
- Gd_3N is the largest cluster encapsulated in a fullerene cage to date
- Gd_3N cluster is responsible for the magnetic properties
 - Theoretical calculations determined two spin multiplicities ($M = 0$ and 22); one is antiparallel to the other two Gd atoms ($M = 0$) and all are parallel aligned ($M = 22$), ferromagnetically coupled
- Kondo Effect
- Possible Spin Logic Device



J. Lu *et al.*, *J. Phys. Chem. B* **110**, 23637 (2006)

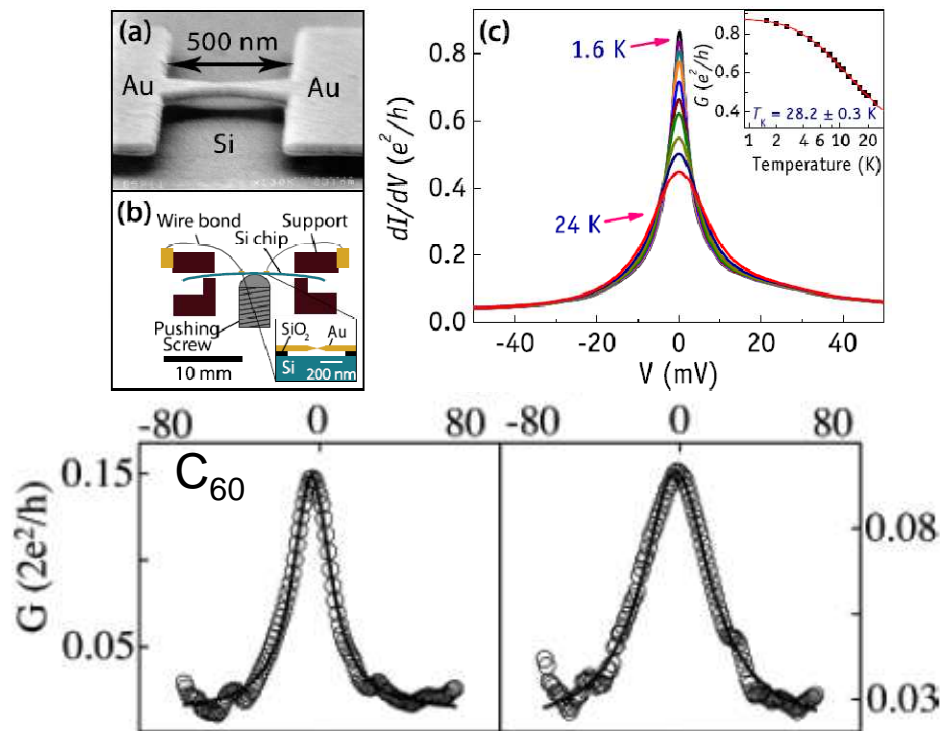


Inelastic Electron Tunneling Spectroscopy (IETS)

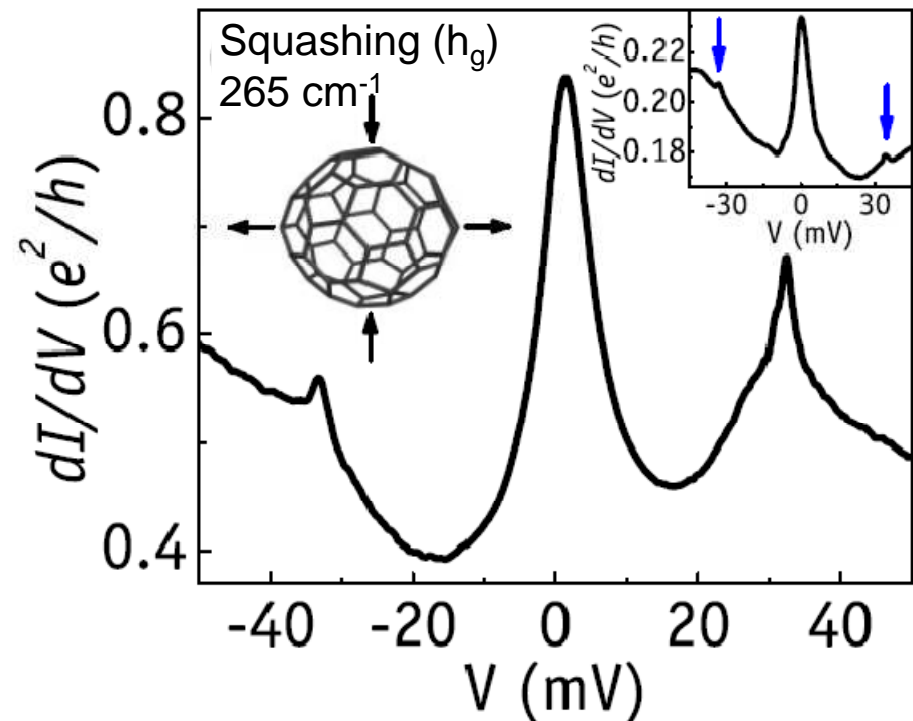


Kondo Effect in Fullerenes (C_{60})

- The Kondo effect is a many-body phenomenon that can arise from the coupling between a localized spin and a sea of conduction electrons
- At low temperature, a spin-singlet state may be formed from a localized spin-1/2 electron and the delocalized Fermi sea, leading to a correlated state reflected in transport as a zero-bias conductance anomaly



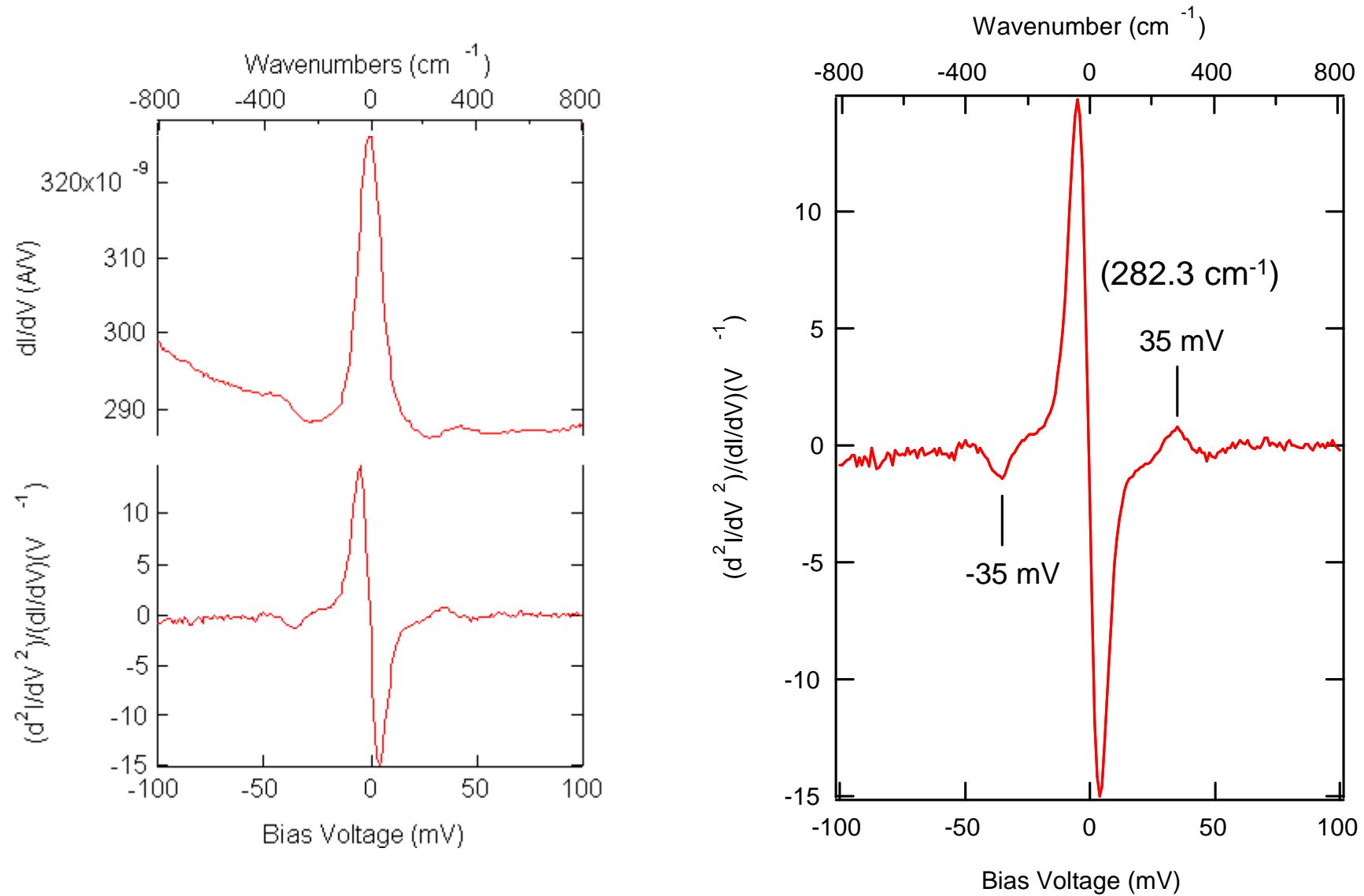
L. Yu and D. Natelson, *Nano Lett.* **4**, 79 (2004)



J.J. Parks *et al.*, *Phys. Rev. Lett.* **99**, 026601 (2007)

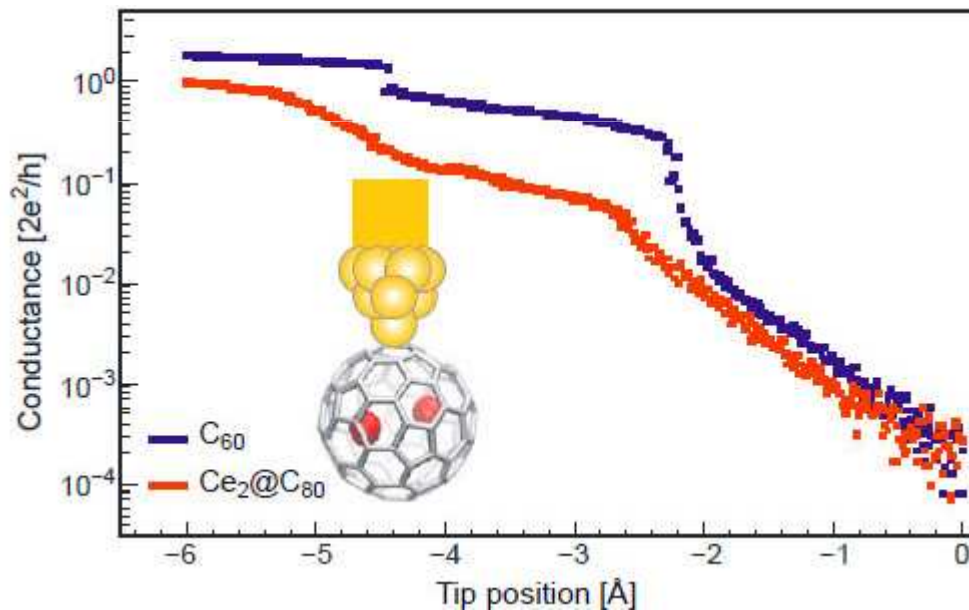


Kondo Effect in $\text{Gd}_3\text{N}@C_{80}$



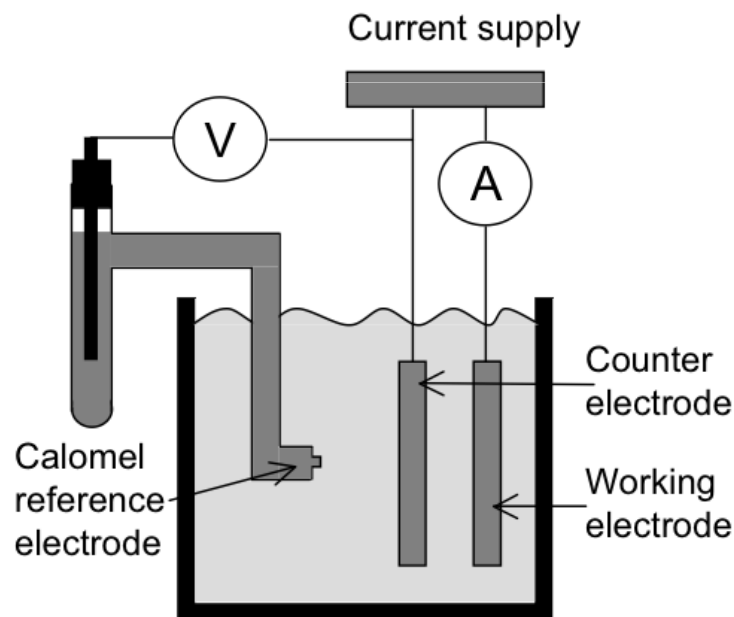
STM of $\text{Gd}_3\text{N}@C_{80}$ (B field dependence)

- Investigate interaction of cage with endocomplex
- Measure tunneling current as a function of magnetic field
- CNMS (Oak Ridge) facility (300 mK, 8 T)



Cyclic Voltammetry (CV)

- Potentiodynamic electrochemical measurement
- Three electrodes (working, counter and reference) are used to measure the current while the working electrode potential is ramped linearly over time
- Identifies redox (reduction-oxidation reaction) couples which change the current as the potential is sweep forward and reversed

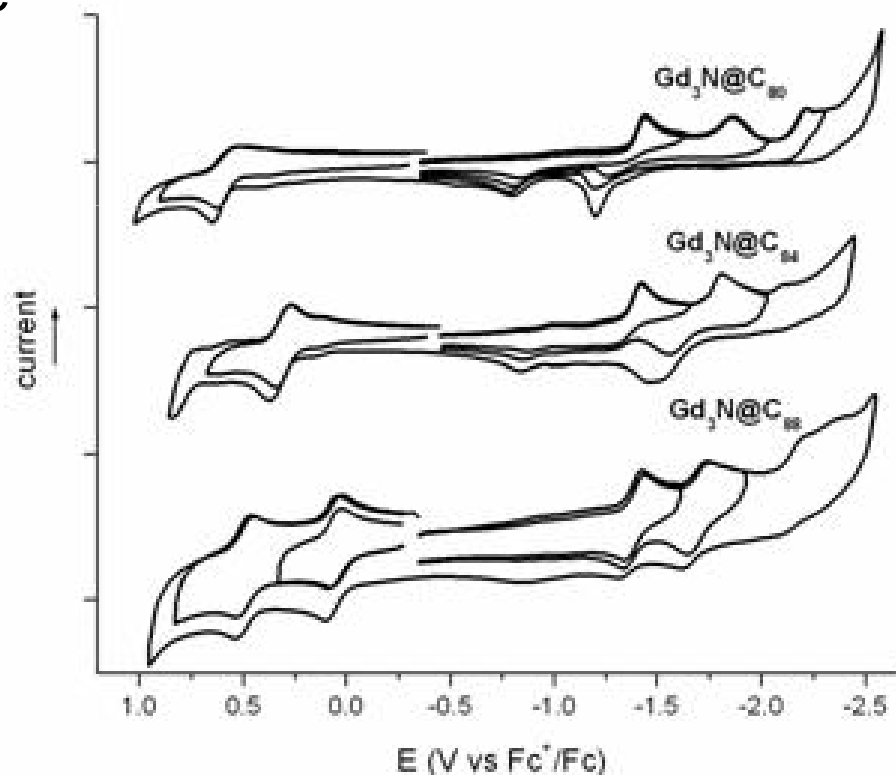


CV of Endofullerenes ($M_3N@C_{8x}$)

- The electrochemical properties change dramatically with the size of the cage, going from irreversible for the C_{80} cage to reversible for $Gd_3N@C_{88}$
- $Gd_3N@C_{88}$ has one of the lowest electrochemical energy gaps for a nonderivatized endofullerene

TNT EMF	$E_{p,red(1)}$	$E_{1/2,red(1)}$	$E_{p,red(2)}$
$Gd_3N@C_{80}$	-1.44		-1.86
$Gd_3N@C_{84}$	-1.37		-1.76
$Gd_3N@C_{88}$	-1.43	-1.38	-1.74

redox potential				
$E_{1/2,red[2]}$	$E_{p,red(3)}$	$E_{1/2,ox1}$	$E_{1/2,ox1}$	ΔE_{gap}
	-2.15	+0.58		2.02
		+0.32		1.69
-1.69		+0.06	+0.49	1.49



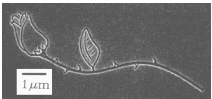
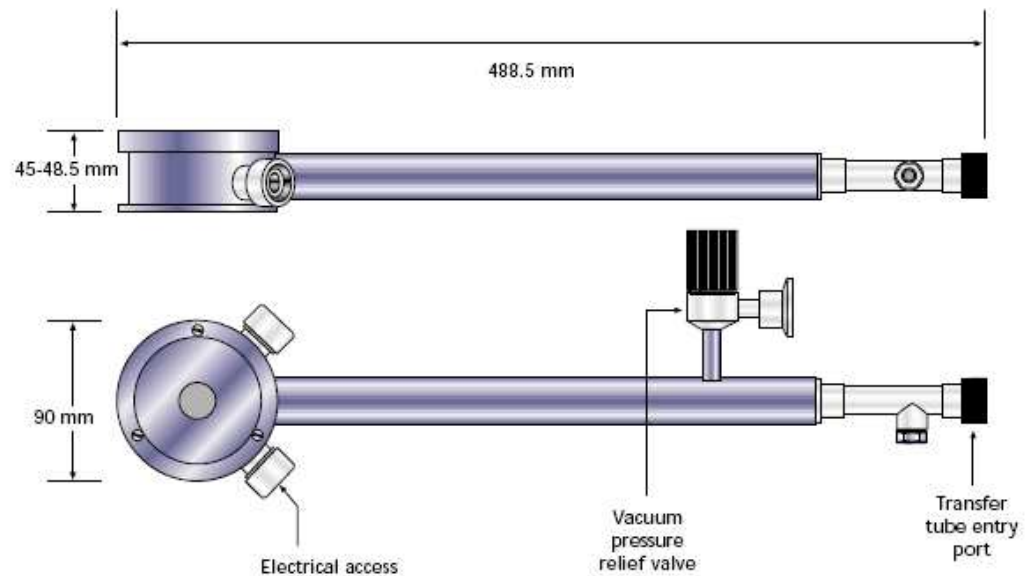
B. Holloway *et al.*, *J. Am. Chem. Soc.* **129**, 14826 (2007)



Magneto-Raman of Endofullerenes (LUNA)

- Six complexes of the form $M_3N@C_{80}$ ($M = Sc, Y, Gd, Er, Lu$ and Ho) will be investigated as a function of magnetic field and temperature
- The species have varying degrees of charge transfer with the cage as well as different moments and sizes, permitting investigation of cage-core mode locking in a methodical manner
- Investigate transition below ~ 10 K with LHe optical cryostat

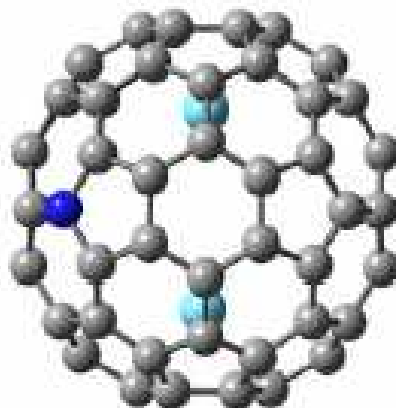
Oxford MicroStat HiRes II



Heterometallofullerenes

- New materials being created (Harry Dorn VT)
- CV and Raman Spectroscopy
- Free electron contained inside cage
- Spin Logic Device

$Y_2@C_{79}N$
 Y_2 Cluster Inside the Cage



H. Dorn *et al.*, *J. Am. Chem. Soc.* **129**, 2035 (2007)

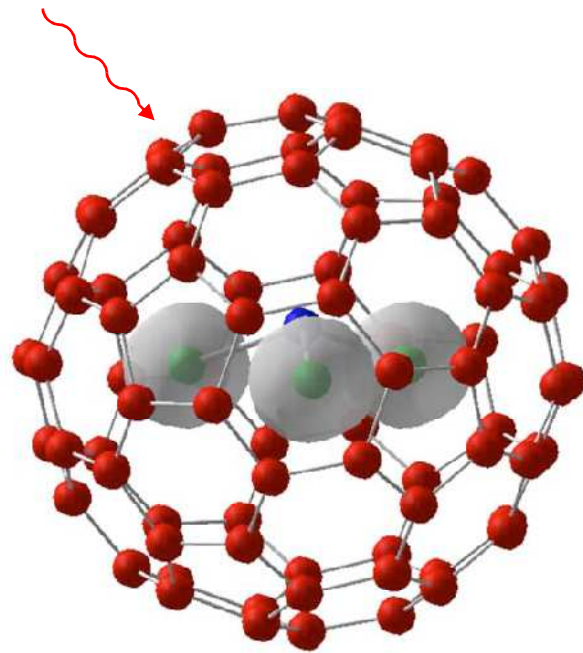


Keith Williams' Nanophysics Group – University of Virginia

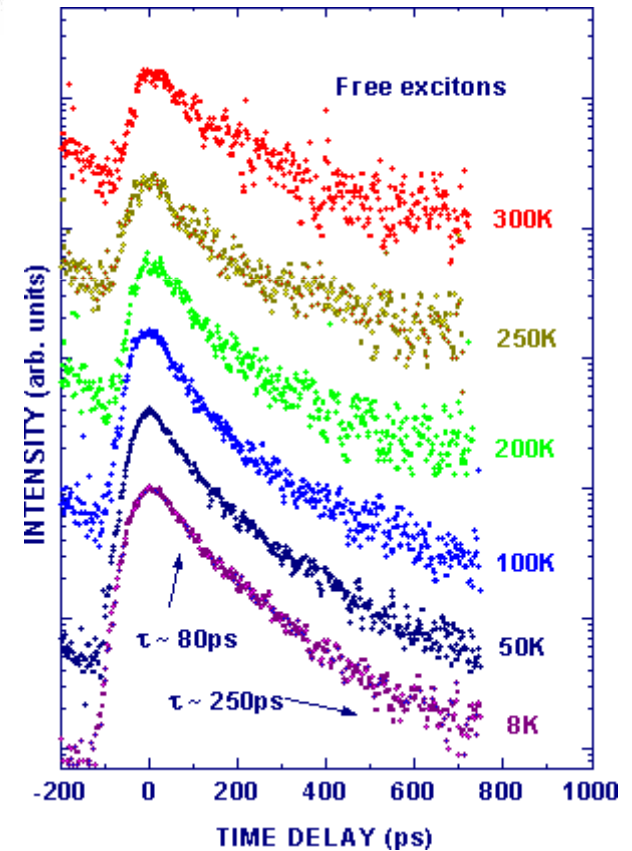
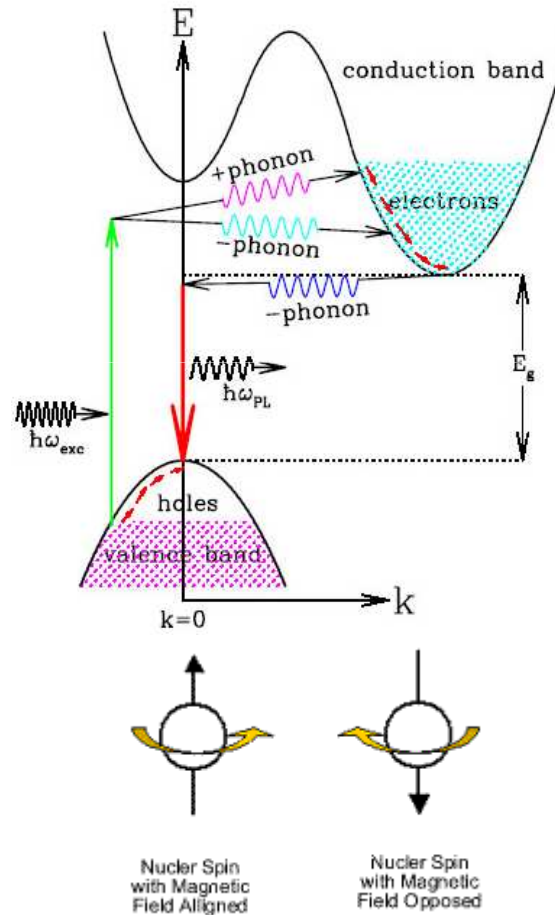
Optically Accessed Memory Device

- Exciton on fullerene cage interacts with core nuclear spin
- Exciton lifetime (τ) should change according to spin state

Laser
Excitation

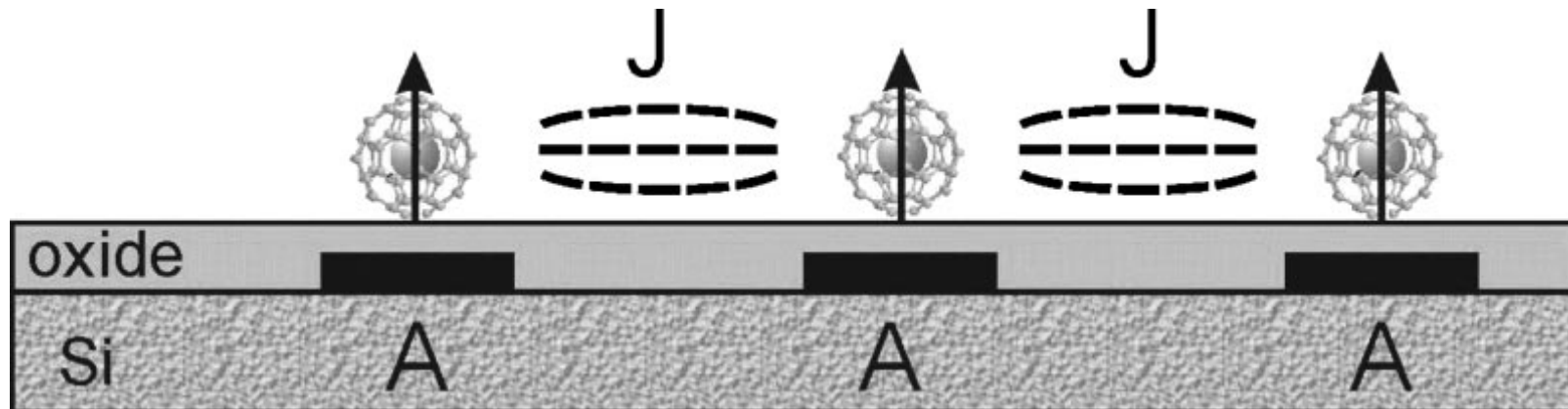


Magnetic
Field



Spin Logic Device

- Scalable solid-state spin quantum computer
- Electron spins are used instead of nuclear spins and the manipulation of fullerene molecules is fairly easy
- Qubits are set and read out via ESR pulses and addressing is provided by local magnetic field or field gradients (Gate A)
- The qubit-qubit interaction is mediated by magnetic dipolar coupling and can be controlled via the direction of the magnetic field with respect to the distance vector of the qubits (J)

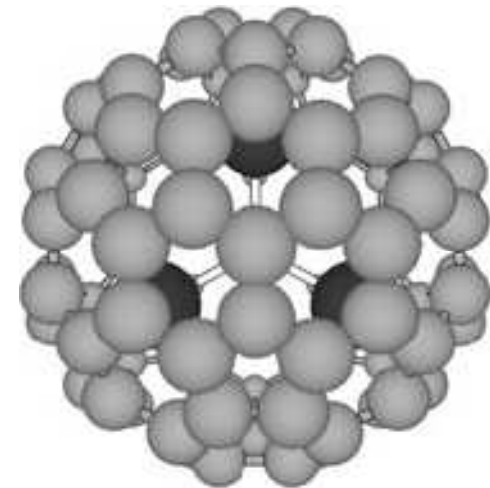
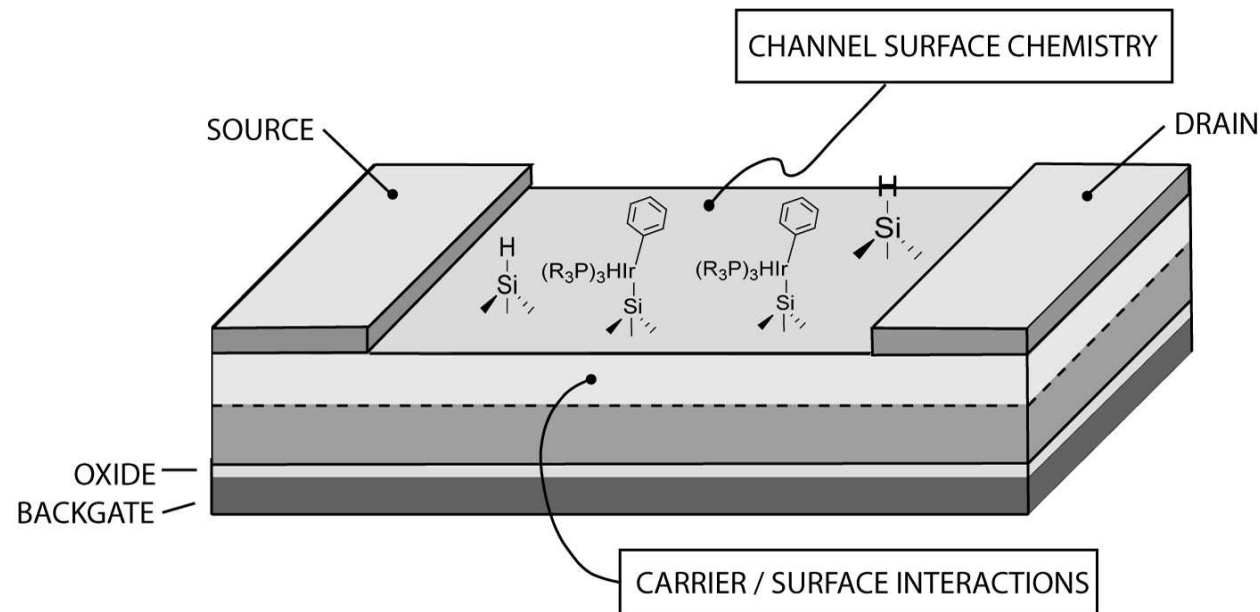


W. Harneit, *Phys. Rev. A* **65**, 032322 (2002)



Summary

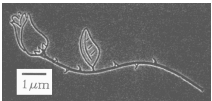
- SurFET device using covalent molecular adsorbates as resonant scattering centers and forming 2DEG-like state at the surface
- Extension of Cardona's p-type silicon data into the submicron region and investigated Fano interference effect for sensing and transport devices
- High resolution Raman data of Endofullerenes

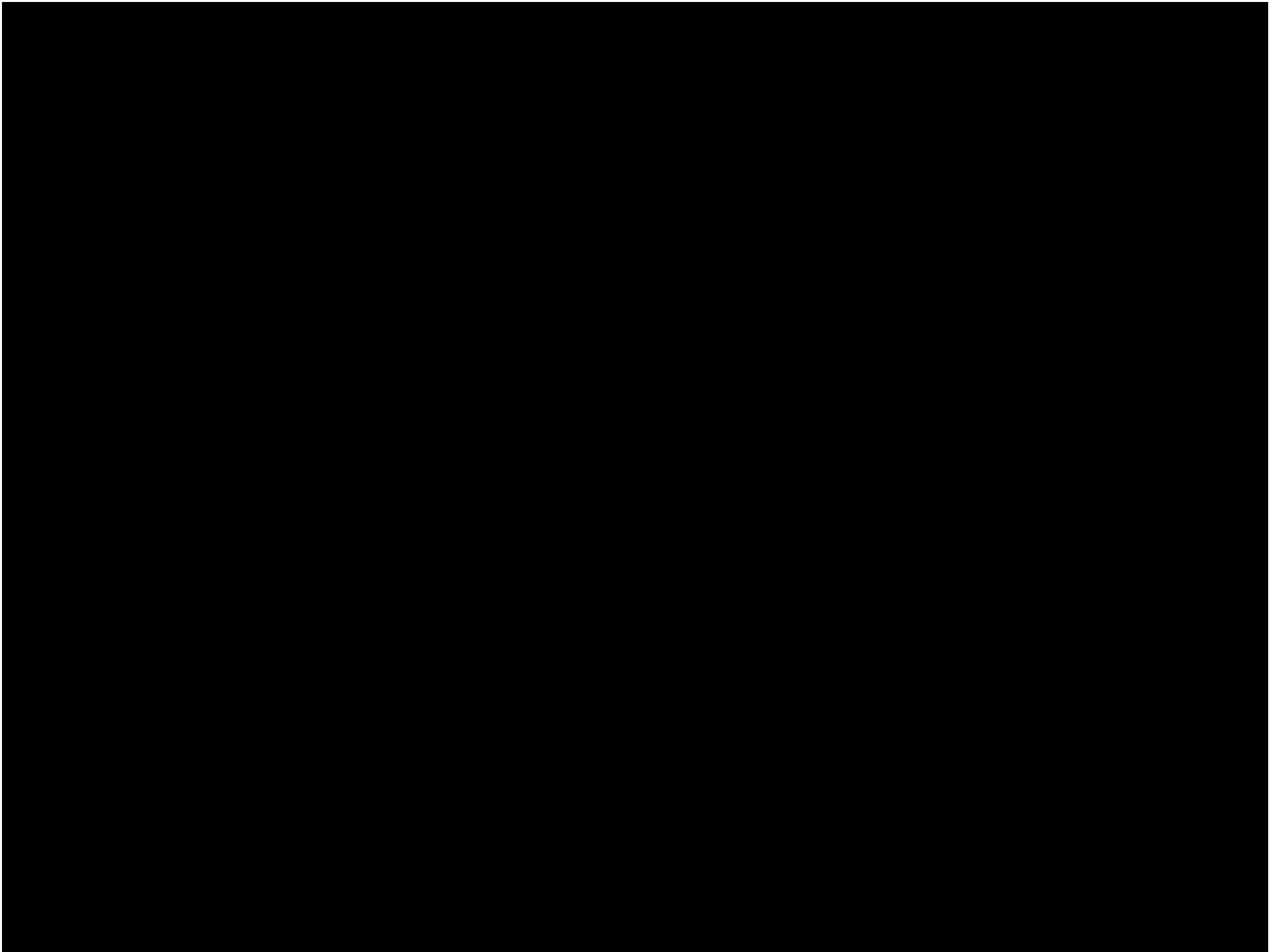


Acknowledgments

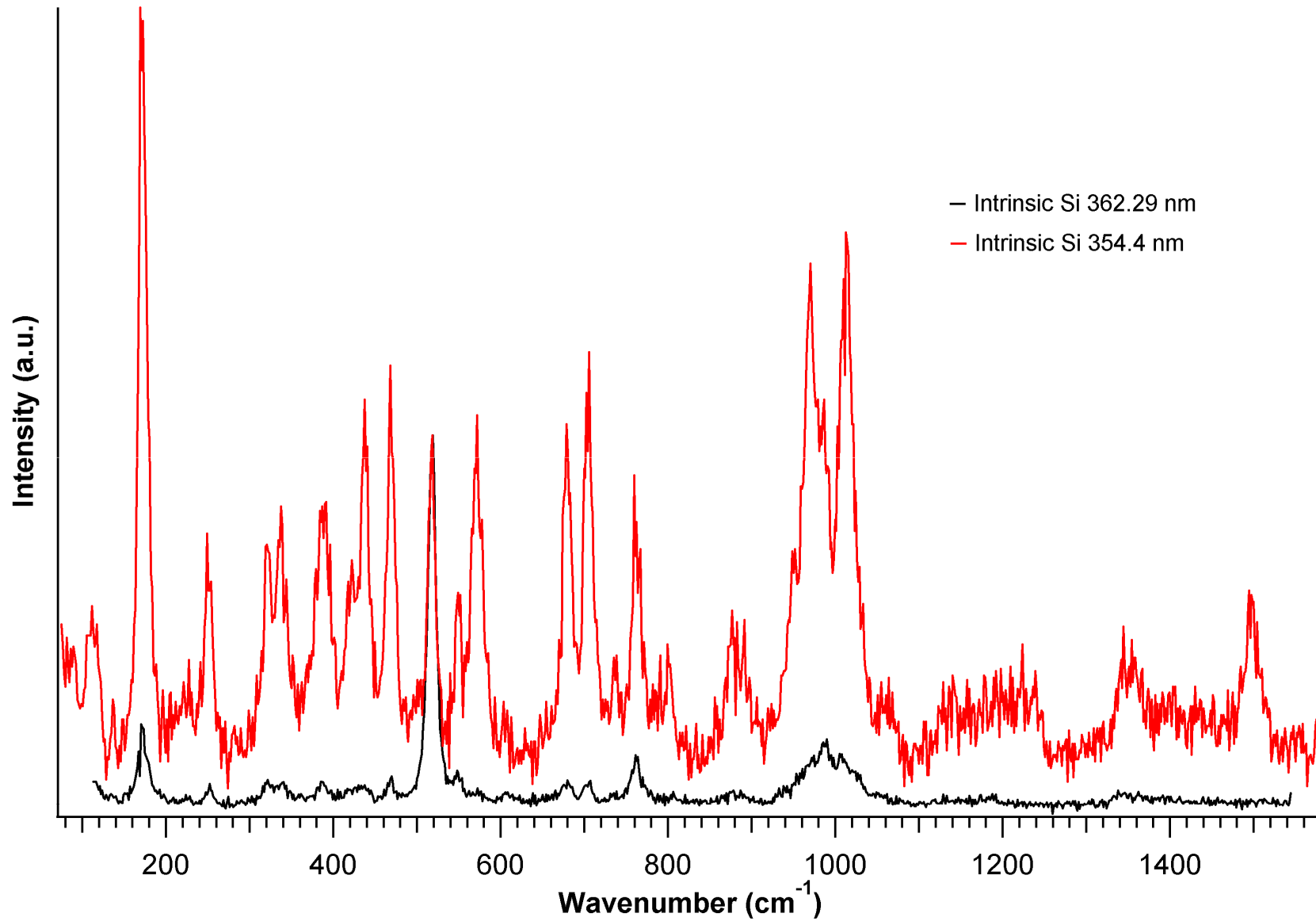
- Keith Williams, Jack Chan and Caixia Bu
- Acar Isin, Jongsoo Yoon, Bob Jones, Wenjing Yin and Josh Gurian
- Mark Turlington and Al Deberardinis (Chemistry)
- Avik Ghosh, Lloyd Harriott, Michael Cabral and Smitha Vasudevan (EE)
- Alex Puretzky and Dave Geohegan (CNMS)
- Shiv Khanna, Meichun Qian and Vince Ong (VCU)

Funding: DARPA, NIRT, LUNA Corp.



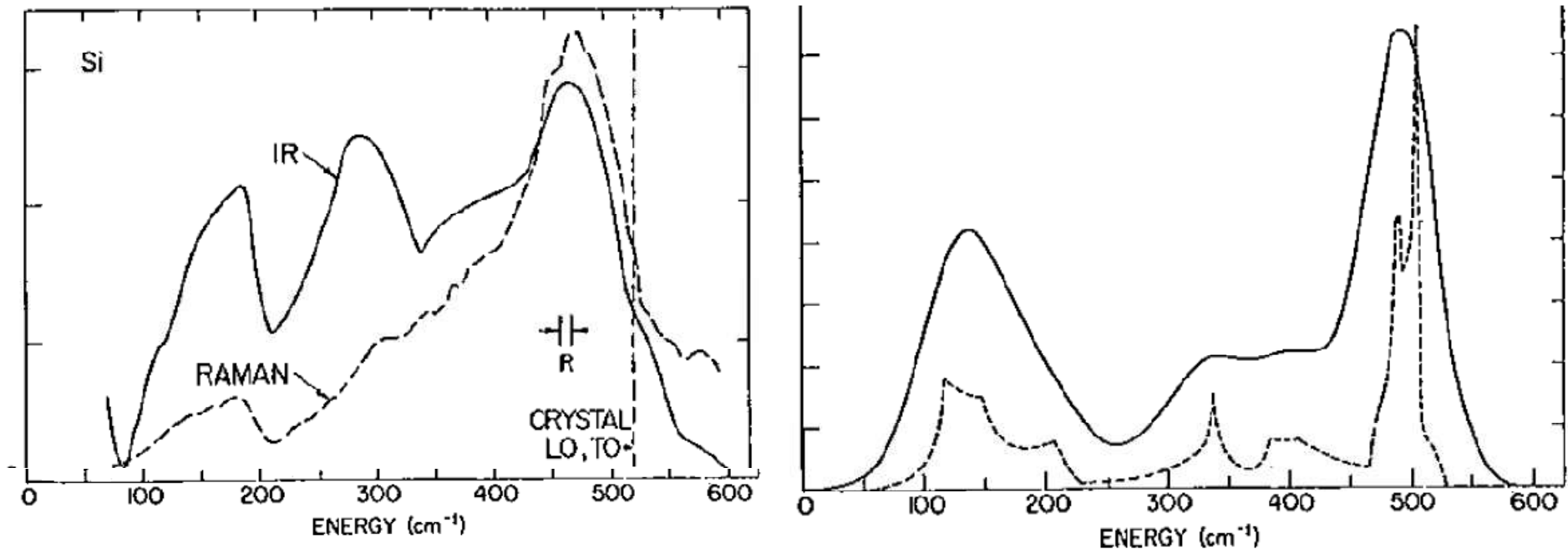


Amorphous Silicon Spectrum



Raman Spectroscopy of Silicon

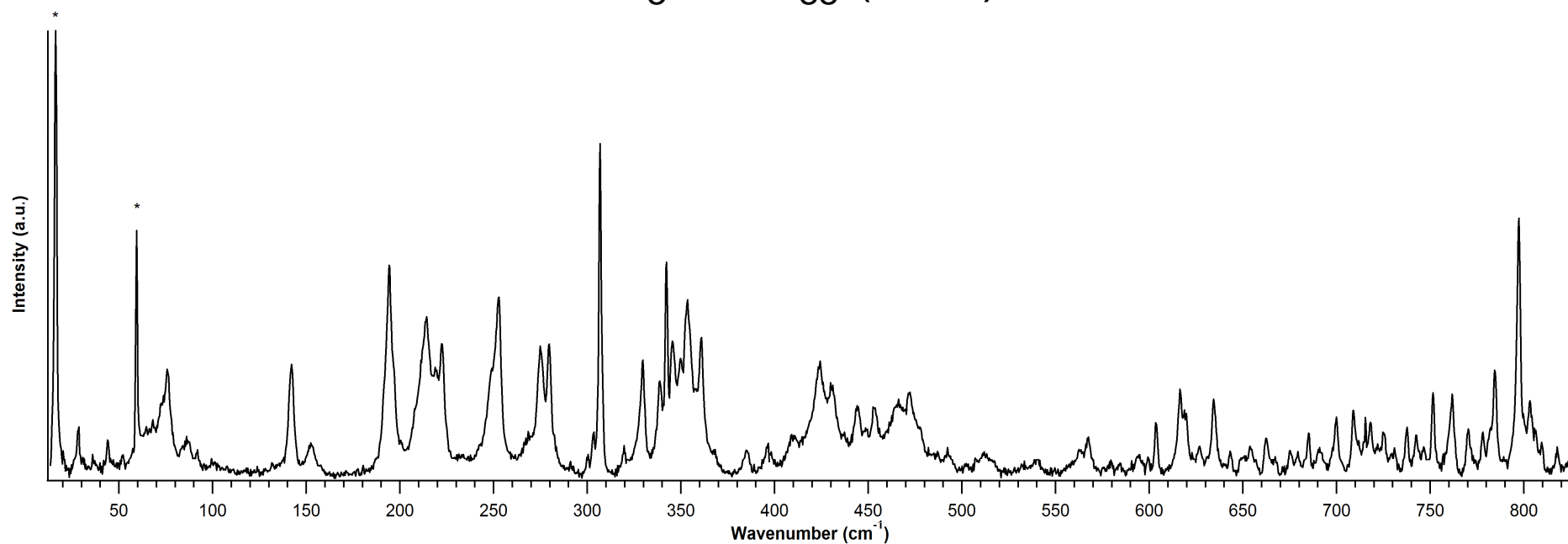
- Crystalline semiconductors exhibit first-order scattering only by phonons with $\mathbf{k} = 0$ (only zone center optical phonon is Raman active)
- In amorphous materials, the first-order Raman spectrum is broad and corresponds to the density of one-phonon states



M. Cardona, *Light Scattering in Solids*, Springer (1975)



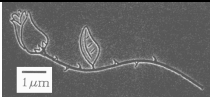
Gd₃N@C₈₈ (90 K)



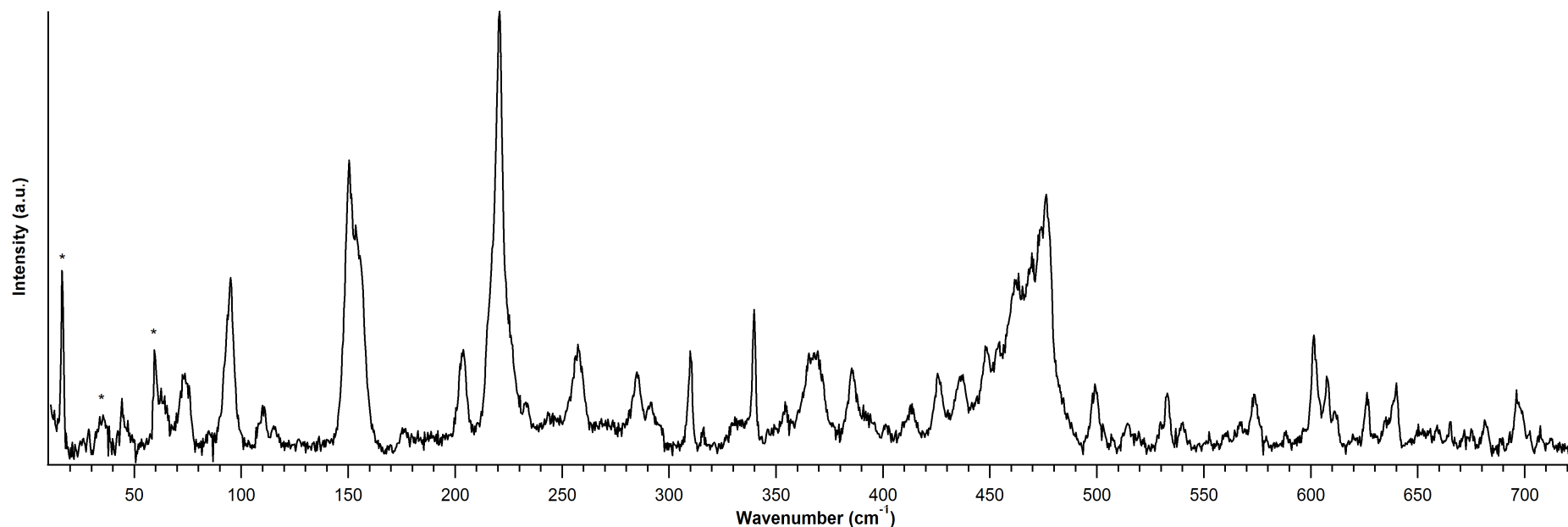
Mode	Raman (cm ⁻¹)	IETS (mV)
	28.5	3.5
	44.3	5.5
	76.0	9.4
	86.0	10.7
	142.2	17.6
	152.5	18.9

Mode	Raman (cm ⁻¹)	IETS (mV)
	194.6	24.1
	214.2	26.5
	222.7	27.6
	252.8	31.3
	274.8	34.1
	279.8	34.7

Mode	Raman (cm ⁻¹)	IETS (mV)
	306.9	38.0
	329.5	40.8
	353.6	43.8
	424.0	52.6
	634.4	78.6
	797.0	98.8



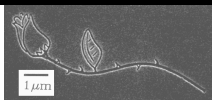
Gd₃N@C₈₄ (90 K)



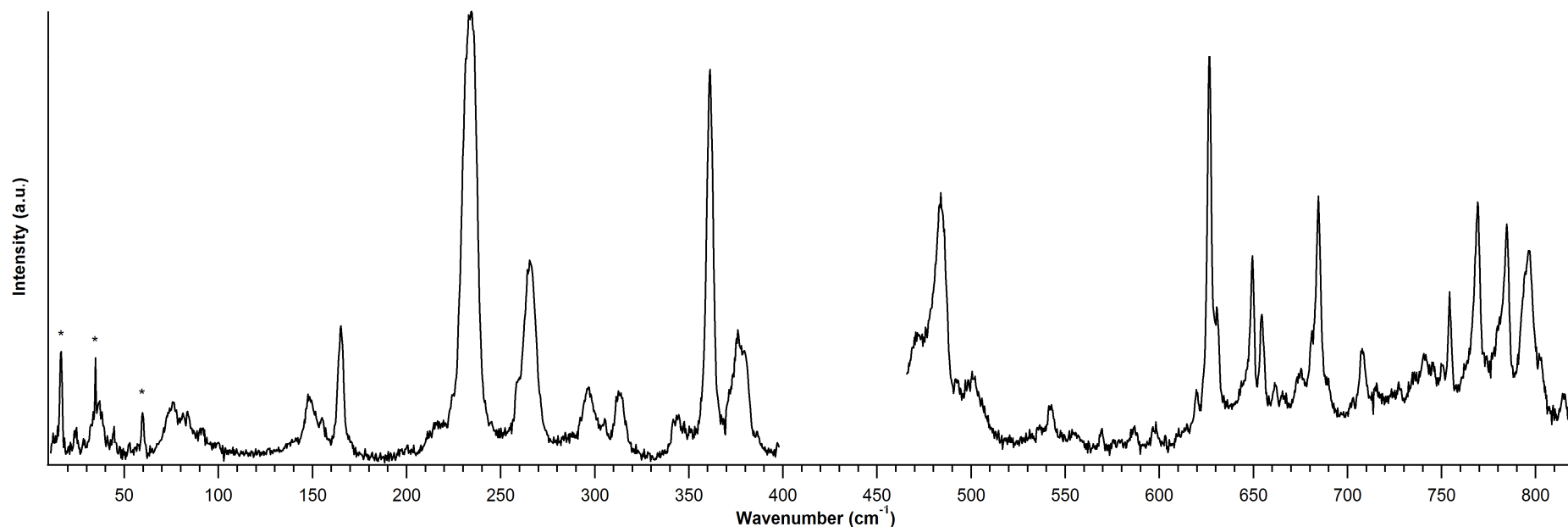
Mode	Raman (cm ⁻¹)	IETS (mV)
	44.2	5.5
	73.7	9.1
	95.0	11.8
	91.5	11.3
	110.8	13.7
	150.4	18.6

Mode	Raman (cm ⁻¹)	IETS (mV)
	203.8	25.3
	220.7	27.4
	257.7	31.9
	310.2	38.5
	339.8	42.1
	367.6	45.6

Mode	Raman (cm ⁻¹)	IETS (mV)
	385.7	47.8
	461.9	57.3
	476.6	59.1
	499.4	61.9
	601.7	74.6
	640.0	79.3



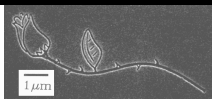
Gd₃N@C₈₀ (90 K)



Mode	Raman (cm ⁻¹)	IETS (mV)
	24.2	3.0
	36.6	4.5
	76.0	9.4
	91.5	11.3
	148.4	18.4
	164.8	20.4

Mode	Raman (cm ⁻¹)	IETS (mV)
	234.1	29.0
	265.7	32.9
	296.4	36.7
	313.2	38.8
	361.0	44.7
	376.1	46.6

Mode	Raman (cm ⁻¹)	IETS (mV)
	483.6	59.9
	626.8	77.7
	684.6	84.9
	769.2	95.3
	784.6	97.3
	797.0	98.8



essential in order for the dips to be observed.

§4. Analysis and Discussion

4.1 Continuum state

Figure 4 shows that dip 1 disappears as the sample is converted into *n*-type through compensation by thermal treatment. This sample treatment neither changes the concentration

of boron impurities, nor introduces any other impurity in the sample. Hence, the dip is observed only if the bound-to-free transition of holes is present. If the acceptor sites are empty because of carrier compensation, the optical phonon cannot be excited even around the acceptor atom. Our experimental results show that the presence of the hole continuum in-

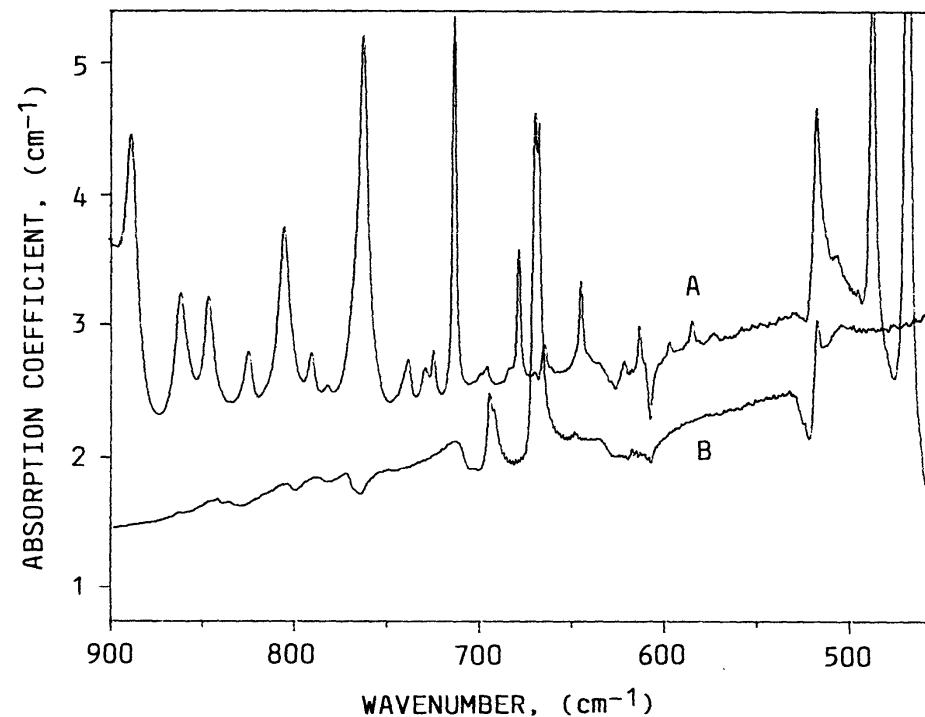


Fig. 4. Infrared absorption spectra of specimens CP-2 before (B) and after (A) heat treatment at 470°C for 550 min.



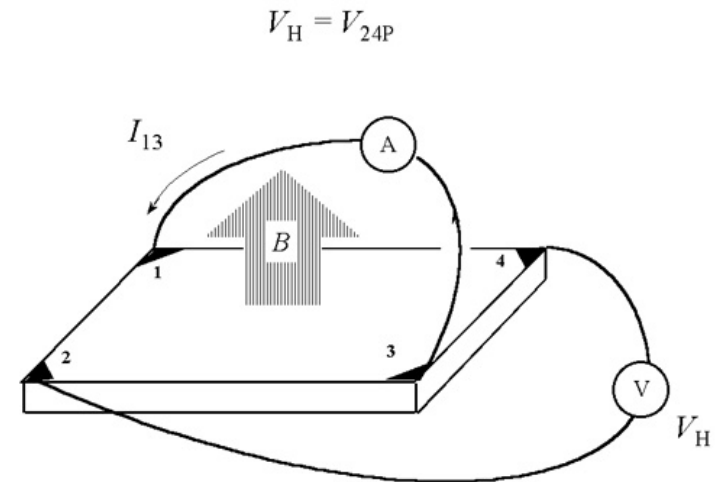
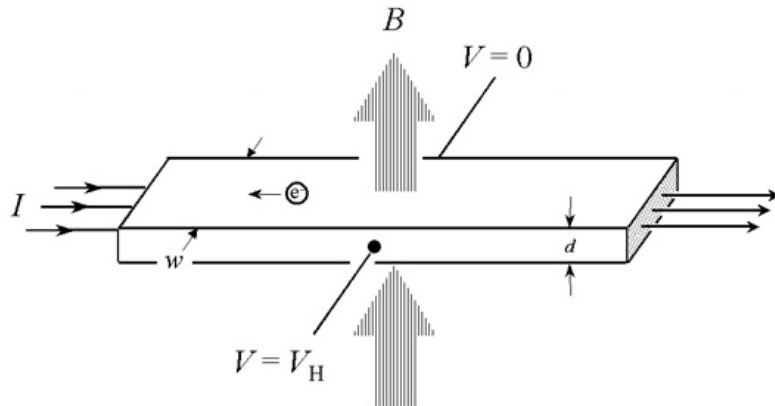
Carrier Concentration Measurements

- Sheet Resistance Measurements

$$\rho = R_s d$$

- Hall Effect Measurements (van der Pauw)

$$n_s = IB/q|V_H|$$



National Institute of Standards and Technology



Research Summary

I. HeCd Laser (325 nm) Capabilities

- i. UV Raman Spectroscopy of Silicon
- ii. Fano Interference (Theory)
- iii. Fano Interference (Experiment)
- iv. Electric Field Dependence Measurements

II. Molecular Doping of Silicon

- i. Decaborane and Allylboronic Acid Pinacol Ester
- ii. Sheet Resistance Measurements

III. Future Work

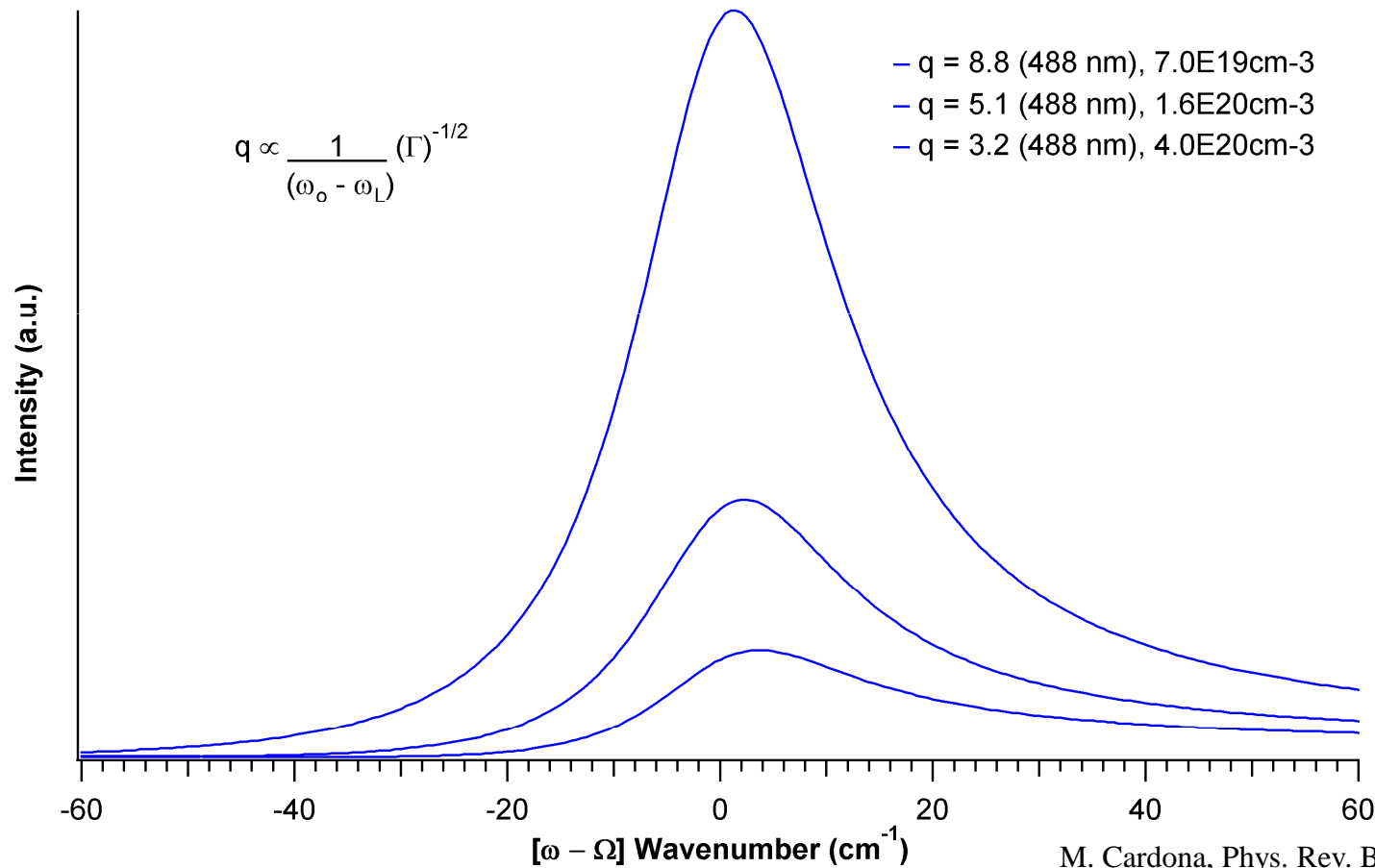
- i. Patterned SurFET Device
- ii. Sensing of Adsorbed Molecules as Surface Scatterers



Debye Length for 488 nm line

$$L_D = \sqrt{\frac{\epsilon_s kT}{q^2 N_A}} = \sqrt{\frac{1.68785 \times 10^7 \text{ m}^{-1}}{N_A}}$$

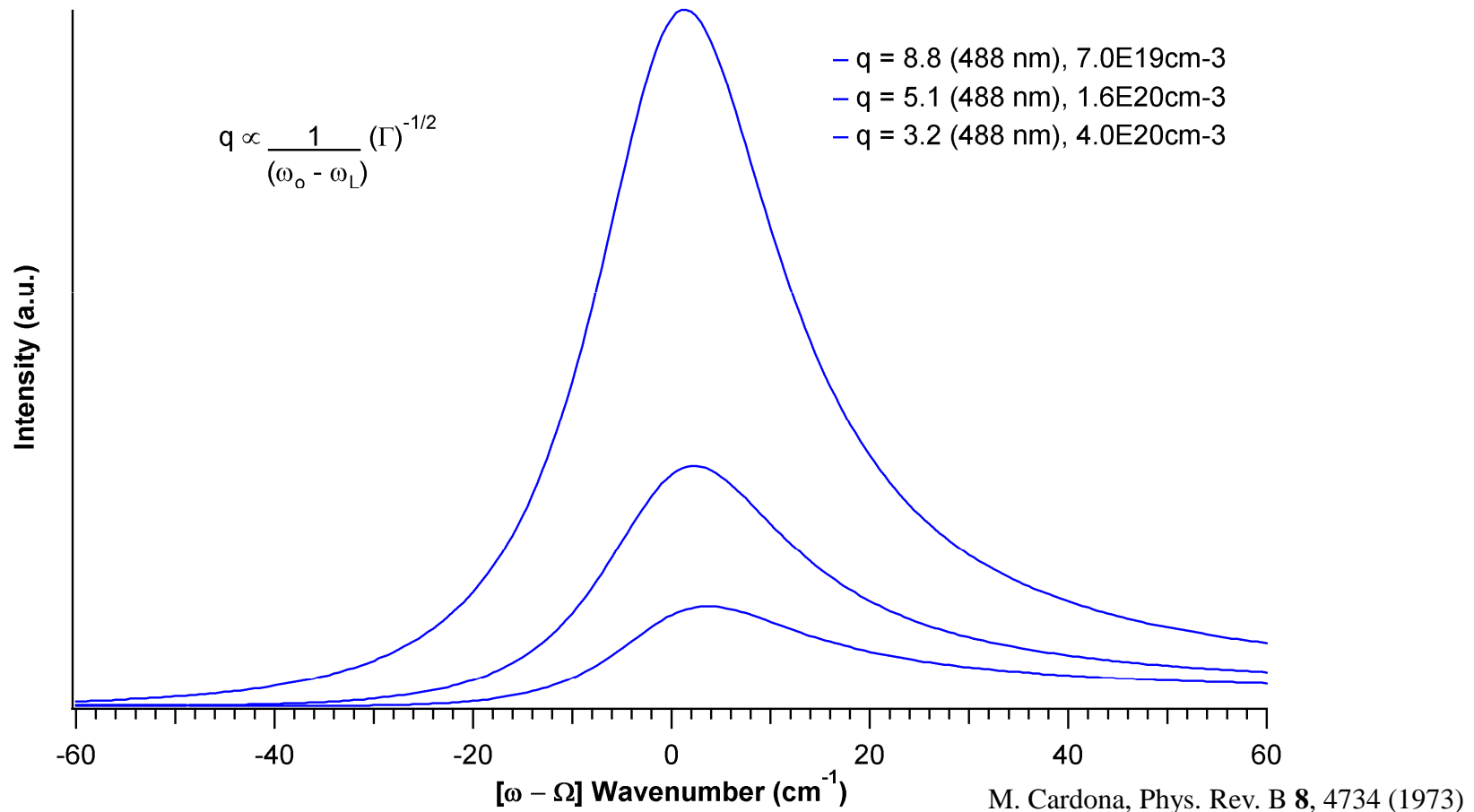
Debye Length (nm)	Doping (m-3)
0.49	7.0E+25
0.32	1.6E+26
0.21	4.0E+26



Depletion Layer for 488 nm line

$$w_d = \sqrt{\frac{2\epsilon_s \phi_s}{qN_A}} = \sqrt{\frac{2\epsilon_s (2\phi_F)}{qN_A}}$$

Depletion Layer (nm)	Doping (m ⁻³)
4.671	7.0E+25
3.145	1.6E+26
2.028	4.0E+26

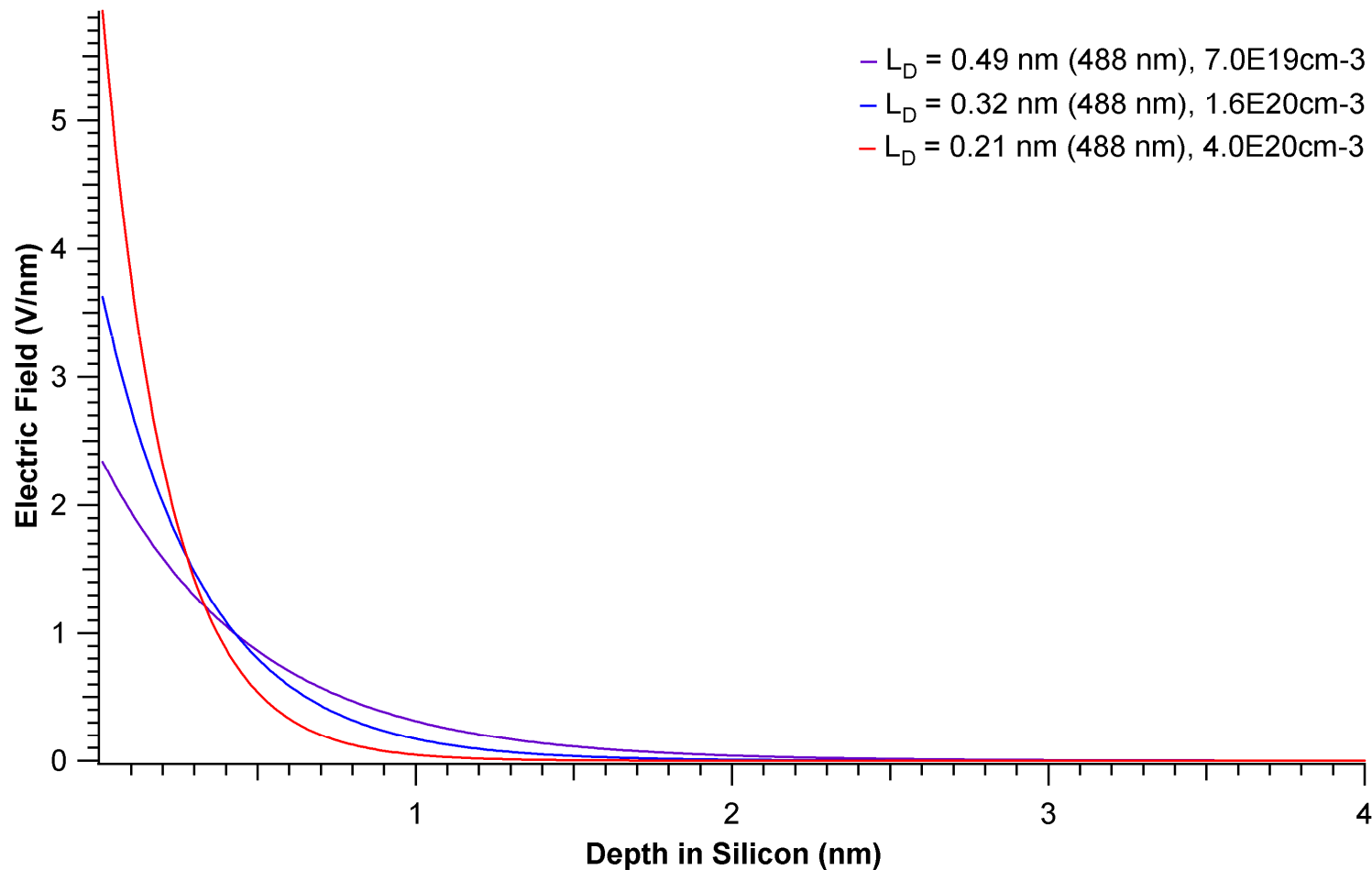


Electric Field Dependence for 488 nm line

$$\vec{E} = \frac{2\phi_F}{L_D} e^{-x/L_D}$$

$$\phi_F = \frac{kT}{q} \ln \frac{N_A}{n_i}$$

Debye Length (nm)	Doping (m-3)
0.49	7.0E+25
0.32	1.6E+26
0.21	4.0E+26



Published Data from Cardona

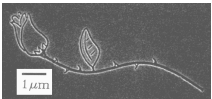
$10^{-19} N$ (cm^{-3})	q	Γ (cm^{-1})			
		$\lambda_L = 4880 \text{ \AA}$	$\lambda_L = 6471 \text{ \AA}$	$\lambda_L = 4880 \text{ \AA}$	$\lambda_L = 6471 \text{ \AA}$
0.6	↑	32.8	18.4	1.1	1.2
1.7		12.4	6.7	2.8	2.8
2.6		14.6	6.4	3.2	3.2
4.0		9.8	4.3	4.4	4.4
7.0		4.7	3.1	6.2	5.9
16		3.7	1.4	8.1	8.1
40		2.8	0.4	10.5	10.7

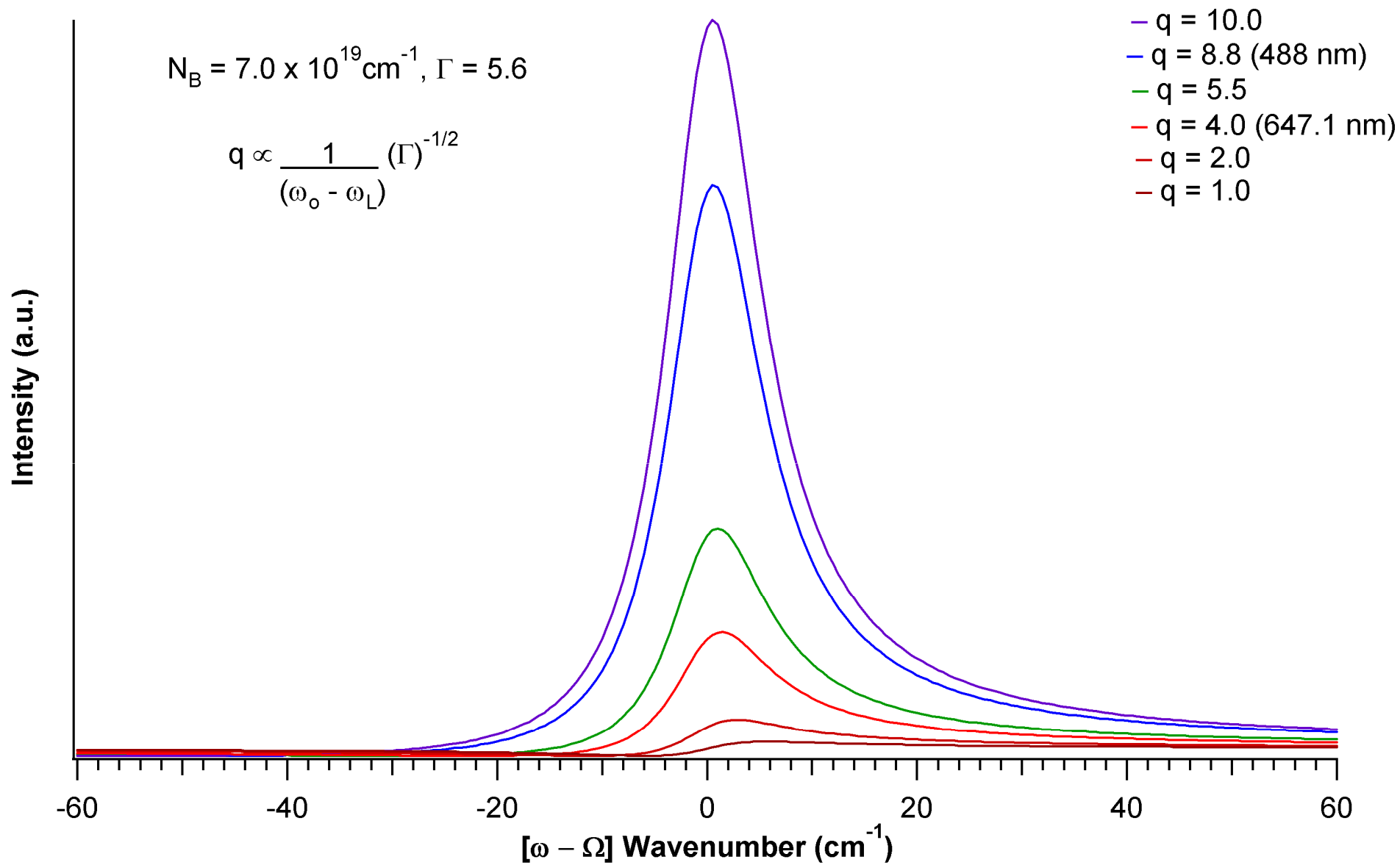
q does show
wavelength
dependence

Γ shows no
wavelength
dependence

$$q \propto \frac{1}{(\omega_o - \omega_L)^{-1/2}}$$

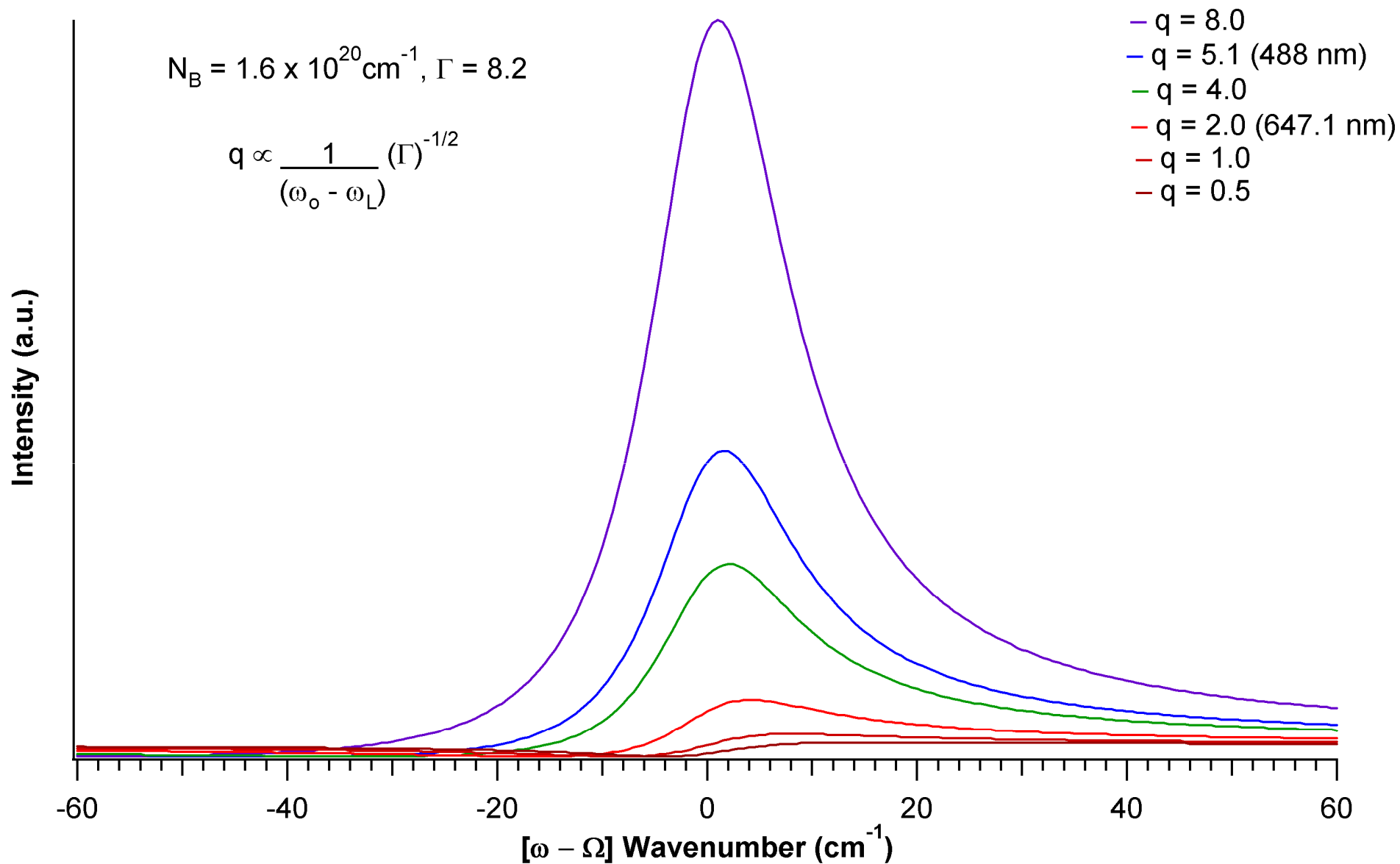
M. Cardona, Phys. Rev. B **8**, 4734 (1973)





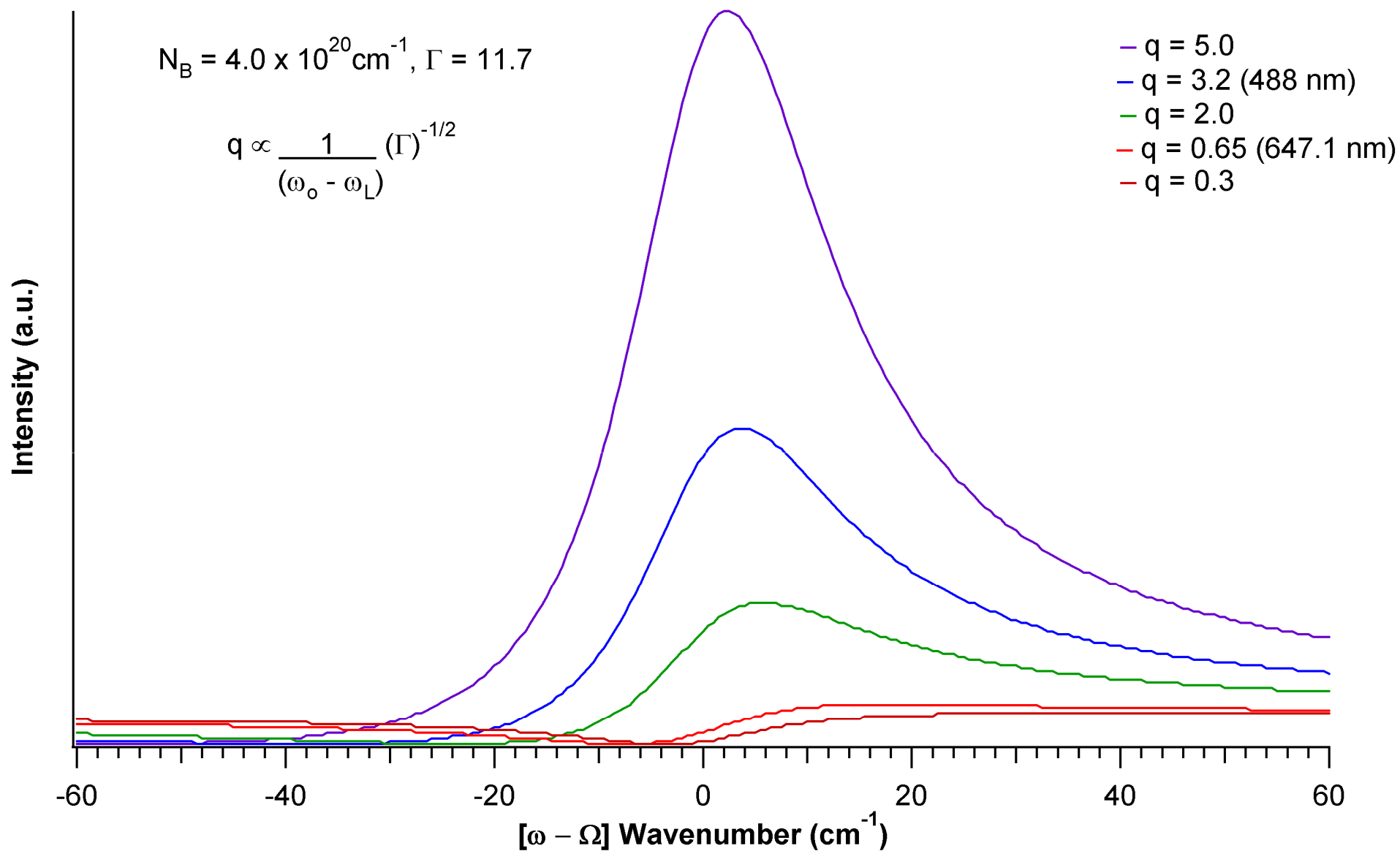
M. Cardona, Phys. Rev. B **8**, 4734 (1973)





M. Cardona, Phys. Rev. B **8**, 4734 (1973)

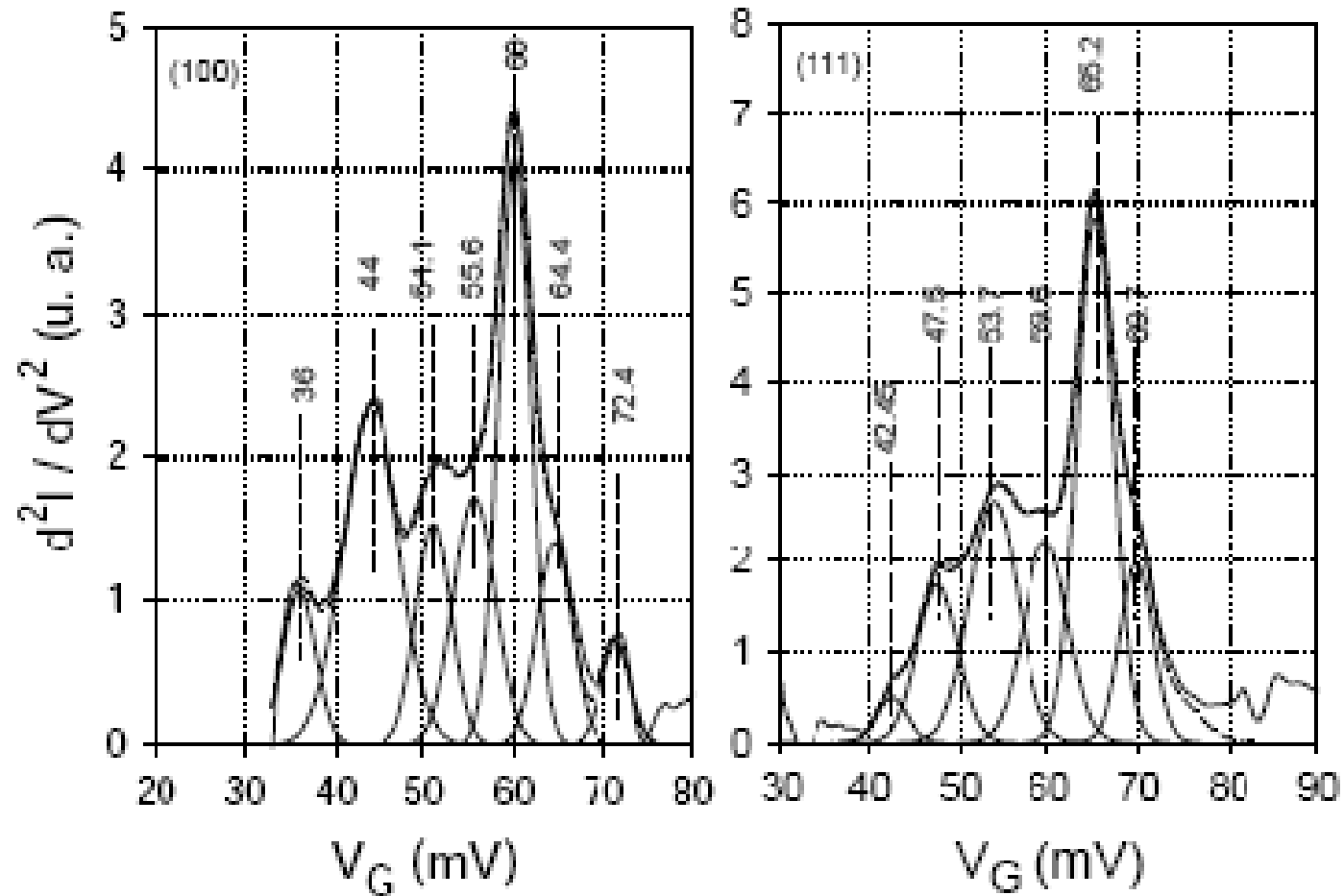




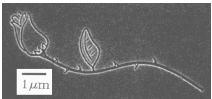
M. Cardona, Phys. Rev. B **8**, 4734 (1973)



IETS of Si(100) and Si(111)

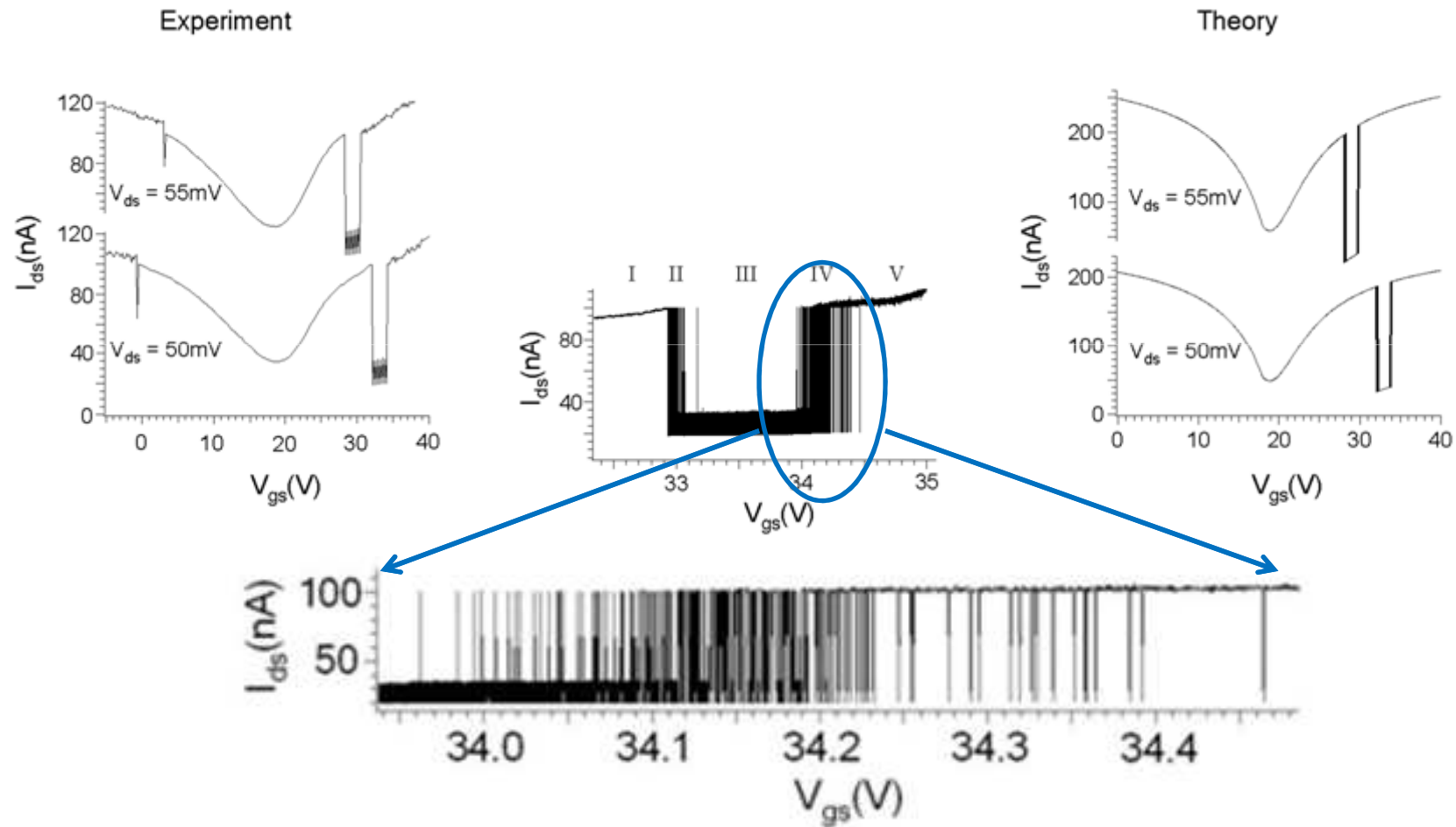


Deconvolution of spectrum for silicon orientation $\langle 100 \rangle$ and $\langle 111 \rangle$.



RTS (Random Telegraph Signals)

- Random trapping and release of charge carriers, observed in MOSFETs and CNT-FETs



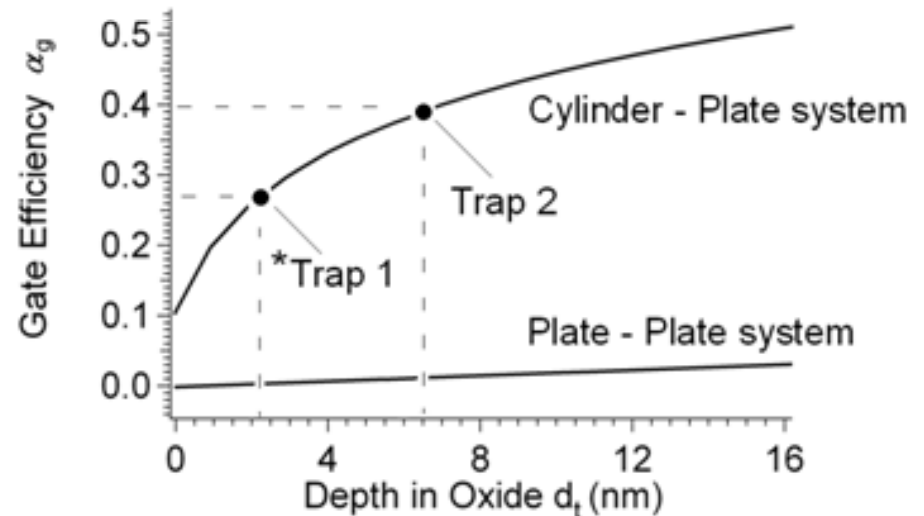
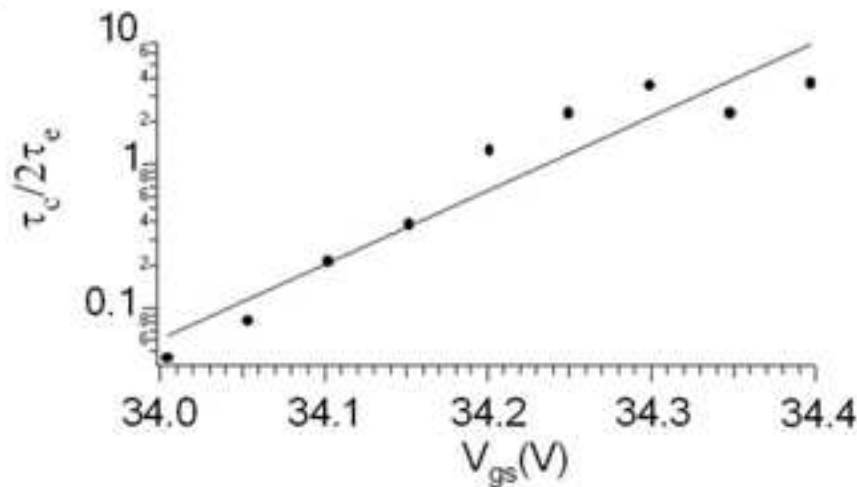
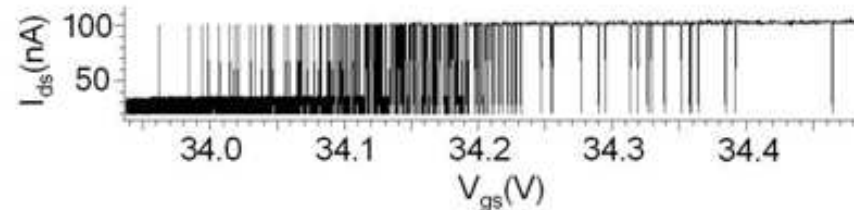
J. Chan *et al.*, *Nano Lett.*, under review



RTS measured in CNT-FET

- Parameters such as trap energy, gate efficiency and trap depth can be determined by analyzing the RTS

$$\frac{\tau_c}{\tau_e} = 2 \exp \left[\frac{-(\epsilon_T - E_F) + \alpha_g |e| (V_{gs} - V_{g0})}{k_B T} \right]$$

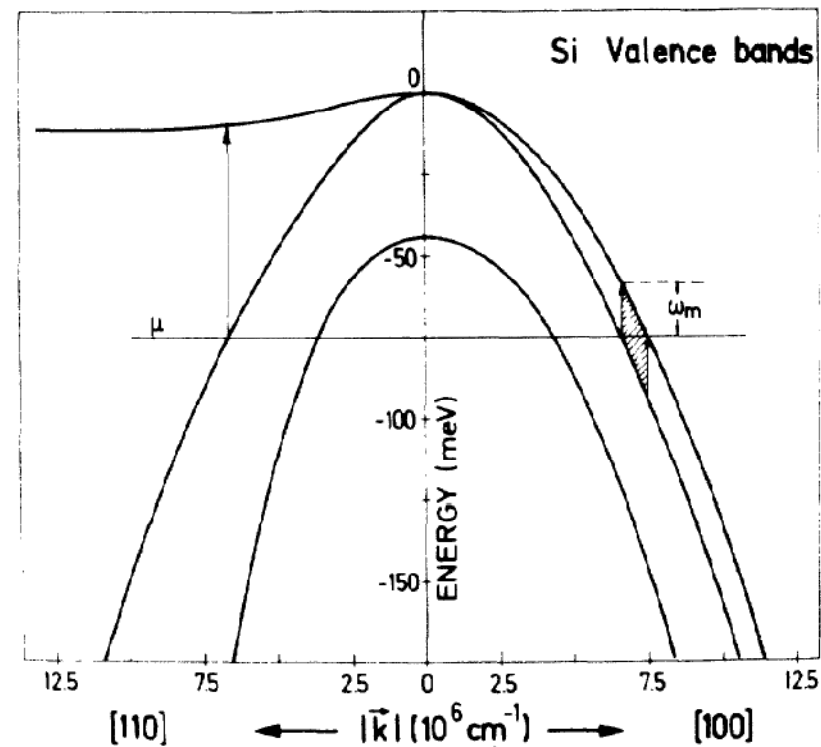


J. Chan *et al.*, *Nano Lett.*, under review



Fano Interference

- The changes in the Raman spectrum of heavily p-type doped silicon with the frequency of the scattering radiation is based on the existence of a continuum of electronic excitations produced by inter-valence band transitions whose energy overlaps with that of the phonon (65 meV)
- The one-electron excitations (infrared forbidden but Raman allowed at $\mathbf{k} = 0$) can also scatter electromagnetic radiation (Raman scattering) giving two competing scattering mechanisms
- One is produced by the continuum of electronic excitations and another by one-phonon scattering
- The continuum extends from a minimum energy ω_m (equal to the smallest separation between bands at the Fermi level) to high energies owing to the flatness of the heavy-hole band in certain directions of k space



M. Cardona, Phys. Rev. B 8, 4734 (1973)



Fano Fitting Parameters

$$I(\epsilon, q) = (q + \epsilon)^2 / (1 + \epsilon^2)$$

$$\epsilon = (\omega - \Omega - \delta\Omega) / \Gamma$$

- Ω is the scattering phonon (critical frequency) and is related to the position of the maximum Ω_m by

$$\Omega = \Omega_m - \Gamma/q$$

- $\delta\Omega$ is the shift of the critical frequency from the intrinsic frequency

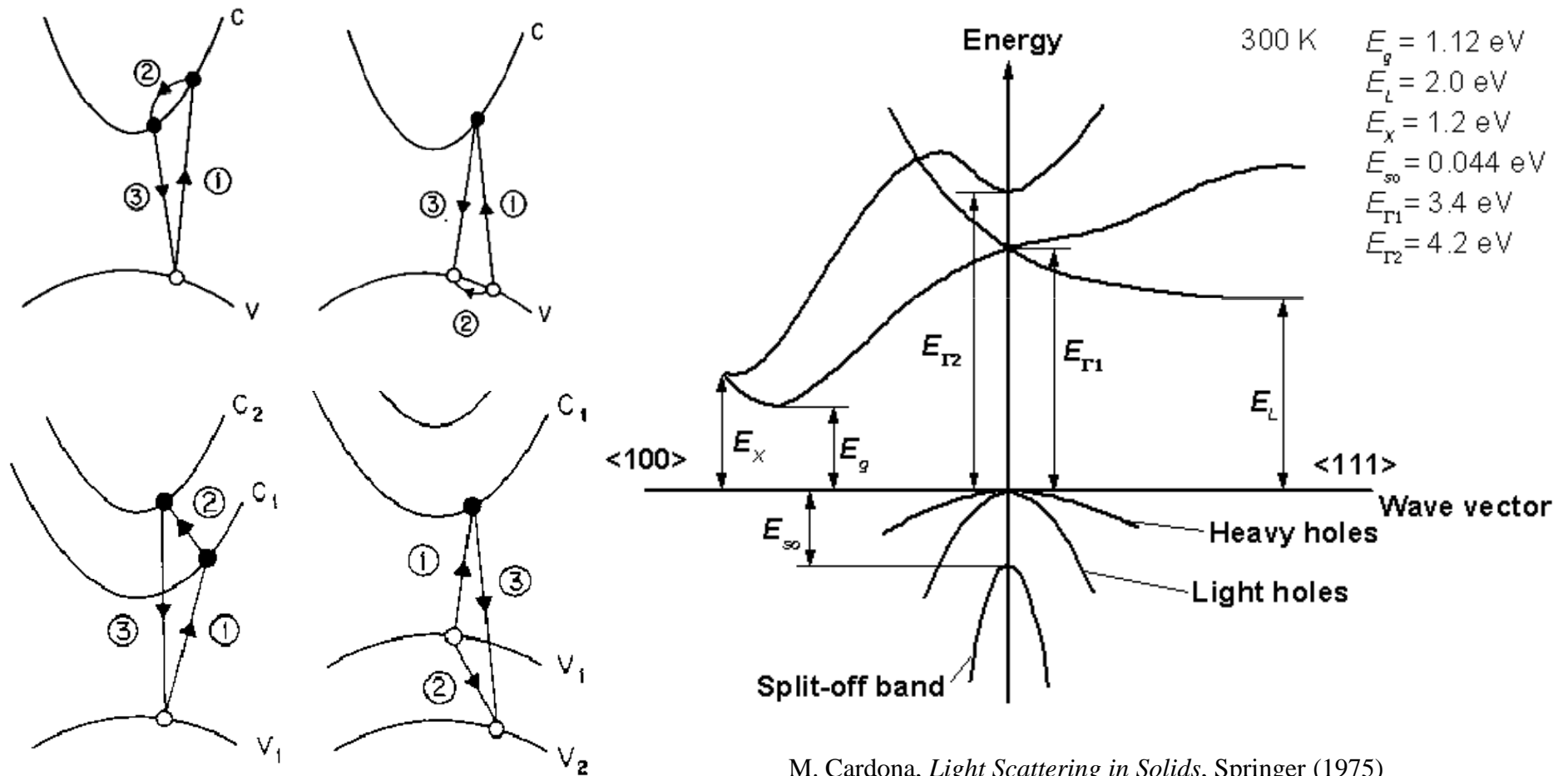
$$\delta\Omega = \Omega - \Omega_{\text{int}}$$

M. Cardona, *Phys. Rev. B* **8**, 4734 (1973)



Intraband and Interband Transitions in Si

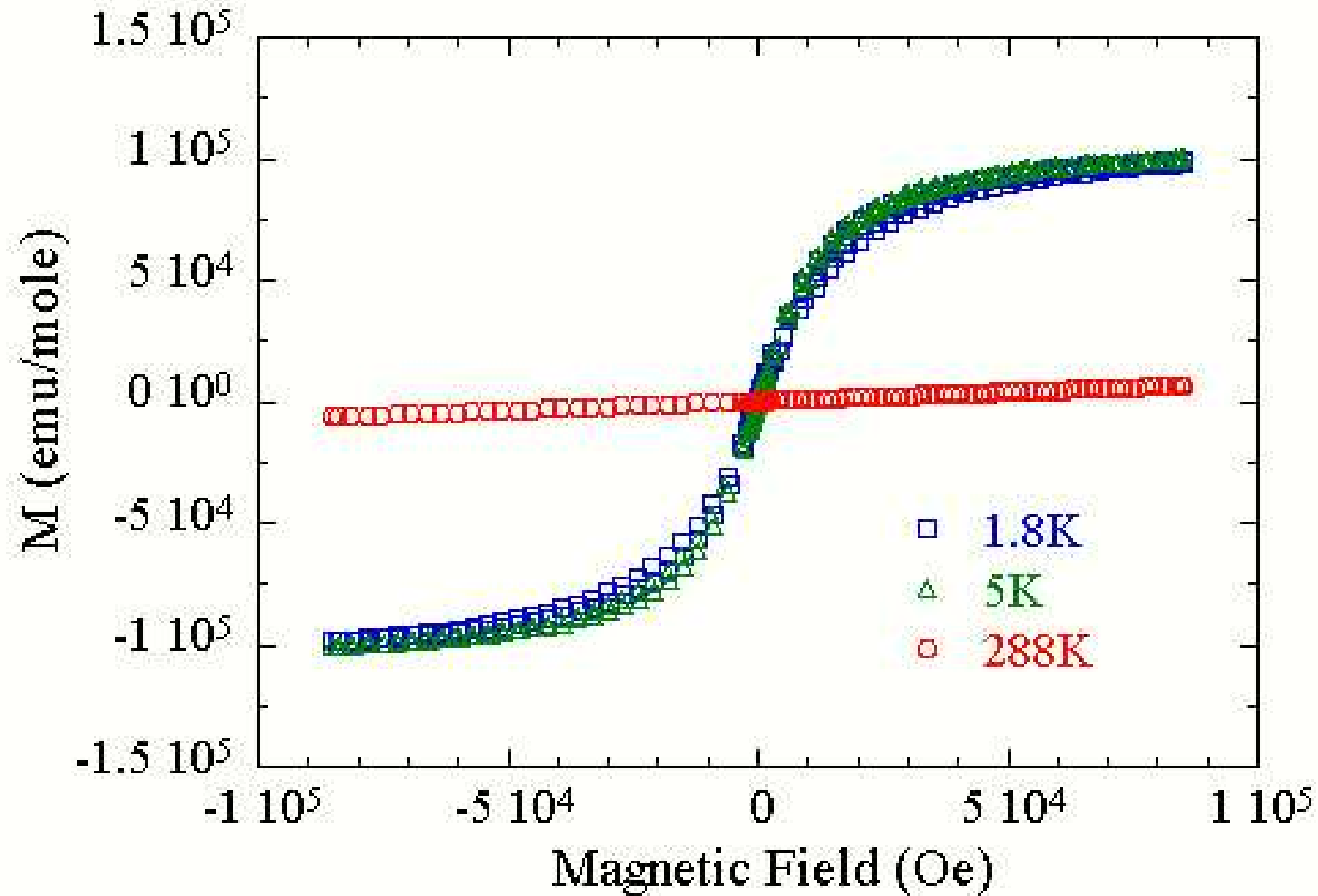
- Cardona approximated the electronic excitation spectrum of silicon as 1D critical points at 3.3 eV and 4.3 eV



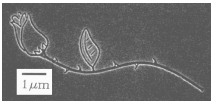
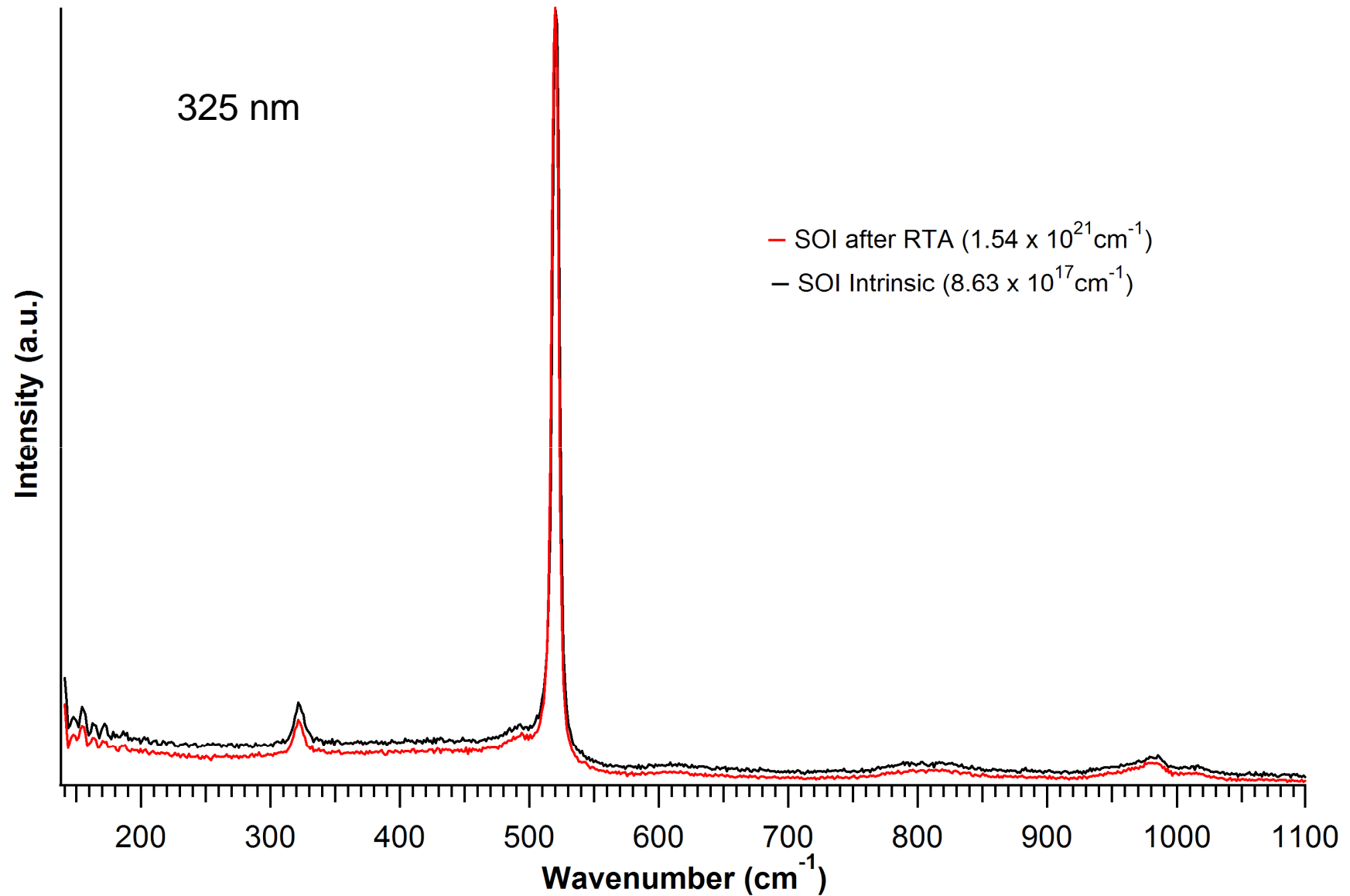
M. Cardona, *Light Scattering in Solids*, Springer (1975)



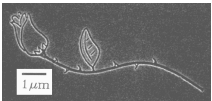
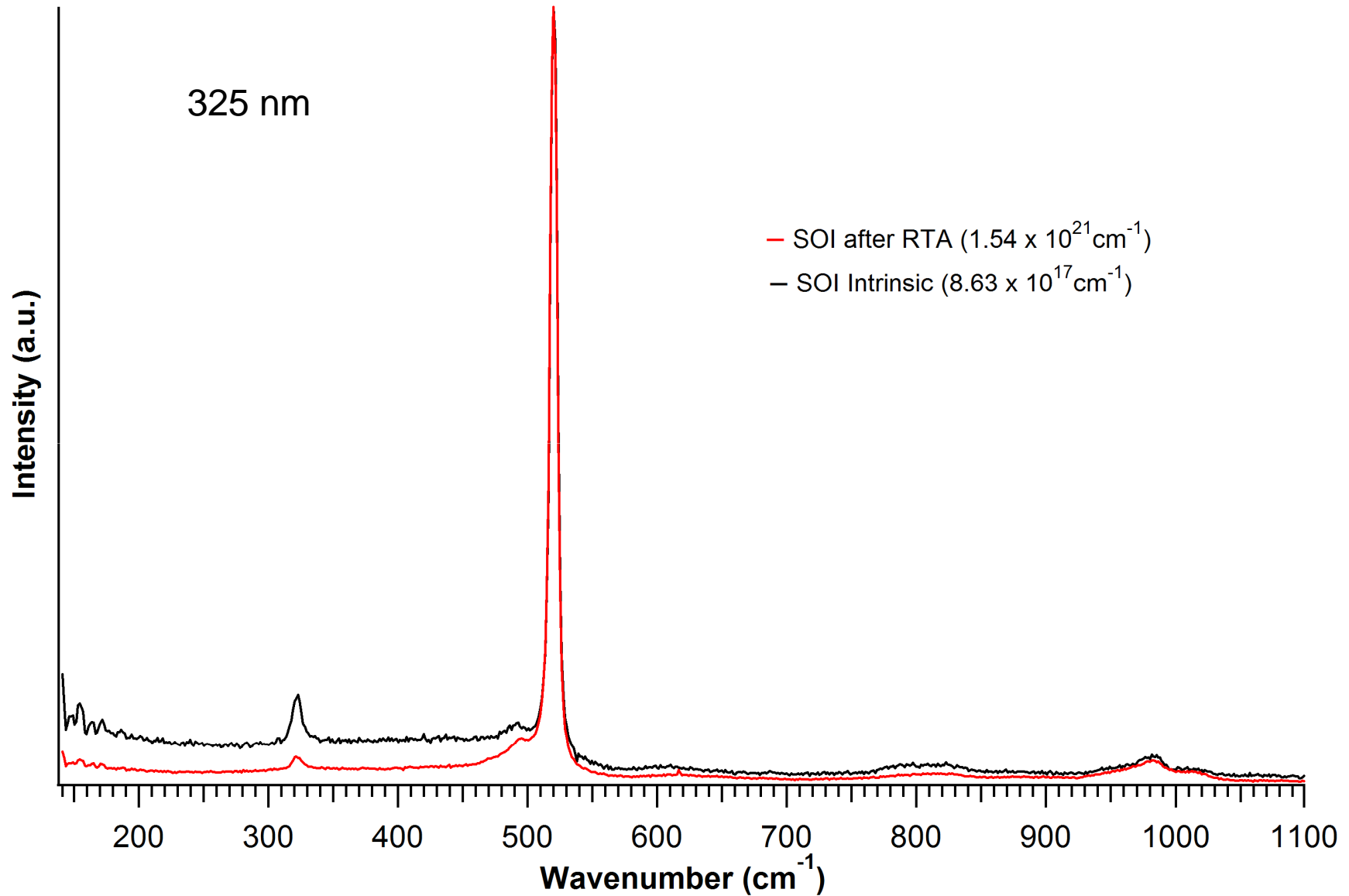
Convincing Data of Local Magnetic Ordering (Gd₃N@C₈₀)



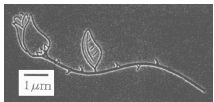
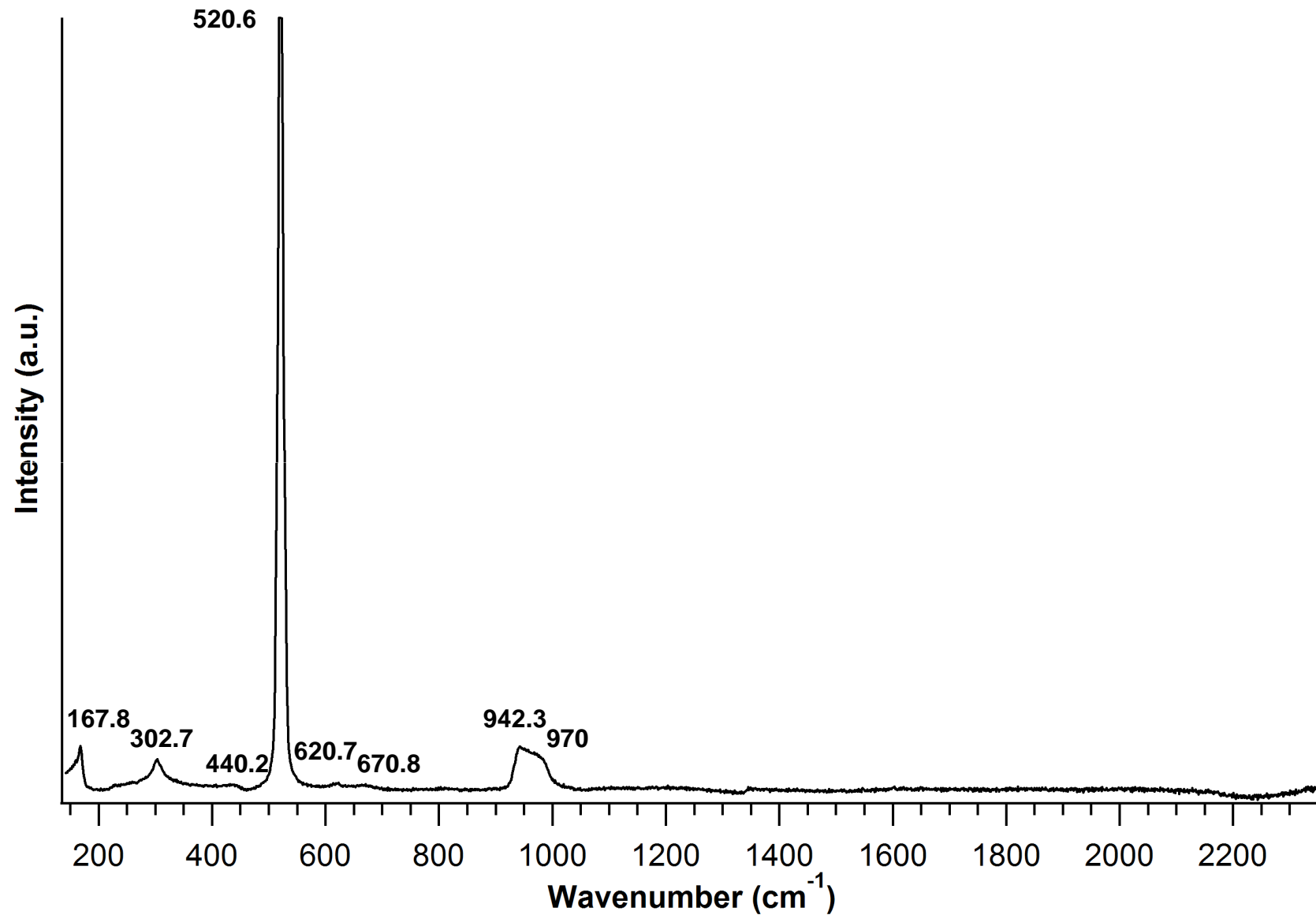
Molecularly Doped SOI (75 nm)



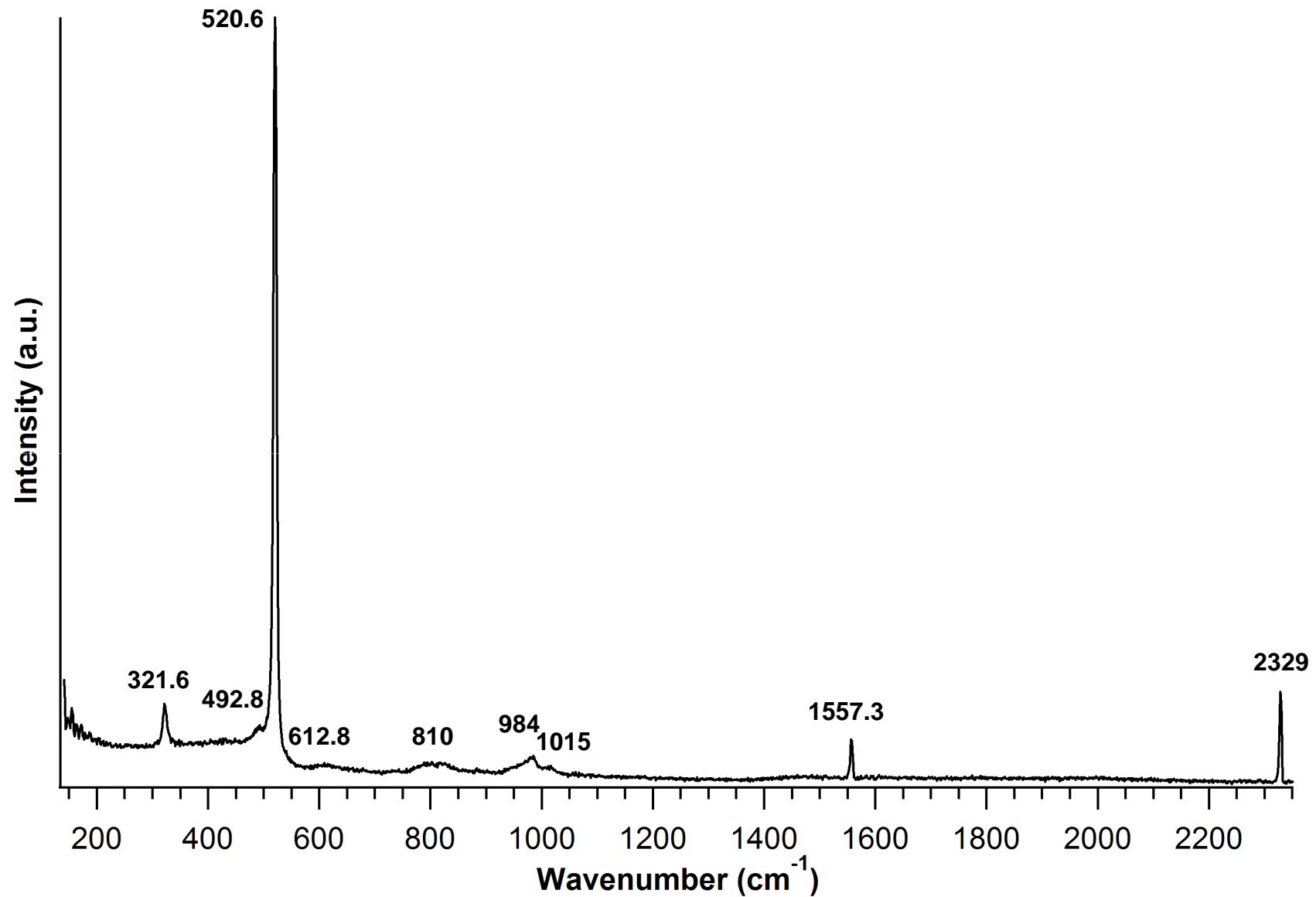
Molecularly Doped SOI (23 nm)



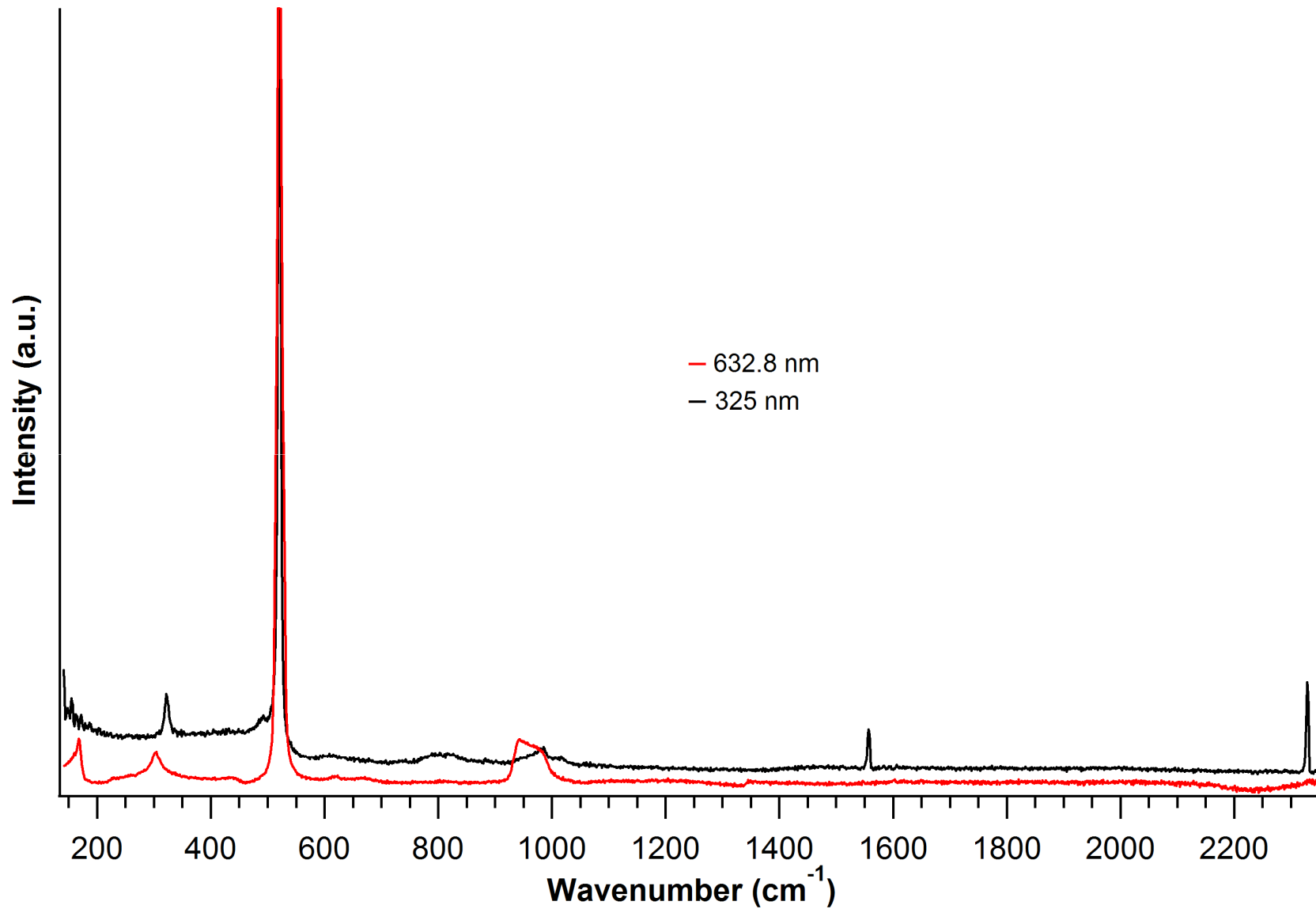
Intrinsic Silicon Spectrum (632.8 nm)



Intrinsic Silicon Spectrum (325 nm)



Intrinsic Silicon Spectrum

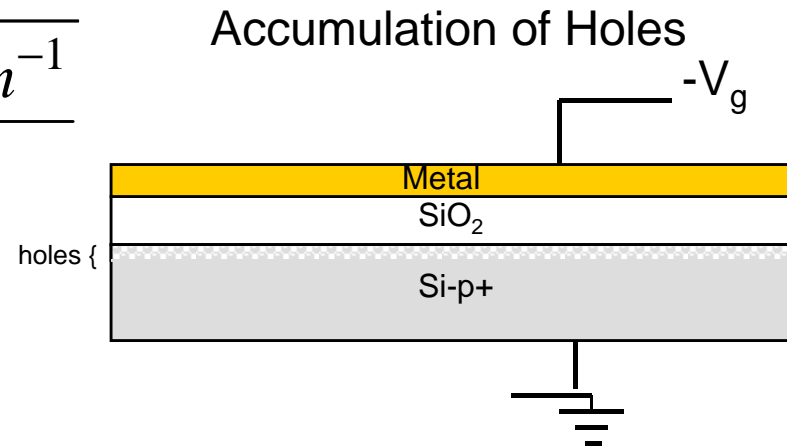


Field Dependence Considerations

- Debye Length

$$L_D = \sqrt{\frac{\epsilon_s kT}{q^2 N_A}} = \sqrt{\frac{1.68785 \times 10^7 \text{ m}^{-1}}{N_A}}$$

For $N_A = 1 \times 10^{19} \text{ cm}^{-3}$, $L_D = 1.299 \text{ nm}$

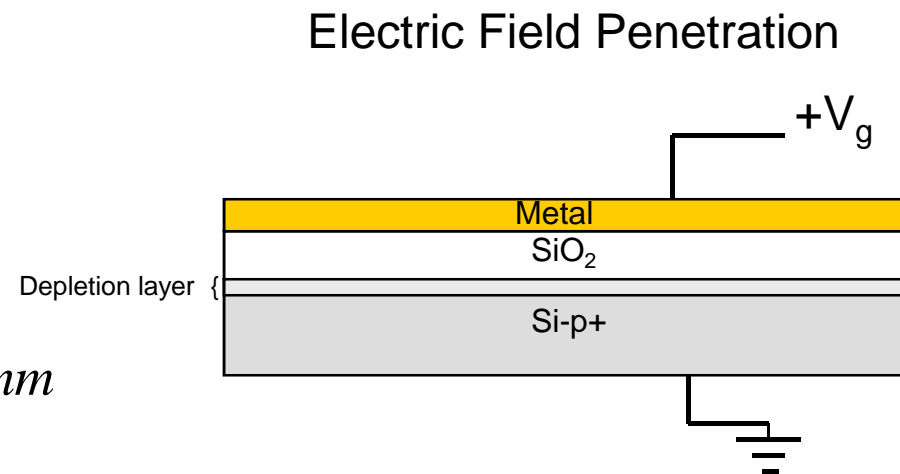


- Depletion Layer

$$w_d = \sqrt{\frac{2\epsilon_s \phi_s}{qN_A}} = \sqrt{\frac{2\epsilon_s (2\phi_F)}{qN_A}}$$

$$\phi_F = \frac{kT}{q} \ln \frac{N_A}{n_i}$$

For $N_A = 1 \times 10^{19} \text{ cm}^{-3}$, $w_d = 11.82 \text{ nm}$

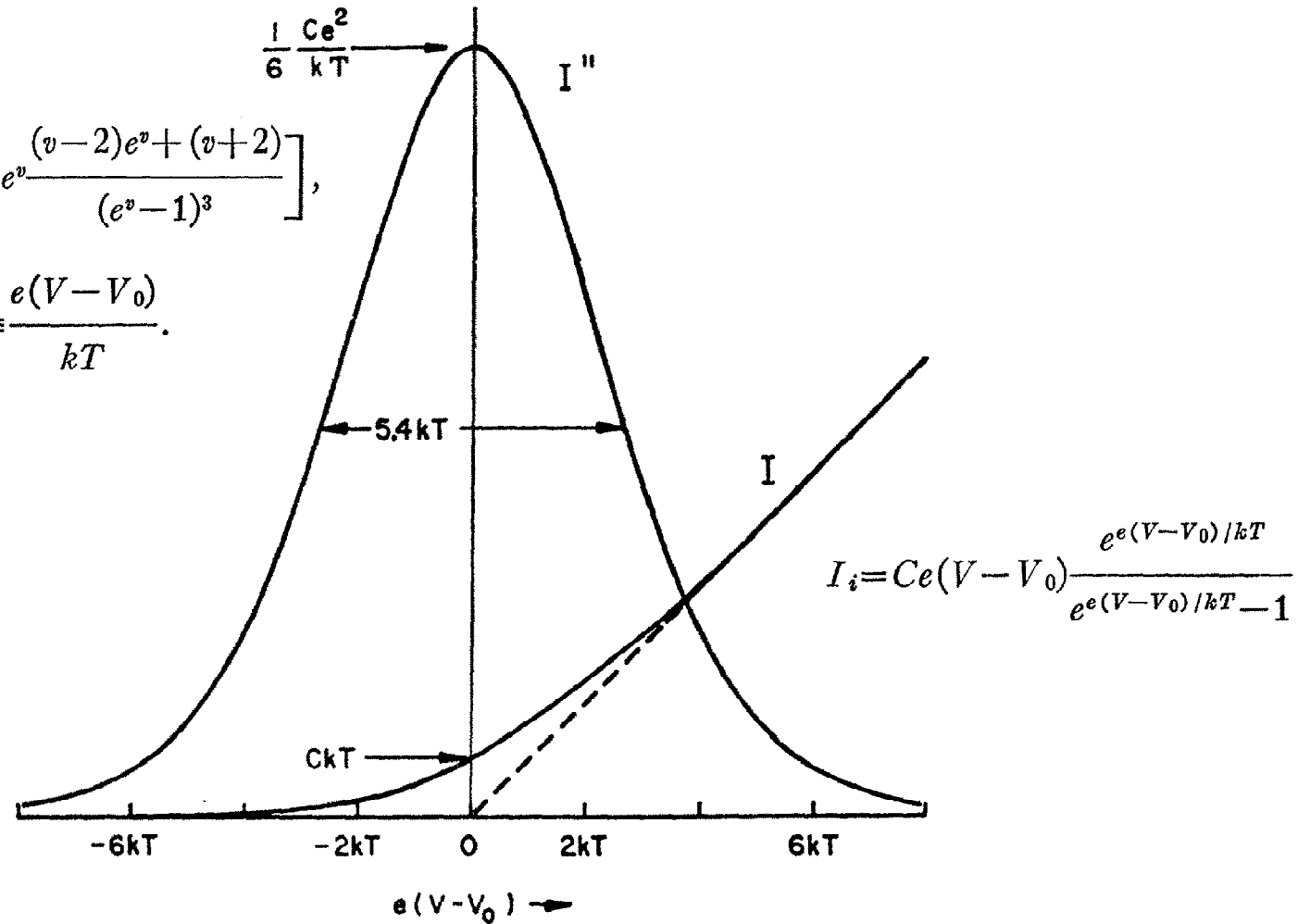


Inelastic Electron Tunneling Spectroscopy (IETS)

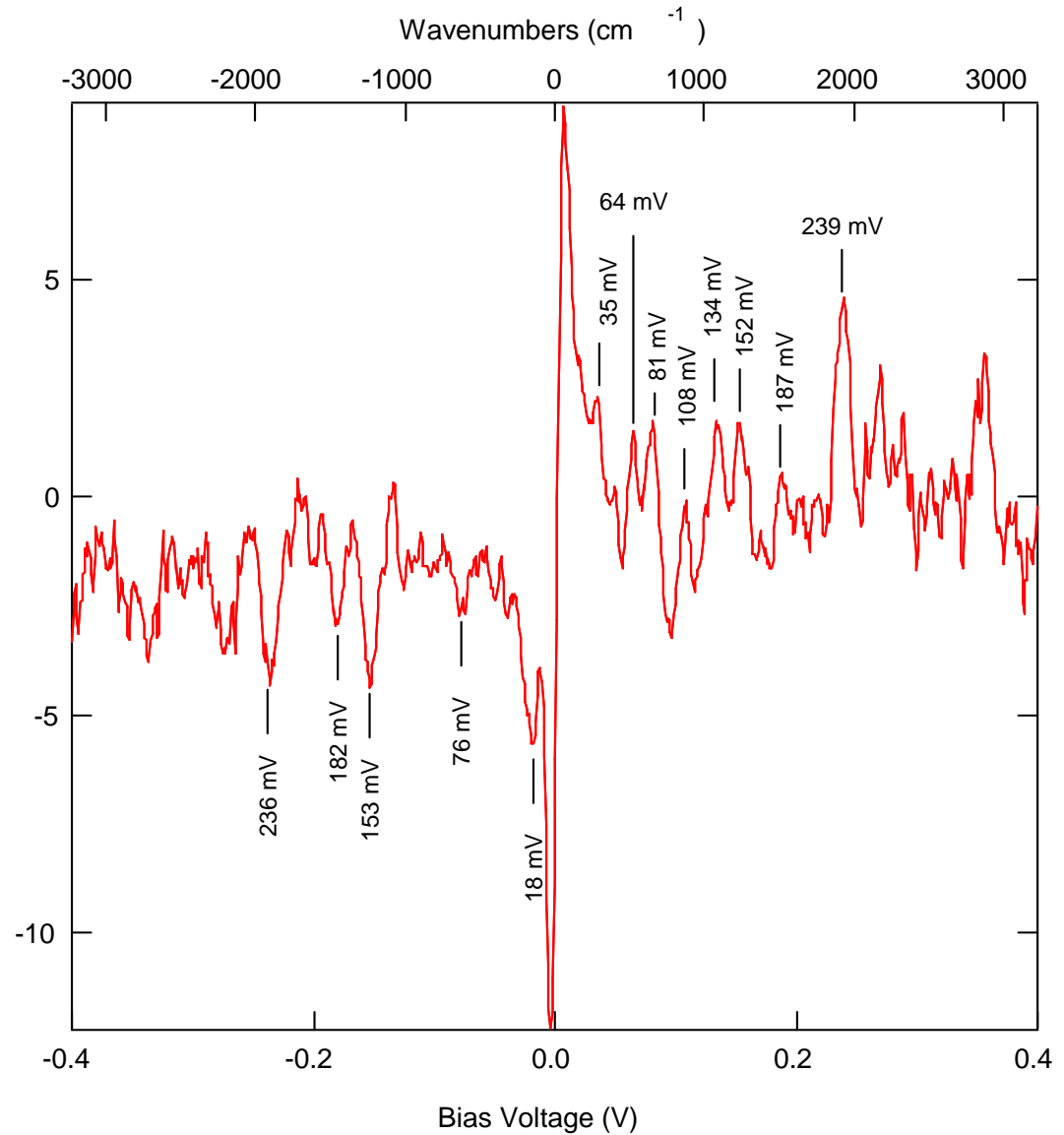
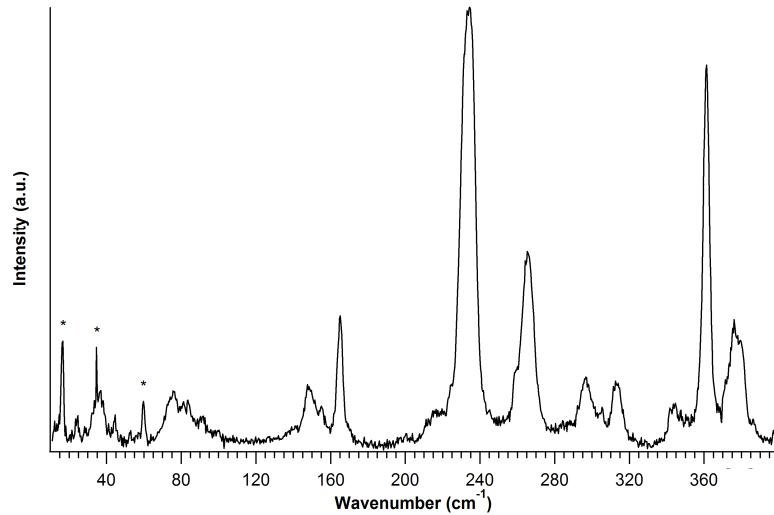
where

$$\frac{d^2 I_i}{dV^2} = C \frac{e^2}{kT} \left[e^v \frac{(v-2)e^v + (v+2)}{(e^v - 1)^3} \right],$$

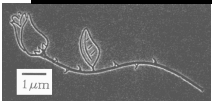
$$v \equiv \frac{e(V - V_0)}{kT}.$$



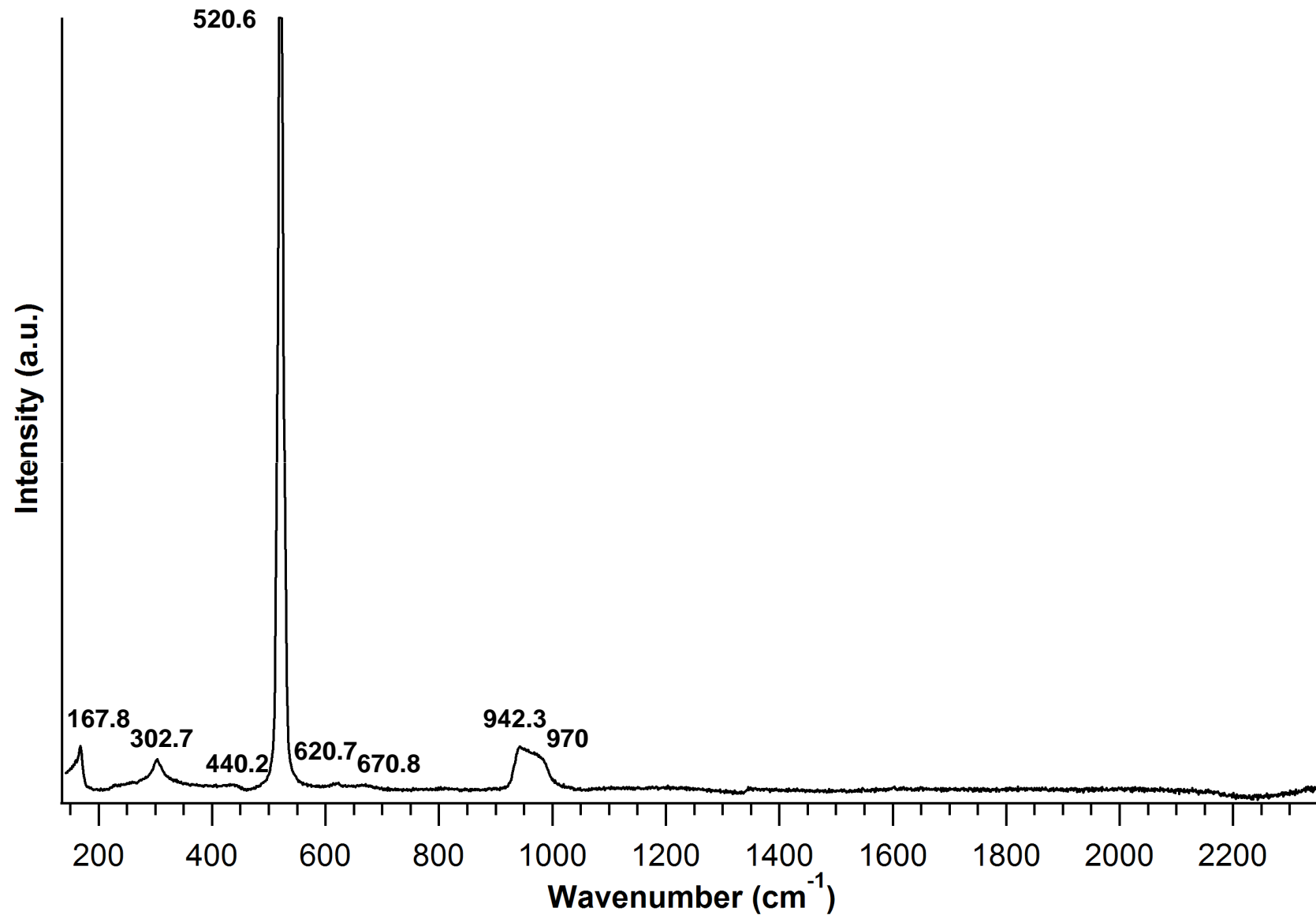
Gd₃N@C₈₀ (Raman and IETS)



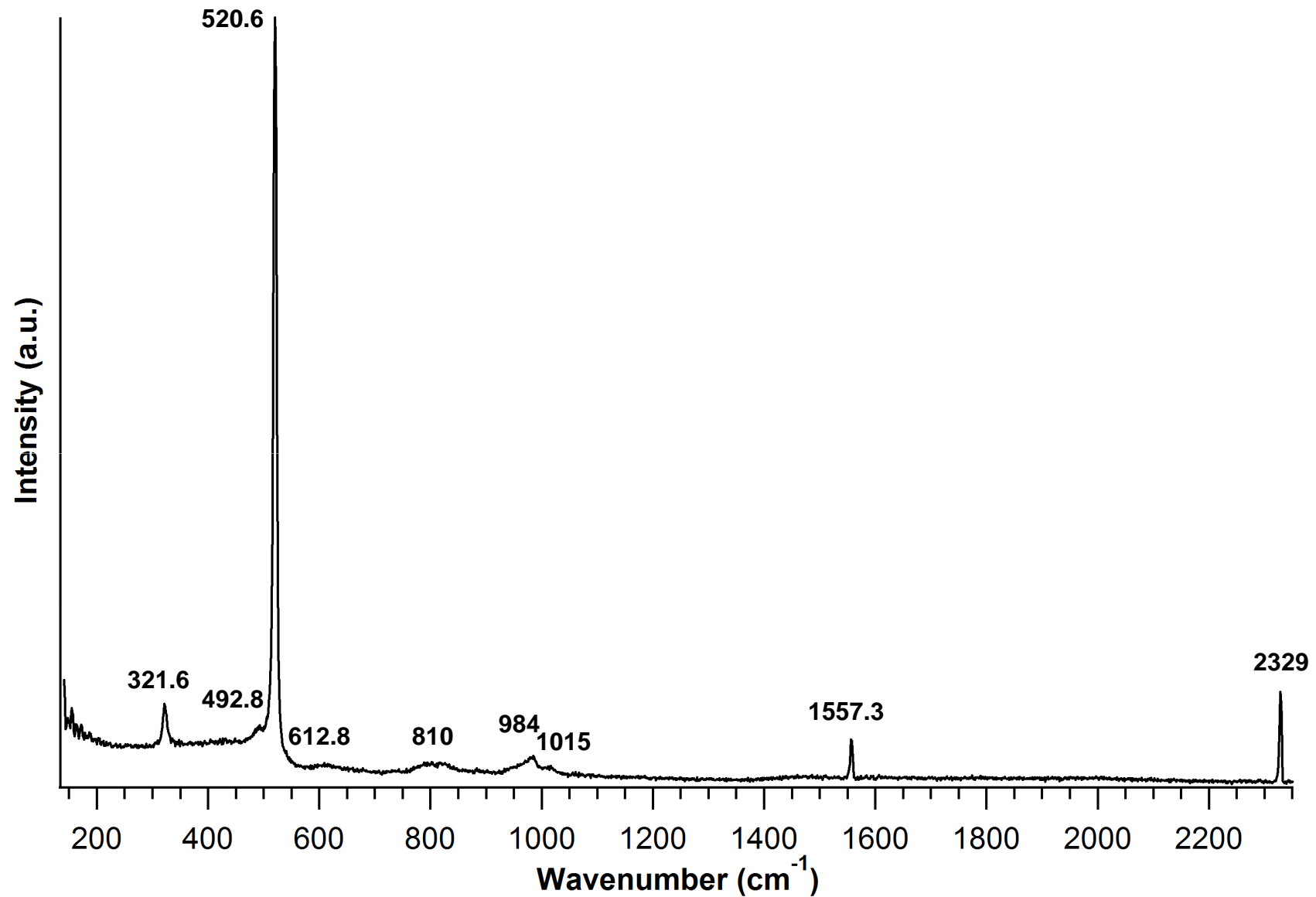
Mode	Raman (cm ⁻¹)	IETS (mV)
	148.4	18.4
	265.7	32.9
	296.4	36.7
	483.6	59.9
	626.8	77.7
	684.6	84.9



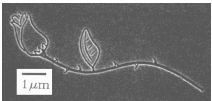
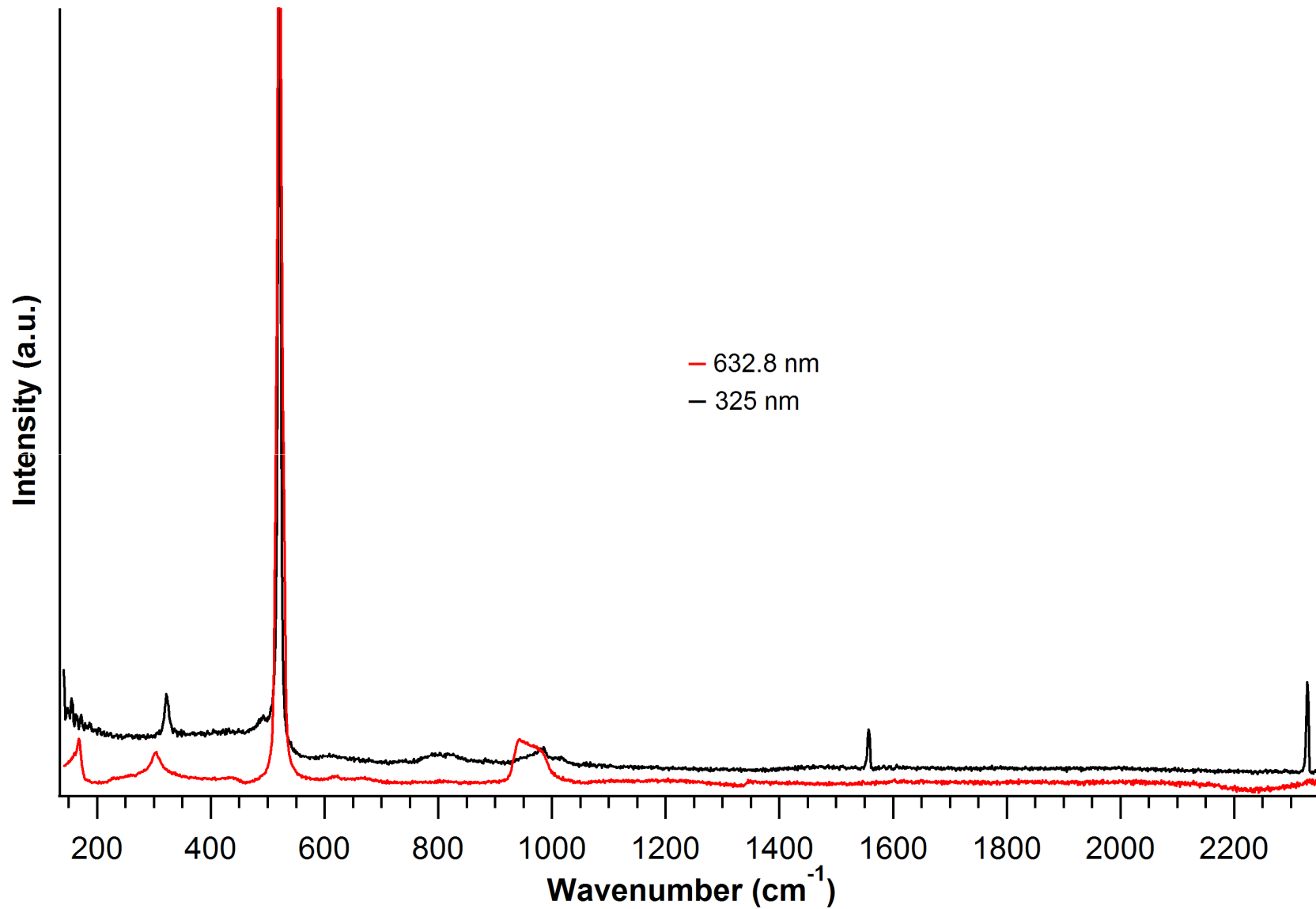
Intrinsic Silicon Spectrum (632.8 nm)



Intrinsic Silicon Spectrum (325 nm)



Intrinsic Silicon Spectrum

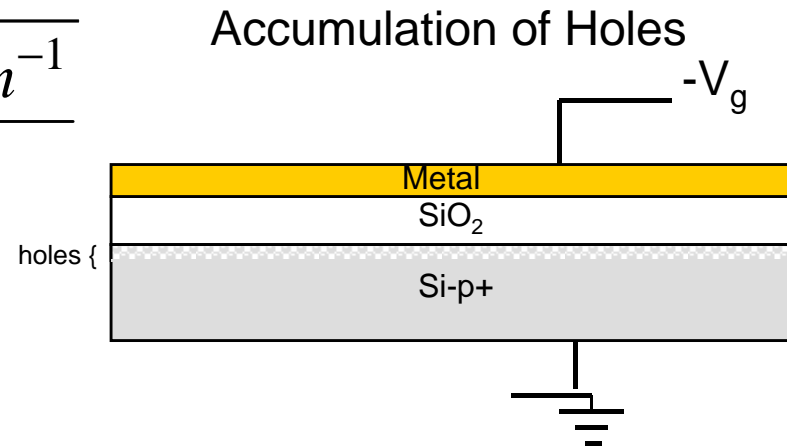


Field Dependence Considerations

- Debye Length

$$L_D = \sqrt{\frac{\epsilon_s kT}{q^2 N_A}} = \sqrt{\frac{1.68785 \times 10^7 \text{ m}^{-1}}{N_A}}$$

For $N_A = 1 \times 10^{19} \text{ cm}^{-3}$, $L_D = 1.299 \text{ nm}$



- Depletion Layer

$$w_d = \sqrt{\frac{2\epsilon_s \phi_s}{qN_A}} = \sqrt{\frac{2\epsilon_s (2\phi_F)}{qN_A}}$$

$$\phi_F = \frac{kT}{q} \ln \frac{N_A}{n_i}$$

For $N_A = 1 \times 10^{19} \text{ cm}^{-3}$, $w_d = 11.82 \text{ nm}$

